Finite Element Methods for Interface Problems Using Unfitted Meshes: Design and Analysis

by

Manuel A. Sánchez Uribe

B.S., University of Concepción, Concepción, Chile, 2010

M.S., Brown University, Providence, RI, 2012

A dissertation submitted in partial fulfillment of the

requirements for the degree of Doctor of Philosophy

in the Division of Applied Mathematics at Brown University

PROVIDENCE, RHODE ISLAND

May 2016

This dissertation by Manuel A. Sánchez Uribe is accepted in its present form by the Division of Applied Mathematics as satisfying the dissertation requirement for the degree of Doctor of Philosophy.

Date________________ ____

Johnny Guzmán, Ph.D., Advisor

Recommended to the Graduate Council

Date________________ ____

Mark Ainsworth, Ph.D., Reader

Date________________ ____

Marcus Sarkis, Ph.D., Reader

Approved by the Graduate Council

Date________________ ____

Peter M. Weber, Dean of the Graduate School

Vitae

Biographical Information

Born on March 14, 1986 in Concepción, Chile.

Education

Brown University, Providence, RI, USA

Ph.D. Applied Mathematics (expected May 2016)
Dissertation Title: Finite Element Methods for Interface Problems using Unfitted Meshes: Design and Analysis.
Advisor: Johnny Guzmán.

M.S. Applied Mathematics, May 2012

University of Concepción, Concepción, Chile

Mathematical Civil Engineer, professional qualification, January 2010
Thesis Title: Analysis of a Velocity-Pressure-Pseudostress Formulation for the Stationary Stokes Equations
Advisor: Gabriel Gatica

B.S. in Mathematical Engineering, January 2010

Research Interests

Numerical Analysis, Scientific Computing, Numerical Solutions of Partial Differential Equations, Finite Elements Methods, Interface Problems, Bernstein Polynomials, Mixed Finite Elements Methods.

Publications

1. Erik Burman, Johnny Guzmán, Manuel A. Sánchez and Marcus Sarkis. "Robust flux error estimation of Nitsche's method for high contrast interface problems". *Submitted to IMA Journal of Numerical Analysis. ArXiv e-prints*, February 2016.

2. Mark Ainsworth and Manuel A. Sánchez. "Computing the Bézier control points of the Lagrangian interpolant in arbitrary dimension". *SIAM Journal of Scientific Computing. Accepted. Arxiv preprint arXiv:1510.09197*, November 2015.

3. Johnny Guzmán, Manuel A. Sánchez, and Marcus Sarkis. A finite element method for high-contrast interface problems with error estimates independent of contrast. *Submitted to Journal of Scientific Computing. ArXiv preprint arXiv:1507.03873*, July 2015.

4. Johnny Guzmán, Manuel A. Sánchez, and Marcus Sarkis. Higher-order finite element methods for elliptic problems with interfaces. *Mathematical Modelling and Numerical Analysis, Accepted. Arxiv preprint arXiv:1505.04347*, November 2014.

5. Johnny Guzmán, Manuel A. Sánchez, and Marcus Sarkis. On the accuracy of finite element approximations to a class of interface problems. *Mathematics of Computations* (2015). *Tech. report Scientific Computing Group, Brown University* 2014-6., March 2014.

6. Johnny Guzmán and Manuel A. Sánchez. Max-norm stability of low order Taylor-Hood elements in three dimensions. *Journal of Scientific Computing, 65(2), 2015.*

7. Gabriel N. Gatica, Antonio Márquez, and Manuel A. Sánchez. Pseudostress-based mixed finite element methods for the Stokes problem in Rn with Dirichlet boundary conditions. I: A priori error analysis. *Commun. Comput. Phys.*, 12(1):109-134, 2012.

8. Gabriel N. Gatica, Antonio Márquez, and Manuel A. Sánchez. A priori and a posteriori error analyses of a velocity-pseudostress formulation for a class of quasi-Newtonian Stokes flows. *Comput. Methods Appl. Mech. Engrg.*, 200(17-20):1619 -1636, 2011.

9. Gabriel N. Gatica, Antonio Márquez, and Manuel A. Sánchez. Analysis of a velocity-pressure-pseudostress formulation for the stationary Stokes equations. *Comput. Methods Appl. Mech. Engrg.*, 199(17-20):1064-1079, 2010.

Presentations

Finite element methods for stationary elliptic interface problems, *CCMA PDEs and Numerical Methods Seminar Series, Department of Mathematics Penn State University (January 14, 2016).*

Finite element methods for high contrast interface problems, *AMS Special Session on The Mathematics of Computation, Joint Mathematics Meetings, Seattle WA* (January 2016).

Finite element methods for high-contrast interface problems, *Finite Element Circus, University of Massachusetts Dartmouth* (October 16-17 2015).

Bernstein polynomial interpolation, Finite Elements Circus, *George Mason University, Fairfax VA* (March 27-28, 2015).

Higher-order FEM for elliptic interface problems, *Minisymposia: Recent Advances in Numerical Methods for Interface Problems, SIAM CSE, Utah* (March 18, 2015).

Higher-order FEM for elliptic interface problems, *Finite Elements Circus, University of Minnesota, Minnesota* (October 24, 2014).

On the accuracy of finite element approximations to a class of interface problems, *DelMar Numerics Day, University of Maryland, Baltimore county* (May 10, 2014).

Max-norm stability of low order Taylor-Hood elements in three dimensions, *Valparaíso Numérico IV. Pontificia Universidad Católica de Valparaíso, Chile* (December 11-13, 2013).

Max-norm Stability of low Taylor-Hood Element in three dimensions, *Finite Element Circus, University of Delaware* (October 18-19, 2013).

Analysis of a velocity-pressure-pseudostress formulation for the stationary Stokes equations, *COMCA 2009 Numerical Analysis, Universidad Católica del Norte, Antofagasta - Chile* (August 5 - 7, 2009).

Poster : FEM for Interface Problems, *Advanced Numerical Methods in the Mathematical Sciences. Institute for Scientific Computation, Texas A&M University, College Station, TX.* May 4-8, 2015.

Poster: Higher-order FEM for the Stokes interface problem, *Minisympostrium on Advances in numerical methods for interface problems, SIAM CSE, Utah*, March 15, 2015.

Poster: Higher-Order FEM to a Class of Interface Problems, *Structure-Preserving Discretizations of Partial Differential Equations, IMA, Minnesota*, October 22-24, 2014.

Poster: Finite Element Approximation to a class of Interface problems, *Robust Discretization and Fast Solvers for Computable Multi-Physics Models ICERM, Providence RI*, May 12-16, 2014.

Finite element methods for interface problems, *Workshop on Integrating Dynamics and Stochastic, Division of Applied Mathematics, Brown University*, November 7, 2014.

Finite Element Approximation to a class of Interface problems, *Graduate student seminar, Division of Applied Mathematics, Brown University*, April 2014.

Honors and Awards

Research Assistantship, Brown University, Fall 2015- Spring 2016

Teaching Assistantship, Method of Applied Mathematics - I, Brown University 2014

Becas Chile Fellowship, Government of Chile for studies abroad, 2011-2015

Thesis project funded by BASAL project, CONICYT, Chile, 2010

Academic Excellence Fellowship, University of Concepción granted to the top 10 entering freshmen, 2004

Professional Service - Peer review in Journals

Computer Methods in Applied Mechanics and Engineering

Journal of Scientific Computing

Journal of Computational and Applied Mathematics

Acknowledgements

I would like to express my gratitude to all those people who have helped me throughout the process of writing this thesis.

My deepest and sincerest gratitude to my advisor, Prof. Johnny Guzmán, who has guided and encouraged me from the very beginning and continues doing it until these days. I have been genuinely influenced and inspired by his dedication and enthusiasm for research. I am very thankful for all I have learned from him during these five years, but I am even more thankful for his precious friendship.

I would like to thank the rest of my dissertation committee Prof. Mark Ainsworth and Prof. Marcus Sarkis for agreeing to read my thesis and for their valuable insights. I am honored to have had the chance to collaborate with them in research projects and I would like to acknowledge the big impact that they have had in my scientific career. I am also grateful to Prof. Chi-Wang Shu for motivated me during the numerous courses I took with him and for his valuable guidance.

I am thankful to my fellow graduate students as well as postdocs and visitors in Applied Mathematics at Brown University for the several discussions and constructive suggestions that contributed to this thesis. In addition, my gratitude to all the friends that me and my family have made here at Providence, their company and support undoubtedly have been essential during this time.

I am profoundly grateful to my parents, Carmen and Victor, and my siblings Victor Hugo, Claudio y Carmen for their support and encouragement throughout my career.

There are no words to express my gratitude to my beloved wife Daniela and my son Daniel for their patience, sacrifices, generosity, caring and love during these 5 years at Brown. They have been my biggest supporters throughout this process. This dissertation is dedicated to them.

Finally, I gratefully acknowledge my scholarship from CONICYT Becas Chile 72110661 that funded me for the first four years of my graduate studies.

Abstract of " Finite Element Methods for Interface Problems Using Unfitted Meshes: Design and Analysis" by Manuel A. Sánchez Uribe, Ph.D., Brown University, May 2016

This dissertation aims to study finite element methods for two-dimensional stationary second order interface model problems on homogeneous and heterogeneous media, under discretizations non-fitted with the interface. We propose novel numerical methods for the model interface problems, proving optimal convergence of the errors and robust error estimates with respect to the curvature of the interface and the physical parameters of the problems.

In the first part of the dissertation, we consider the Poisson and Stokes interface problems on homogeneous media. In both cases, we design correction terms relying on the interface jump conditions of the problem for each unknown variable, which are then added to the right-hand side of the system. This technique is developed for arbitrary polynomial order of the finite element subspace, by means of higher order derivative jumps of the solution derived from the problem. We provide pointwise error analyses of the methods obtaining optimal convergence of the errors.

The second part assesses the classical elliptic interface model problem on heterogeneous media: Poisson equations with discontinuous constant coefficients. In particular, we examine the case in which the contrast of the diffusion coefficients is high. We present an a priori analysis of the regularity in order to develop error estimates for the numerical methods consistent with the behavior of the solution. Furthermore, we propose and analyze two finite element methods, following distinct approaches, for the high contrast Poisson interface problem. The first method follows the philosophy of Immersed Finite Element methods, incorporating the jump conditions of the problem strongly in the finite element subspace. Optimal error estimates independent of the contrast of the diffusion coefficients are proved. A detailed anal-

ysis incorporating the curvature of the interface and the regularity of the solution is presented, guaranteeing robustness of the method. The second numerical approximation is based on a Nitsche finite element method, with flux stabilization terms. This approach imposes the jumps conditions of the problem weakly, in the form of penalty terms with support on the interface that are added to the system. Optimal error estimates independent of the high-contrast are demonstrated, including a novel error estimate for the flux of the solution.

Finally, numerical evidence of the properties of the finite element approximations are displayed for each problem, corroborating the theoretical findings.

Contents

List of Tables

List of Figures

Chapter One

Introduction

In this dissertation we design and study numerical approximations by finite element methods to two-dimensional, second order, elliptic interface problems, using meshes that are non-aligned with the interface. We present stability and error analyses of the numerical methods with emphasis on: the autonomy of the discretizations with respect to the interface, proofs of optimal errors estimates based on the energy and L^2 norms, and the study of the dependence (or independence) of these error estimates with respect to the physical quantities or parameters corresponding to the sub-domains interacting through the interface.

Broadly speaking, *Interface Problems* are systems of partial differential equations with jump conditions satisfied across an interface immersed in the physical domain of study. These problems arise as mathematical models in physical sciences and engineering, as for example: biological flows interacting with elastic structures (heart models), multi-phase flows, cell and bubble dynamics, front tracking in porous media flows, animal locomotion, plasma dynamics and electromagnetic problems, etc. As one can anticipate, solutions to these problems are in general non-smooth, or even discontinuous across the interface depending on the jump conditions. Consequently, numerical methods that rely on the global regularity of the solution perform poorly, rendering suboptimal convergence of the errors or even in some cases lack of convergence near the interface.

A common feature of interface problems, independent of the complexity of the governing equations or the dimension of the space, is the geometry: typically, a bounded domain Ω contained in $\mathbb{R}^d$ and an interface or elastic boundary Γ, of at least one dimension less than Ω, immersed in the domain are considered. The domain and the interface interact by means of interface or transmission conditions presented in the partial differential equations arising from the physical model. Naturally, we are interested in numerical approximations of the solution of this system of equations.

A key step in this direction, for most of the numerical methods, is the discretization of the physical domain (mesh construction). In interface problems, we can divide the numerical methods, depending on how the discretization is constructed, into two approaches: methods with meshes that are aligned or fitted with the interface, or methods with meshes that are non-aligned or non-fitted (unfitted) with the interface. See Figure 1.1 for an illustration of both cases. Evidently, the first approach is much more restrictive in terms of mesh generation. In particular, for problems where the interface evolves in time, re-meshing in each time step could present some drawbacks, as for instance: a high computational cost of the mesh generation, the structure of the mesh could be totally destroyed, the well-conditioning of the stiffness matrix could be progressively deteriorated, and possible instabilities of the numerical approximation might appear. Considering these obstacles, the second approach presents significant advantages, allowing much simpler discretizations, as for example, Cartesian grids or uniform triangulations. The discussion in this dissertation focuses exclusively in the latter approach, designing finite element methods based on meshes that are non-fitted with the interface.

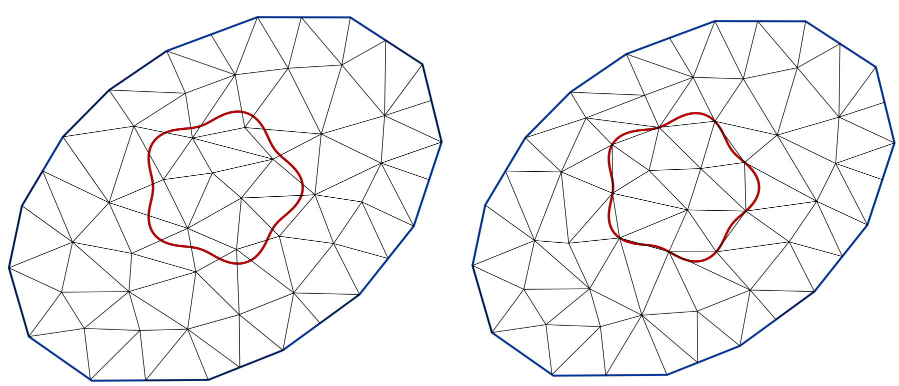

Figure 1.1: Illustration of discretizations of a two-dimensional polygonal domain with an immersed interface. Left figure: non-fitted with the interface. Right figure: fitted with the interface (right).

In the next section we present an overview of some numerical methods, based on meshes that are non-fitted with the interface, that influenced our work.

1.1 Background on numerical methods for interface problems

A widely known, flexible, and certainly remarkable numerical method for interface problems is the finite differences based *Immersed Boundary Method* (IBM) by Peskin [96, 98]. Originally, the IBM was designed to approximate numerically a blood flow model in the human cardiac muscle. Since then, the method has found several applications in biophysics, fluid-structure interactions, and aerodynamic, including: blood flow in the heart [90], vibrations of the cochlear basilar membrane [57], blood clotting [111], aquatic locomotion (swimming of eels, sperm and bacteria)[52], flow with suspended particles [53], insect flight [93]. See the review article [97] for a complete review of the method and detailed applications of it. Although we are presenting here IBM as a numerical method for interface problems, the initial equations were not quite written the interface setting with jump conditions. In order to illustrate this, we introduce one of the first models studied by Peskin: Consider a closed elastic curve (massless) immersed in a two-dimensional incompressible fluid.

The equations of motion of the problem are

$$\rho(\frac{\partial \boldsymbol{u}}{\partial t} + \boldsymbol{u} \cdot \nabla \boldsymbol{u}) + \nabla p = \mu \Delta \boldsymbol{u} + \boldsymbol{f}_b, \tag{1.1a}$$

$$\nabla \cdot \boldsymbol{u} = 0, \tag{1.1b}$$

$$\boldsymbol{f}_b(x,t) = \int_0^L \boldsymbol{\beta}(s,t)\delta(x - \boldsymbol{X}(s,t))ds, \tag{1.1c}$$

$$\frac{\partial \boldsymbol{X}}{\partial t}(s,t) = \boldsymbol{u}(\boldsymbol{X}(s,t),t), \tag{1.1d}$$

$$f(s,t) = \frac{\partial}{\partial s}(T\boldsymbol{t}), \tag{1.1e}$$

$$T = S(\left|\frac{\partial \boldsymbol{X}}{\partial s}\right| - 1), \tag{1.1f}$$

$$\boldsymbol{t} = \frac{\partial \boldsymbol{X}/\partial s}{|\partial \boldsymbol{X}/\partial s|}, \tag{1.1g}$$

where : $\boldsymbol{u}(x,t)$ is the fluid velocity, $p(x,t)$ is the fluid pressure, $\boldsymbol{f}_b(x,t)$ is the force-density generated by the boundary, ρ density of the fluid (constant), μ viscosity of the fluid (constant), $\boldsymbol{X}(s,t)$ is the boundary configuration, L is the unstressed length of the boundary, $T(s,t)$ is the boundary tension, and $\boldsymbol{t}$ the tangential vector to the boundary.

The model (1.1), studied by Peskin in [96, 99, 98], does not have interface conditions written explicitly, the force $\boldsymbol{f}_b$ generated by the boundary immersed (or interface) in the domain is considered instead. This force is described by means of a delta function with support on the immersed boundary. Peskin and Printz [99] would show later that this force is in fact equivalent to some jump conditions across the immersed boundary, as in the standard interface setting. Specifically, they showed that, under the non-slip assumption ($[u] = 0$), the jumps across the boundary are given by

$$\mu \boldsymbol{t} \cdot [(\nabla \boldsymbol{u})\boldsymbol{n}] = -\frac{\boldsymbol{\beta} \cdot \boldsymbol{t}}{|\partial \boldsymbol{X}/\partial s|} \tag{1.2}$$

$$[p] = \frac{\boldsymbol{\beta} \cdot \boldsymbol{n}}{|\partial \boldsymbol{X}/\partial s|} \tag{1.3}$$

where $\boldsymbol{n}$ denotes the normal vector to the boundary.

One of the key and distinguishable ideas of the IBM is the approximation of the delta function by a discrete smooth delta function. On the other hand, in the variational formulation of problem (1.1) an integral over the boundary appears, replacing the delta function. This observation caught the attention of variational methods, in particular Finite Element Methods (FEM), which have proven to be very powerful and robust in terms of implementation and analysis. Perhaps one of the most important finite element approaches to the Immersed Boundary Method is the *Finite Element Immersed Boundary method* (FEIBM) developed by Boffi et al. [22, 23, 24, 25, 20, 19, 21]. Among the contributions of FEIBM are for instance CFL conditions, numerical stability of the method, and conservation properties. In this framework, the construction of the discrete delta function is avoided and replaced by discretization of the integrals along the boundary. In spite of all the advantages that IBM presents, the method for both approaches (the finite difference and finite element approach) is in general only first order accurate. The optimal second order accuracy is obtained for special cases when the solution is smooth. In this dissertation we will present a methodology to obtain higher order finite element approximations considering cases where the solution is not necessarily smooth across the boundary, at least for basic model problems.

Another notable and well-known numerical method, also finite differences based, is the *Immersed Interface Method* (IIM) by LeVeque and Li [77, 78, 76, 75, 81]. The

IIM was motivated by the IBM, but first developed in a much simpler framework. The model problem for which IIM was first applied is the Poisson equation with discontinuous diffusion coefficients. We now present the problem in order to illustrate ideas. A connected, bounded and open domain $\Omega \subset \mathbb{R}^2$ is assumed to have an immersed closed interface Γ, separating the domain into two sub-domains Ω^- and Ω^+. See Figure 1.2 for an illustration of these definitions. We seek for the solution u of the equations:

$$-\nabla \cdot (\rho(x)\nabla u(x)) = f(x) \qquad x \in \Omega^{\pm}, \tag{1.4a}$$

$$u(x) = 0 \qquad x \in \partial\Omega, \tag{1.4b}$$

$$[u(x)] = \alpha(x) \qquad x \in \Gamma, \tag{1.4c}$$

$$[\rho(x)\nabla u(x) \cdot \boldsymbol{n}(x)] = \beta(x) \qquad x \in \Gamma, \tag{1.4d}$$

with the function ρ defined to be piecewise constant in Ω^- and Ω^+ as follows

$$\rho(x) = \begin{cases} \rho^-, & x \in \Omega^-; \\ \rho^+, & x \in \Omega^+. \end{cases} \tag{1.5}$$

Despite the apparent simplicity of the model problem (1.4), its accurate numerical

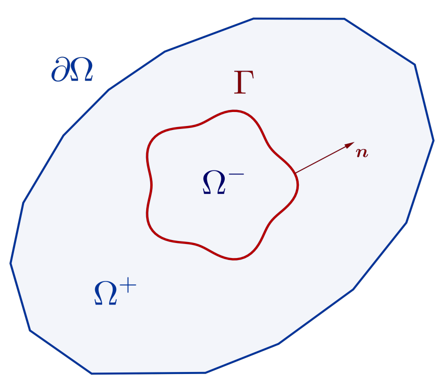

Figure 1.2: Illustration of the standard geometry of the domain for interface problems.

resolution is key in many applications such as: plasma particle simulations and electromagnetic problems [85, 72], solving multi-phase flows [37, 42, 69], topology optimization problems [18], to name a few. For a more extended list of applications of model problem (1.4) and other interface problems in heterogeneous media see [80, 66]. In contrast to the IBM, the IIM intents to accurately capture the discontinuities of the solution across the interface, imposing the interface jump conditions exactly or approximately on points of the grid. As one can expect, this approach gives a more accurate approximation of the solution near the interface. In effect, Beale et al. [14] proved an optimal second order convergence of the Immersed Interface Method for the Poisson equations with discontinuous coefficients. Not long after the appearance of this method, a finite element version following the idea of imposing strongly the interface conditions emerged. The first contribution in this direction is due to Li [79] for the one-dimensional model problem. After this, several publications addressing finite element formulations of the IIM have appeared. See for example [83, 82, 58, 59, 35, 66, 67, 68, 17, 112, 1, 84, 86]. For instance, for the two dimensional case Li et al. [83, 82] proposed and analyzed conforming and nonconforming immersed finite element methods for the Poisson equations with discontinuous constant coefficients and homogeneous jump conditions. These methods are known as Immersed Finite Element methods (IFEM) or Immersed-Interface Finite Element methods. A natural question that has not been satisfactorily answered by these methods, even for the Poisson model problem with discontinuous coefficients, is the independence of the error estimates with respect to the contrast ρ^+/ρ^- of the discontinuous constant coefficients (1.5). One of the main objectives of this dissertation is to obtain error estimates independent of the contrast of the parameters associated with the subdomains separated by the interface. We will rigorously prove, among other things, the first error estimates totally independent of the contrast for a method in the immersed finite element class.

In the same context, another numerical method that has shown desirable properties to approximate interface problems with a large contrast of the coefficients is the *Nitsche finite element method*. This method was initially designed as a technique to impose Dirichlet boundary conditions in finite element methods (see [95]), an alternative to other well-known methodologies as, for example, Lagrange multipliers [7] or penalty methods [7, 13]. The original Nitsche's method can be interpreted as a variant of the penalty methods in order to recover consistency [106]. Now, in the context of interface problems, we can describe the dynamics as the interaction of problems on two non-overlapping domains by means of boundary conditions satisfied on a common interface. In this sense, the interface conditions will naturally appear as a result of formulation of Nitsche's method in both domain. For instance see the contribution by Hansbo et al. [65, 64]. Subsequently, different forms of this method have appeared. In the quest of a robust method in terms of the configuration of the computational mesh with respect to the interface and how small can the elements be cut, an interesting approach was given by Burman et al. [30]. They proposed stabilization techniques, a penalty term is added with the aim of improving the stability in the elements cut by the interface. Such a term is usually called the *ghost penalty term*, see Burman [29]. Despite all the efforts and techniques utilized to design a method independent of the contrast of the coefficients, explicit error estimates stating the desired result are not found in the literature. In this thesis this result is achieved, proving optimal error estimates, based on the L^2 and energy norm, independent of the contrast of the discontinuous coefficients presented in the Poisson interface model problem. Furthermore, a novel optimal error estimate for the flux variable, totally independent of the coefficients, is derived.

Other notable examples in the literature of numerical methods for interface problems (or similar problems) on discretizations that are non-fitted with the interface are: *Partition of Unity method* (PUM), *Generalized Finite Element method* (GFEM), and *eXtended Finite Element method* (XFEM). As it is mentioned in [54] and [8], these methods are closely related. The common feature is the so called "enrichment" which can be seen as special function added to the standard finite dimensional space, by means of partition of unity techniques [92]. The idea behind this enrichment is to capture properties of the unknown solution in order to obtain a better approximation. The partition of unity technique was first proposed in [10], under the name of Special Finite Element methods, using a particular partition of unity based on standard finite element hat-functions. The idea is generalized in [91], where the hat-functions are replaced by any partition of unity [11, 92]. This is the Partition of Unity method or Partition of Unity Finite Element method. The Generalized Finite Element method (see also meshless methods) would appear later [40, 107, 108, 109, 9] using hat-functions partition of unity and enrichment that are not necessarily polynomials. About the same time and totally independent of GFEM, eXtended Finite Element method were developed for crack propagation problems [16, 45]. The XFEM uses analogous techniques for the enrichment, although the emphasis is on a local enrichment of the spaces (on the nodes near the crack or interface). In addition, the *multi-scale finite element methods* [49] have also been applied to interface problems, even addressing problems with high-curvature of the interface [38, 70].

In the next section we elaborate on the concepts introduced above and discuss our early motivations and influences.

1.2 Motivation and overview

An early motivation for our research was the article [94] by Mori, where pointwise error estimates for the Immersed Boundary Method applied to the Stokes problem with an immersed boundary are presented. In order to fix ideas, consider the following model problem: Let Γ be a one dimensional closed curve (interface) immersed in a two-dimensional fluid domain Ω. Let $\boldsymbol{X}(s)$ be the arc-length parameterization of Γ. Let $\boldsymbol{\beta}$ be a boundary force given in function of the curve parameterization. The problem is to find the fluid velocity field $\boldsymbol{u}$ and pressure p under Stokes flow,

$$-\Delta\boldsymbol{u} + \nabla p = \boldsymbol{f} - \boldsymbol{f}_b \qquad \text{in } \Omega, \tag{1.6a}$$

$$\nabla\cdot\boldsymbol{u} = 0 \qquad \text{in } \Omega, \tag{1.6b}$$

$$\boldsymbol{u} = \boldsymbol{0} \qquad \text{on } \partial\Omega, \tag{1.6c}$$

where the singular external force field $\boldsymbol{f}_b$ is expressed in terms of the boundary force $\boldsymbol{\beta}$ as follows:

$$\boldsymbol{f}_b(x) = \int_0^{|\Gamma|} \boldsymbol{\beta}(s)\delta(x - \boldsymbol{X}(s))ds, \quad x \in \Omega,$$

and δ denotes the Dirac delta function.

In [94], Mori studied the periodic version of problem (1.6), proving pointwise error estimates optimal for points away from the boundary Γ. One of the merits of this work is that it was able to quantify the distance to the boundary at which the errors converge optimally. An important consequence of this is that the loss of convergence is a local behavior. In the beginning of our research we decided to study this phenomenon using the variational formulation and finite element methods applied to the Stokes equations (1.6), with the aim to achieve a numerical method that totally recovers the optimal convergence. In order to fully understand the problem, we began with an even simpler model problem: Poisson equations with an immersed boundary. Consider the same geometry as in (1.6), a two dimensional bounded domain Ω and an immersed curve Γ. We seek a solution of

$$-\Delta u = f - f_b \qquad \text{in } \Omega, \tag{1.7a}$$

$$u = 0 \qquad \text{on } \partial\Omega, \tag{1.7b}$$

$$\tag{1.7c}$$

where the singular force f_b is written in terms of a given boundary force $\beta(s)$ and $\boldsymbol{X}(s)$ the arc-length parameterization of Γ

$$f_b(x) = \int_0^{|\Gamma|} \beta(s)\delta(x - \boldsymbol{X}(s))ds, \quad x \in \Omega. \tag{1.8}$$

As it was mentioned before, singular forces can be written as interface conditions across Γ by means of the variational formulation of the problem. To see this, consider the non-overlapping sub-domains Ω^+ and Ω^-, resulting from the presence of Γ, i.e. $\overline{\Omega} = \overline{\Omega^-} \cup \overline{\Omega^+}$ and $\partial\Omega^- \cap \partial\Omega^+ = \Gamma$. Consider a test function $v \in C^\infty(\Omega)$ with support in Ω. Then, multiplying by v, integrating equation (1.7a) over Ω, and using integration by parts (assuming that u is continuous across Γ), gives

$$\int_{\Omega^-} \nabla u^- \cdot \nabla v + \int_{\Omega^+} \nabla u^+ \cdot \nabla v - \int_\Gamma [\nabla u \cdot \boldsymbol{n}]\, v ds = \int_\Omega f v - \int_\Omega f_b v,$$

where $[\cdot]$ denotes the jump on Γ defined by

$$[\nabla u \cdot \boldsymbol{n}] = \nabla u^+ \cdot \boldsymbol{n}^+ + \nabla u^- \cdot \boldsymbol{n}^-,$$

for $u^\pm \equiv u|_{\Omega^\pm}$ and $\boldsymbol{n}^\pm$ the outward pointing unit normal vector to $\Omega^\pm$. Now, using the definition of the delta function it follows

$$\int_\Omega f_b(x)v(x)dx = \int_\Omega \Big(\int_0^{|\Gamma|} \beta(s)\delta(x - \boldsymbol{X}(s))ds \Big) v(x)dx = \int_0^{|\Gamma|} \beta(s)v(\boldsymbol{X}(s))ds.$$

Therefore, taking test functions with support in Ω^-, Ω^+ and on a thin strip with Γ on the center (collapsing towards Γ), the interface problem is derived as

$$-\Delta u^\pm = f \qquad \text{in } \Omega^\pm, \tag{1.9a}$$

$$u = 0 \qquad \text{on } \partial\Omega, \tag{1.9b}$$

$$[\nabla u \cdot \boldsymbol{n}] = \beta \qquad \text{on } \Gamma. \tag{1.9c}$$

An additional jump condition for the function u can also be considered in the Poison interface problem (1.9), i.e. $[u] = \alpha$.

In order to illustrate the difficulties of this problem, consider the standard finite element formulation for equations (1.9) using continuous piecewise linear functions. Let $\Omega = (-1, 1)^2$ and the interface Γ be the circle centered at the origin and of radius $1/3$. We consider a continuous exact solution with a constant jump on Γ of the form (1.9c) (solution is not in H^2). Table 1.1 displays the errors obtained by the finite element approximation in: the L^2 and L^∞ norms, and the H^1 and $W^{1,\infty}$ semi-norms. In addition, the experimental order of convergence (eoc) is computed for each error. In Table 1.1 convergence is observed for L^2 and L^∞ norm, but are far from optimal (second order). The error in the $W^{1,2}$ semi-norm barely converges, whilst the error in the $W^{1,\infty}$ semi-norm does not seem to converge. Figure 1.3 shows plots of the approximate solution and the pointwise errors at the nodes of the mesh. We observe in the latter plot that larger errors are concentrated in a small region around the interface.

h	e_h^0	eoc	e_h^∞	eoc	e_h^1	eoc	$e_h^{1,\infty}$	eoc
1.8e-1	1.02e-1		1.63e-1		4.71e-1		7.01e-1	
8.8e-2	1.57e-2	2.70	4.09e-2	2.00	1.38e-1	1.78	3.26e-1	1.10
4.4e-2	6.72e-3	1.22	2.85e-2	0.52	1.30e-1	0.09	5.48e-1	-0.75
2.2e-2	2.02e-3	1.74	1.07e-2	1.42	7.88e-2	0.72	5.87e-1	-0.10
1.1e-2	7.65e-4	1.40	7.24e-3	0.56	6.16e-2	0.36	6.24e-1	-0.09
5.5e-3	2.71e-4	1.50	4.39e-3	0.72	4.27e-2	0.53	6.24e-1	0.00
2.8e-3	9.09e-5	1.58	2.04e-3	1.11	2.83e-2	0.59	7.80e-1	-0.32
1.4e-3	3.53e-5	1.36	1.38e-3	0.57	2.24e-2	0.34	8.78e-1	-0.17

Table 1.1: Errors based on L^2 and L^∞ norms, and H^1 and $W^{1,\infty}$ semi-norms of the approximate solution by standard FEM, and their respective experimental order of convergence.

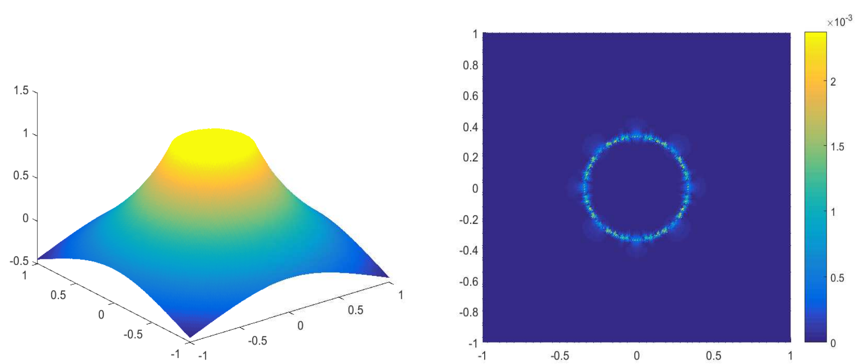

Figure 1.3: Standard FEM applied to interface problem (1.7). Left figure: plot of the approximate solution. Right figure: plot of the errors at the nodes of the triangulation.

Driven by the local behaviour of the error and testing our variational formulation with an interpolant of the solution we derived higher-order finite element methods for the interface problem (1.9). These are presented in Chapter 3. The error analysis, as in Mori's work, is on the L^∞ norm and $W^{1,\infty}$ semi-norm, and is carried on by means of standard Green's function techniques for finite elements. One of the notable properties of these new methods is that only the right-hand side is modified (i.e. the load vector), maintaining the stiffness matrix intact.

In this dissertation, problems (1.9) and (1.7) are referred as interface problems on homogeneous media since it is implicitly assumed that the physical properties of Ω^- and Ω^+ are the same. This is certainly not the general case for applications of interface problems. Indeed, problems where the governing equations are satisfied in sub-domains separated by an interface and the characteristic coefficients are heterogeneous have several applications. For example: computational mechanics for deformation of multiple material bodies [65], or geosciences for flow and mass transport [32]. A model problem that has caught the attention of the numerical-methods community for years and motivated this thesis is the Poisson interface problem with heterogeneous coefficients, problem (1.4) before introduced.

The model problem (1.4) has been extensively studied by several authors who have proposed various numerical methods. In particular, for finite element methods studying this problem see [6, 110, 84, 113, 15, 33, 31, 114, 29, 65, 64, 68, 58, 88, 12, 89, 1, 38], to name a few. Among methods utilizing discretizations on meshes that are non-fitted with the interface, very little has been said on *high contrast problems*, i.e. cases where the contrast of the constant coefficients ρ^- and ρ^+ is high (i.e. $\rho^+/\rho^- \gg 1$). The importance of achieving error estimates independent of contrast is that this guarantees a robust method with respect to the characteristics of the materials, avoiding deterioration of the error estimates with respect to the increment of the contrast of the coefficients. Consider, for example, the standard finite element method with piecewise linear polynomials applied to problem (1.4) with homogeneous jumps on a non-fitted triangulation. Note that this method is suboptimal, only first order accurate since the solution is not in $H^2(\Omega)$. An exact solution is available in terms of ρ^- and ρ^+ with a circle of radius $1/3$ as interface (see equation (4.47)). In order to test the dependence of the contrast we fix the value of ρ^- and increment ρ^+ consistently. Table 1.2 displays the errors obtained for the approximate solution on a fix mesh and different values of ρ^+. Observe that, in

ρ^+	$\|u - u_h\|_{L^2(\Omega)}$	$\|\rho\nabla(u - u_h)\|_{L^2(\Omega)}$
2	3.7e-4	5.5e-2
8	1.0e-3	8.0e-2
32	1.7e-3	1.2e-1
128	2.1e-3	1.9e-1
512	2.3e-3	2.6e-1

Table 1.2: Errors based on L^2 norm and H^1 semi-norm of the approximate solution u_h of problem (1.4) (with $\rho^- = 1$) by standard FEM for a mesh of size $h = 2^{-(1/2+5)}$.

addition to the sub-optimality of the method, the errors also decrease in accuracy as the value of ρ^+ increments.

In the literature two articles can be found addressing and analyzing problem (1.4) for high contrast of the coefficients. Burman et al. [33] introduced an unfitted Nitsche method with averages and stabilization techniques for arbitrarily high contrast problems, presenting bounds for the condition number of the stiffness matrix, although a rigorous error analysis was not given in that paper. The other article by Chu et al. [38] uses multi-scale techniques to build basis functions, an approach that seems well suited for high curvature problems (e.g. inclusions completely contained in a triangle). However, in regions where the curvature of the interface is small it appears that their main a priori estimate degenerates (see Theorem 3.9 in [38]), forcing them to refine the mesh on those regions in order to be aligned with the interface. In this thesis, two contributions (see Chapter 4 and 5) to the design and analysis of finite element methods for high contrast problems are provided. These, however, come from two quite different approaches.

The first approach seeks to strongly enforce the jump conditions of the problem, i.e., the flux conservation and the continuity. This is achieved, for example, by defining the basis functions of the finite element space so that the satisfy the jumps on Γ at certain points. This is an important and marked feature of the Immersed Interface Method using a finite element formulation. In this context several authors have contributed [1, 59, 58, 38, 68, 67]. For example, Adjerid et al. [1] proposed to penalize jumps of the trial functions across the edges. Similar penalty terms were added by Lin et al. [84] proving optimal error estimates. However, in their analysis they do not consider high contrast problems. This dissertation study problem (1.4) and introduces a method following the immersed finite element approach that differs from [1] and [84] by having an additional stabilization term. This term allows us to prove error estimates that are independent of the contrast ρ^+/ρ^-. Specifically, we prove

$$\|\sqrt{\rho^-}\nabla(u-u_h)\|_{L^2(\Omega^-)} + \|\sqrt{\rho^+}\nabla(u-u_h)\|_{L^2(\Omega^+)} \leq \frac{C}{\sqrt{\rho^-}} h\|f\|_{L^2(\Omega)}, \tag{1.10}$$

where u is solution of problem (1.4), u_h is the approximation that we shall introduce in Chapter 4, and $C > 0$ is a constant independent of h, ρ^- and ρ^+. By stabilization term we mean a penalization of the jumps of the normal derivatives of the approximation across the edges that belong to triangles intersecting Γ. This idea was used before by Burman et al. [33], however, here we use different stabilization parameters (and of course different basis functions). Roughly speaking, the reason this flux stabilization is important for high contrast problems, is that one does not want to move estimates from Ω^+ to Ω^- because ρ^+ could be much larger than ρ^-. However, triangles that are cut by Γ might have a thin part in Ω^+, and therefore, inverse estimates might be affected. By adding the jumps of derivatives we can transfer the estimates to a neighboring triangle that will have a larger portion in Ω^+.

On the other hand, the second approach seeks to weakly enforce the jump conditions of the problem, doubling the degrees of freedom on the elements cutting the interface, and adding penalty terms with support on the interface. This approach corresponds to the Nitsche method class previously named. The inspiration of our contribution is the article by Burman et al. [33], where they demonstrated, as we commented before, that in addition to penalizing the jumps across Γ, it is necessary to add a flux stabilization term. This method is the so-called stabilized unfitted Nitsche method. The stabilization term penalizes the jumps of the gradient on edges that belong to triangles that intersect the interface. As Burman et al. [33] showed, in order to obtain a method that is robust with respect to the contrast of the coefficients and robust with respect to the way Γ cuts triangles, this type of penalization is necessary. However, their work fails to explicitly state the independence of the errors and the contrast.

In addition to this result, this thesis also includes a novel estimate for the error of the flux ($\rho\nabla u$) totally independent of ρ^- and ρ^+, i.e.

$$\|\rho^-\nabla(u-u_h)\|_{L^2(\Omega^-)} + \|\rho^+\nabla(u-u_h)\|_{L^2(\Omega+)} \leq Ch\|f\|_{L^2(\Omega)}, \tag{1.11}$$

where u is solution of problem (1.4), u_h is the approximation that we shall introduce in Chapter 5, and $C > 0$ is a constant independent of h, ρ^- and ρ^+. Note that estimate (1.10) does not directly imply (1.11). It does imply the estimate on Ω^-, simply multiplying by $\sqrt{\rho^-}$, i.e.

$$\|\rho^- \nabla(u - u_h)\|_{L^2(\Omega^-)} \leq Ch\|f\|_{L^2(\Omega)}.$$

However, the same trick does not work on Ω^+, where we would obtain

$$\|\rho^+ \nabla(u - u_h)\|_{L^2(\Omega^+)} \leq C\frac{\sqrt{\rho^+}}{\sqrt{\rho^-}}h\|f\|_{L^2(\Omega)},$$

being dependent of the contrast ρ^+/ρ^-.

1.2.1 Organization of the dissertation

The remainder of this dissertation is organized as follows. The next chapter introduces notation and general results with the aim of laying the bases for the posterior discussion. Chapter 3 deals with the interface problems on homogeneous media. Arbitrary order finite element methods are provided, as well as, proofs of the optimal pointwise error estimates for the approximations. In Chapter 4 we propose and analyze an Immersed Finite Element Method-type, based on piecewise linear functions, for the Poisson interface problem with heterogeneous coefficients, paying particular attention to the high contrast problem. Error analyses for the the L^2 and energy norms are studied, achieving the first estimates independent of contrast for this type of methods. Chapter 5 analyzes our version of the unfitted Nitsche method for the high contrast Poisson interface problem. The analysis includes a novel error estimate for the flux variable totally independent of contrast. Finally, concluding remarks are presented at the end of each chapter, addressing the contributions of this thesis, extension of the results and directions in terms of research that we would like pursue in the future.

Chapter Two

Preliminaries

The aim of this chapter is to introduce notation and terminology that will be used throughout the dissertation. In addition, we discuss our assumptions and some theoretical results necessary for the analysis of our numerical methods.

2.1 Sobolev spaces and norms

Consider a domain $\Omega \subseteq \mathbb{R}^d$. Let $1 \leq p \leq \infty$ and define the function spaces

$$L^p(\Omega) := \{v : \Omega \to \mathbb{R},\ v \text{ is Lebesgue measurable and } \|v\|_{L^p(\Omega)} < \infty\},$$

where the norms $\|\cdot\|_{L^p(\Omega)}$ are defined by:

$$\|v\|_{L^p(\Omega)} := \left(\int_\Omega |v|^p\right)^{1/p}, \quad 1 \leq p < \infty;$$

and for $p = \infty$,

$$\|v\|_{L^\infty(\Omega)} := \operatorname{ess\,sup}\{|v(x)| : x \in \Omega\}.$$

Let $L^1_{loc}(\Omega)$ denotes the set of locally integrable functions. Let k be a nonnegative integer and $1 \leq p \leq \infty$. We define the Sobolev spaces by

$$W^{k,p}(\Omega) := \{v \in L^1_{loc}(\Omega) : \|v\|_{W^{k,p}(\Omega)} < \infty\},$$

with Sobolev norms:

$$\|v\|_{W^{k,p}(\Omega)} := \left(\sum_{\boldsymbol{\alpha} \leq k} \|D^{\boldsymbol{\alpha}} v\|^p_{L^p(\Omega)}\right)^{1/p}, \quad 1 \leq p < \infty;$$

and for $p = \infty$,

$$\|v\|_{W^{k,\infty}(\Omega)} = \max\{\|D^{\boldsymbol{\alpha}} v\|_{L^\infty(\Omega)} : |\boldsymbol{\alpha}| \le k\}.$$

In this definition $D^{\boldsymbol{\alpha}} v$ denotes the weak derivative of v, for a multi-index $\boldsymbol{\alpha}$.

Remark 2.1. For the case $p = 2$, the Sobolev space is a Hilbert space and is denoted by $H^k = W^{2,k}$.

2.2 Finite element basics

We begin this section with standard definitions and concepts related to finite element discretizations.

2.2.1 The finite element

We follow classical finite element definitions from the books of Ciarlet [39] and Brenner and Scott [27]).

Definition 2.2.1. Let

- $K \subset \mathbb{R}^d$ be a bounded open set with nonempty interior and piecewise smooth boundary (the *element domain*),
- P_K be a finite-dimensional space of functions on K (the space of *shape functions*), and
- $\Sigma_K = \{\psi_1, \psi_2, ..., \psi_k\}$ be a basis for $(P_K)'$, dual space of P_K (the set of *nodal variables*).

Then (K, P_K, Σ_K) is called a *finite element*.

Remark 2.2. Note that we consider open elements instead of the classical definitions using closed elements.

Definition 2.2.2. Let (K, P_K, Σ_K) be a finite element. The basis $\{\phi_1, \phi_2, \ldots, \phi_n\}$ of P_K dual to Σ_K (i.e., $\psi_i(\phi_j) = \delta_{i,j}$) is called the *nodal basis* of P_K.

Definition 2.2.3. In $\mathbb{R}^d$, a (non-degenerate) *d-simplex* is the convex hull K of $(d+1)$-points $\{a_1, a_2, \ldots, a_{d+1}\} \in \mathbb{R}^d$, which are called *vertices* of the d-simplex, and which are not all contained in a hyperplane. For any integer $0 \leq m \leq d$, an *m-face* of the d-simplex K is any m-simplex whose $(m+1)$ vertices are also vertices of K. Any $(d-1)$-face is simply called a *face* and a 1-face is called an *edge*.

Definition 2.2.4. The *barycentric coordinates* $\lambda_j = \lambda_j(x)$, $1 \leq j \leq d+1$, of any point $x \in \mathbb{R}^d$, with respect to the $(d+1)$ points a_j, are the (unique) solutions of the linear system

$$\sum_{j=1}^{d+1} a_j \lambda_j = x, \quad \sum_{j=1}^{d+1} \lambda_j = 1.$$

Let K be any d-simplex with vertices $\{a_1, a_2, \ldots, a_{d+1}\} \in \mathbb{R}^d$. The d-dimensional *Lagrange nodes* (equidistant) are defined by the set

$$L_k(K) := \Big\{ x = \sum_{j=1}^{d+1} \lambda_j a_j; \sum_{j=1}^{d+1} \lambda_j = 1,\ \lambda_j \in \big\{0, \frac{1}{k}, ..., \frac{k-1}{k}, 1\big\},\ 1 \leq j \leq d+1 \Big\}.$$

Example 2.1. Consider K a d-simplex. Let $P_K = \mathbb{P}^k$, the space of polynomials of degree k in $\mathbb{R}^d$. Let $\Sigma_K = \{\psi_1, \psi_2, \ldots, \psi_{n_k}\}$ where

$$\psi_i(v) = v(a_i), \quad v \in P_K,\ \forall a_i \in L_k(K),\ i = 1, \ldots, n_k,$$

and $n_k := \dim(\mathbb{P}^k)$. Then (K, P_K, Σ_K) is a finite element. The nodal basis for the case $k = 1$ are the barycentric coordinates $\{\lambda_1, \lambda_2, \lambda_3\}$.

Remark 2.3. The element defined in Example 2.1 is called the Lagrange element.

We now characterize the discretization of a domain by simplices.

Definition 2.2.5. A *triangulation* (or simplicial triangulation) of a polygonal domain $\Omega \in \mathbb{R}^d$ is a finite collection of d-simplex element domains $\{T_i\}$ such that

- $T_i \cap T_j = \emptyset$, if $i \neq j$ and
- $\bigcup \overline{T_i} = \overline{\Omega}$.
- Any face of any d-simplex $T_1 \in \mathcal{T}_h$ is either a subset of the boundary $\partial\Omega$, or a face of another d-simplex $T_2 \in \mathcal{T}_h$.

Definition 2.2.6. Let Ω be a given domain and $\{\mathcal{T}_h\}$ be a family of triangulations of Ω, with maximum mesh size $h = \max\{h_T : h_T := \operatorname{diam} T,\, T \in \mathcal{T}_h\} \leq 1$. The family is said to be *quasi-uniform* if there exists $\gamma_0 > 0$ such that

$$\min\{\operatorname{diam} B_T : T \in \mathcal{T}_h\} \geq \gamma_0 h, \tag{2.1}$$

where B_T is the largest ball contained in T. The family is said to be *shape-regular* or non-degenerate if there exists $\gamma_0 > 0$ such that for all $T \in \mathcal{T}_h$

$$\operatorname{diam} B_T \geq \gamma_0 h_T. \tag{2.2}$$

Remark 2.4. If a family of triangulations is quasi-uniform, then it is shape-regular, but not conversely.

Next, standard finite element notation is introduced.

Definition 2.2.7. Consider an element T of a triangulation $\mathcal{T}_h$. We define the patch of elements ω_T of T as the union of elements sharing boundary with T, i.e.

$$\omega_T := \operatorname{int}\Big\{ \bigcup_{K\in\mathcal{T}_h} \overline{K} \,:\, \overline{K}\cap\overline{T} \neq \emptyset \Big\}. \tag{2.3}$$

For a vertex x of the triangulation $\mathcal{T}_h$, we define the patch of elements ω_x of x as the union of elements sharing x as a vertex, i.e.

$$\omega_x := \operatorname{int}\Big\{ \bigcup_{K\in\mathcal{T}_h} \overline{K} \,:\, x \text{ is a vertex of } K \Big\}. \tag{2.4}$$

Definition 2.2.8. Given a triangulation $\mathcal{T}_h$ of a polygonal domain $\Omega \subset \mathbb{R}^d$, we denote by $\mathcal{E}_h$ the set of all faces ($d = 2$ edges) of $\mathcal{T}_h$. Now, for a piecewise smooth function v with support on $\mathcal{T}_h$, we define its average and jump across an interior face $e \in \mathcal{E}^h \backslash \partial\Omega$, shared by elements T_1 and T_2, as

$$\{v\} := \frac{v|_{T_1} + v|_{T_2}}{2}, \qquad [\![v]\!] := v|_{T_1}\boldsymbol{n}_1 + v|_{T_2}\boldsymbol{n}_2, \tag{2.5}$$

where $\boldsymbol{n}_1$ and $\boldsymbol{n}_2$ are the outward pointing unit normal vectors to T_1 and T_2, respectively. Similarly, if $\boldsymbol{\tau}$ is a vector-valued function, piecewise smooth on $\mathcal{T}_h$, its average and normal jump across an interior face e are defined as

$$\{\boldsymbol{\tau}\} := \frac{\boldsymbol{\tau}|_{T_1} + \boldsymbol{\tau}|_{T_2}}{2}, \qquad [\![\boldsymbol{\tau}]\!] := \boldsymbol{\tau}|_{T_1}\cdot\boldsymbol{n}_1 + \boldsymbol{\tau}|_{T_2}\cdot\boldsymbol{n}_2. \tag{2.6}$$

For a boundary face $e \in \mathcal{E}_h \cap \partial\Omega$ of an element T_1 we simply define

$$\{v\} := v|_{T_1}, \qquad [\![v]\!] := v|_{T_1}\boldsymbol{n}_1, \qquad \{\boldsymbol{\tau}\} := \boldsymbol{\tau}|_{T_1}, \qquad [\![\boldsymbol{\tau}]\!] := \boldsymbol{\tau}|_{T_1}\cdot\boldsymbol{n}_1.$$

2.2.2 Interpolation operators

Definition 2.2.9. Given a finite element (K, P_K, Σ_K), let the set $\{\phi_i : 1 \leq i \leq n\} \subseteq P_K$ be the basis dual to Σ_K (i.e., $\psi_i(\phi_j) = \delta_{i,j}$). If v is a function for which all $\psi_i \in \Sigma_K$, $i = 1, ..., n$, are defined, then we define the *local interpolant* by

$$I_K v := \sum_{i=1}^{n} \psi_i(v)\phi_i.$$

Definition 2.2.10. Let $\Omega \subset \mathbb{R}^d$ be a polygonal domain with a triangulation $\mathcal{T}_h$. Assume each element in the triangulation is equipped with some type of shape function and nodal variables. Let m be the order of the highest derivative involved in the nodal variables. For $v \in C^m(\overline{\Omega})$, the *global interpolant* is defined by

$$I_h v|_K := I_K v, \quad \forall K \in \mathcal{T}_h.$$

Definition 2.2.11. (Lagrange interpolant) Let $\Omega \subset \mathbb{R}^d$ be a polygonal domain with a triangulation $\mathcal{T}_h$. Let K be a d-simplex and $P_K = \mathbb{P}^k$. Let $\Sigma_K = \{\psi_1, \psi_2 ..., \psi_{n_k}\}$ defined by $\psi_i(v) = v(a_i)$, for a_i Lagrange nodes of T, $i = 1, ..., n_k$. Let $\{\phi_1, \phi_2, \ldots, \phi_{n_k}\}$ be a basis of P_K dual to Σ_K. Then the *local Lagrange interpolant* is defined by

$$(I_T v)(x) := \sum_{i=1}^{n_k} \psi_i(v)\phi_i(x) = \sum_{i=1}^{n_k} v(a_i)\phi_i(x), \tag{2.7}$$

for a_i Lagrange node of T, $i = 1, ..., n_k$. Consequently, the *global Lagrange interpolation operator* $I_h : C(\overline{\Omega}) \to V_h^k$ is

$$(I_h v)|_T := I_T v, \quad \forall T \in \mathcal{T}_h, \tag{2.8}$$

where V_h^k is the finite-dimensional space of piecewise continuous polynomials of degree k on $\mathcal{T}_h$.

Lemma 2.2.1. *(Lagrange interpolant approximation) Let* $\{\mathcal{T}_h\}$ *be a shape regular family of triangulations of a polyhedral domain* $\Omega \subset \mathbb{R}^d$*. Let* l*,* m *and* $1 \leq p \leq \infty$ *such that, either* $m-l-n/p > 0$ *when* $p > 1$ *or* $m-l-n \geq 0$ *when* $p = 1$*. Then there exists a positive constant* C *depending on* m, p *and the shape regularity constant* γ_0 *in* (2.2) *such that, for* $0 \leq s \leq m$

$$\left(\sum_{T \in \mathcal{T}_h} \|v - I_h v\|^p_{W^{s,p}(T)} \right)^{1/p} \leq C h^{m-s} |v|_{W^{m,p}(\Omega)}, \tag{2.9}$$

for all $v \in W^{m,p}(\Omega)$*, where the left-hand side should be interpreted, in the case* $p = \infty$*, as* $\max_{T \in \mathcal{T}_h} \|v - I_h v\|_{W^s_\infty(T)}$.

Next, we introduce the Scott-Zhang interpolation operator. We follow the definition from [104].

Definition 2.2.12. (Scott-Zhang interpolation operator) Let $\Omega \subset \mathbb{R}^d$ be a connected, open, bounded, polygonal domain with a triangulation $\mathcal{T}_h$. Let $\{a_i\}_{i=1}^N$ be the set of all the Lagrange interpolation nodes of the triangulation $\mathcal{T}_h$ and $\{\phi_i\}_{i=1}^N$ be the corresponding nodal basis, i.e., $\phi_i(a_j) = \delta_{i,j}$, for $i, j = 1, \ldots, N$. We choose, for each Lagrange node a_i, either a d-simplex or a $(d-1)$-simplex, σ_i, according to the type of node, a_i, as follows.

- If a_i is an interior node of some d-simplex, $K \in \mathcal{T}_h$, we let $\sigma_i = K$.
- If a_i is an interior point of some face (which is a $(d-1)$-simplex), K', of a d-simplex, K, we let $\sigma_i = K'$.
- For the rest of the a_i, which must be on some $(d-2)$-simplex, there is a considerable freedom in picking σ_i. We may pick any $(d-1)$-simplex, K', such

that $a_i \in \overline{K'}$, subject only to the restriction $K' \in \partial\Omega$ if $a_i \in \partial\Omega$.

For face $(d-1)$-simplex, K', of K, there is a natural restriction of (K, P_K, Σ_K) that defines a finite element:

$$(K', P_{K'}, \Sigma_{K'}) = (K, P_K, \Sigma_K)|_{K'}.$$

Let's denote by $n_0(\sigma_i)$ the dimension of $\mathbb{P}^k(\mathbb{R}^{\dim \sigma_i})$. Let $a_{i,1} = a_i$, and let $\{a_{i,j}\}_{j=1}^{n_0}$ be the set of nodal points in σ_i. We introduce the $L^2(\sigma_i)$-dual basis $\{\psi_{i,j}\}_{j=1}^{n_0}$ of the nodal basis $\{\phi_{i,j}\}_{j=1}^{n_0}$:

$$\int_{\sigma_i} \psi_{i,j}(x)\phi_{i,\ell}(x)dx = \delta_{j,\ell}, \quad j, \ell = 1, \ldots, n_0.$$

Denote $\psi_i = \psi_{i,1}$. Therefore we have

$$\int_{\sigma_i} \psi_i(x)\phi_j(x)dx = \delta_{i,j}, \quad i, j = 1, \ldots, N.$$

The *Scott-Zhang interpolation operator* $I_h : W^{m,p}(\Omega) \to V_h^k$ is defined by

$$I_h v(x) := \sum_{i=1}^{n} \phi_i(x) \int_{\sigma_i} v(\xi)\psi_i(\xi)d\xi,$$

where $m \geq 1$ if $p = 1$ and $m > 1/p$ otherwise.

Lemma 2.2.2. *(Scott-Zhang interpolant approximation) Let $v \in W^{m,p}(\Omega)$, for m, p satisfying $m \geq 1$ if $p = 1$ and $m > 1/p$ otherwise. Let $\mathcal{T}_h$ be a shape regular triangulation of Ω and I_h be the Scott-Zhang interpolant defined in Definition 2.2.12. Then*

$$\left(\sum_{K \in \mathcal{T}_h} \|v - I_h v\|_{W^{s,p}(K)}^p \right)^{1/p} \leq C h^{m-s} \|v\|_{W^{m,p}(\Omega)}, \quad 0 \leq s \leq m \leq d+1.$$

2.3 Interface-triangulation interaction

In this section we introduce some basic notation regarding the interface-triangulation interaction. As it was mentioned in the introductory chapter, we are interested in finite element approximations of interface problems without restricting the triangulation to the interface, i.e. our discretization of the domain is not fitted with the interface.

2.3.1 Geometric considerations

We shall analyze interface problems with the following geometric setting: Consider a two dimensional, connected, open and bounded polygonal domain $\Omega \subset \mathbb{R}^2$ and an immersed and closed one dimensional interface Γ contained in Ω, such that Γ divides Ω into two open sub-domains Ω^+ and Ω^-, i.e. $\overline{\Omega} = \overline{\Omega^+} \cup \Gamma \cup \overline{\Omega^-}$ and $\Gamma = \overline{\Omega^+} \cap \overline{\Omega^-}$. We further assume that the interface Γ encloses either Ω^+ or Ω^-. The interface Γ is assumed to be smooth (C^2) admitting an arc-length parameterization $\boldsymbol{X}$.

In the following lemma we introduce the concept of r-tubular neighborhood of the interface Γ (see [44, 48]). We will be interested in the radius r of this neighborhood, and we will make a key assumption on the size of the finite element triangulation ($2h < r$). This assumption will alow us to establish rigourous analysis for the elements-interface interactions. The lemma presented below is a simplification to one dimensional curves of Proposition 1 in [44]. We include an adaptation of the proof in [44] for this case for completeness.

Proposition 2.3.1. *(Existence of r-tubular neighborhood) Let Γ be a regular, simple, and compact C^2 curve. For every $x \in \Gamma$ consider the line segment $N_x(r)$ of length $2r$*

centered at x and perpendicular to Γ at x. Define the tubular neighborhood of radius r of Γ by $Tub(r) = \cup_{x\in\Gamma} N_x(r)$. Then, there exists $r > 0$ such that for any two points $x_1, x_2 \in \Gamma$, $x_1 \neq x_2$, the line segments $N_{x_1}(r)$ and $N_{x_2}(r)$ are disjoint.

Proof. Let $x_0 \in \Gamma$, with $x_0 = \boldsymbol{X}(s_0)$. Consider map $F : [0, |\Gamma|) \times \mathbb{R} \to \mathbb{R}^2$

$$F(s;\tau) = \boldsymbol{X}(s) + \tau \boldsymbol{n}(s),$$

where $\boldsymbol{n} = (n_x, n_y)$ is the unit normal vector of $\boldsymbol{X}(s) = (x(s), y(s))$. Geometrically, F maps the point $(s;\tau)$, of the "rectangle" $[0, |\Gamma|)$, into the point of the normal line to Γ at a distance τ from $\boldsymbol{X}(s)$. The map F is clearly differential and its Jacobian at $\tau = 0$ is given by

$$\begin{vmatrix} \frac{\partial x}{\partial s} & \frac{\partial y}{\partial s} \\ n_x & n_y \end{vmatrix} = \|\boldsymbol{n}\|_2 \neq 0.$$

By the inverse function theorem, there exists a rectangle in $[0, |\Gamma|) \times \mathbb{R}$, say

$$s_0 - \delta < s < s_0 + \delta, \quad -\epsilon < \tau < \epsilon$$

restricted to which F is one to one. But this means that in the image Γ_{x_0} of F by the interval $s_0 - \delta < s < s_0 + \delta$, the segments of the normal lines with centers $x \in \Gamma_{x_0}$ and of length less than 2ϵ do not meet.

Now we proceed by a covering argument. By compactness is possible to choose a finite number of image set Γ_{x_0}, say $\Gamma_1, \ldots, \Gamma_k$ (corresponding to $\epsilon_1, \ldots, \epsilon_k$) such that $\cup_{i=1}^k \Gamma_i = \Gamma$. We shall show that the required r is given by

$$r = \min\{\epsilon_1, ..., \epsilon_k, \frac{\delta_L}{2}\},$$

where δ_L is the Lebesgue measure of the family $\{\Gamma_i\}$ (see Prop. 2.3.2). In fact, let two points $x_1, x_2 \in \Gamma$. If both belong to some Γ_i, $i = 1, ..., k$, the segments of the normal lines with center in x_1 and x_2 and length $2r$ do not meet, since $r < \epsilon_i$. If x_1 and x_2 do not belong to the same Γ_i, the $\text{dist}(x_1, x_2) \geq \delta_L$; were the segments of the normal lines, centered in x_1 and x_2 and of length $2r$, to meet at a point $x_3 \in \mathbb{R}^2$, we would have

$$2r \geq \text{dist}(x_1, x_3) + \text{dist}(x_3, x_2) \geq \text{dist}(x_1, x_2) \geq \delta_L,$$

which contradicts the definition of r. $\square$

The next proposition is a standard property of compact sets. See [44] 2-7 Property 3.

Proposition 2.3.2. *Let $\Gamma \subseteq \mathbb{R}^2$ be a compact set and $\{\Gamma_i\}$ a family of open sets of Γ such that $\bigcup \Gamma_i = \Gamma$. Then there exists a number $\delta > 0$ (the Lebesgue measure of the family $\{\Gamma_i\}$) such that whenever two points $x_1, x_2 \in \Gamma$ area at a distance* $\text{dist}(x_1, x_2) < \delta$ *then x_1 and x_2 belongs to some Γ_i.*

2.3.2 Interface-triangulation notation

Consider the two dimensional Ω, the interface Γ and the sub-domains Ω^- and Ω^+ as in the beginning of Section 2.3.1. let $\{\mathcal{T}_h\}_{0<h<1}$ be a family of triangulations of Ω. We remark that we are adopting the convention that elements T and element edges e are open sets. We use over-line symbol to refer to their closure. For each triangular element $T \in \mathcal{T}_h$, let h_T denotes its diameter and define the global parameter of the triangulation by $h = \max_T h_T$. Henceforth we will consider the following definitions:

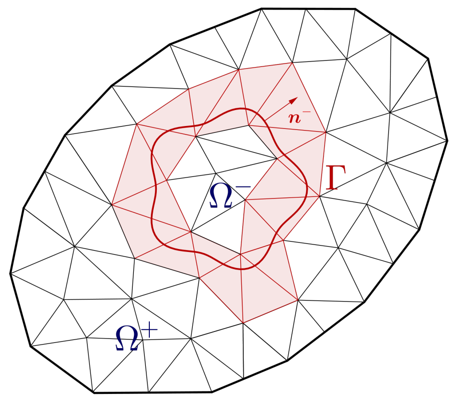

Figure 2.1: Illustration of the collection of elements intersecting the interface, $T \in \mathcal{T}_h^\Gamma$.

Definition 2.3.1. We define the following sets of elements subsets of $\mathcal{T}_h$:

$$\mathcal{T}_h^\pm := \{T \in \mathcal{T}_h : T^\pm \neq \emptyset\}, \quad T^\pm := T \cap \Omega^\pm. \tag{2.10}$$

We are naturally interested in the set of elements intersecting the interface, we denote it by

$$\mathcal{T}_h^\Gamma := \{T \in \mathcal{T}_h^- : \overline{T} \cap \Gamma \neq \emptyset\}. \tag{2.11}$$

For $T \in \mathcal{T}_h^\Gamma$ we denote the interface segment contained in T by

$$T_\Gamma := \overline{T} \cap \Gamma. \tag{2.12}$$

Moreover, considering the patch of elements ω_T of $T \in \mathcal{T}_h$, we define the restriction of ω_T to $\Omega^\pm$, and the interface segment intersection of ω_T with Γ by

$$\omega_T^\pm := \omega_T \cap \Omega^\pm, \quad \omega_T^\Gamma := \omega_T \cap \Gamma. \tag{2.13}$$

Remark 2.5. Observe that the definition of $\mathcal{T}_h^\Gamma$ guarantees that the union of curve segments T_Γ conforms the interface Γ, i.e. $\sum_{T\in\mathcal{T}_h^\Gamma} |T_\Gamma| = |\Gamma|$.

2.3.3 Assumptions on the triangulation

From now on we will work under the following assumptions.

Assumption 2.1. *Given Lemma 2.3.1 we make the following assumptions on the triangulation:*

1. *We assume that the triangulation is shape-regular.*
2. *We assume that the mesh size $h < r/2$, where r is the radius of the tubular neighborhood of Γ.*
3. *If the interface passes through the interior of an element, then it intersects the boundary of the element at most twice and at different edges.*

We make use of these assumptions to prove technical lemmas (see Lemmas 4.3.1, 4.3.6, A.1.4).

Remark 2.6. In general, the numerical methods presented in this dissertation will render optimal convergence of the errors under the Assumption 1 on the triangulation. However, we will use the more restrictive quasi-uniformity assumption, for some technical proofs, as for example, the error estimates in the max-norms in Chapter 3.

Remark 2.7. Assumption 2 restricts the size of the mesh by the geometric parameter r, radius of the tubular neighborhood of the interface Γ defined in Proposition 2.3.1. It is well known that $r \leq 1/\kappa$, where $\kappa := \|\boldsymbol{X}''\|_{L^\infty}$ assumed to be bounded since Γ is a C^2 curve, and hence by our assumption $h < 1/(2\kappa)$. The radius r also bounds from below how close the curve Γ comes from self-intersecting (e.g. consider a dumbbell with a thin middle section). Avoiding cases where, for example, the interface separates an element into three regions.

Remark 2.8. Assumption 3 is only considered for the sake of simplicity of the presentation. For instance, when an edge e is considered we will define its restriction to Ω^+ and Ω^-. Assuming that the interface does not intersect the edge twice we can uniquely define the two connected pieces e^+ and e^-. However, the methods that we will propose in this dissertation apply without this restriction.

2.4 Theoretical results on interface problems

In this section we establish some theoretical extension and regularity results of the solution of model interface problem (1.4) with homogeneous jump conditions, i.e. we consider

$$-\nabla \cdot \left(\rho^{\pm} \nabla u^{\pm}\right) = f \qquad \text{in } \Omega^{\pm}, \tag{2.14a}$$

$$u = 0 \qquad \text{on } \partial\Omega, \tag{2.14b}$$

$$[u] = 0 \qquad \text{on } \Gamma. \tag{2.14c}$$

$$[\rho \nabla u \cdot \boldsymbol{n}] = 0 \qquad \text{on } \Gamma. \tag{2.14d}$$

2.4.1 Regularity results for Poisson interface problem

A solution u of the elliptic interface problem (2.14) is, in general, only in $H_0^1(\Omega)$, instead of $H^2(\Omega)$. However, it is well known [6, 36, 73, 74] that under an assumption on the smoothness of Γ (namely C^2 curve), the restrictions of the solution to Ω^- and Ω^+ enjoy H^2 regularity, i.e. $u^- \in H^2(\Omega^-)$ and $u^+ \in H^2(\Omega^+)$. This implies the following estimate

$$\|u\|_{H^2(\Omega^-)} + \|u\|_{H^2(\Omega^+)} \leq C\|f\|_{L^2(\Omega)}.$$

Since we shall be interested in high contrast problem ($\rho^+/\rho^- \gg 1$) we need to specify the dependence of constant $C > 0$ above in terms of the coefficients ρ^- and ρ^+. A result that states this dependence can be found in [71]. At this point we recall that we are assuming that $0 < \rho^- \leq \rho^+$.

Lemma 2.4.1. *(Corollary 2.1 [71]) Assume that $\Gamma \cap \partial\Omega = \emptyset$. Then, a solution u of* (2.14)*, with $u^- \in H^2(\Omega^-)$ and $u^+ \in H^2(\Omega^+)$, satisfies:*

- *If $\partial\Omega^- = \Gamma$ (i.e. Ω^- is the inclusion), it holds*

$$\rho^- \|u\|_{H^2(\Omega^-)} \leq C\|f\|_{L^2(\Omega)}, \quad \rho^+ \|u\|_{H^2(\Omega^+)} \leq C\|f\|_{L^2(\Omega)}, \tag{2.15}$$

- *If $\partial\Omega^+ = \Gamma$ (i.e. Ω^+ is the inclusion), it holds*

$$\rho^+ \|u\|_{H^2(\Omega^+)} \leq C\left(\frac{\rho^+}{\rho^-}\right)\|f\|_{L^2(\Omega)}, \quad \rho^- \|u\|_{H^2(\Omega^-)} \leq C\|f\|_{L^2(\Omega)}, \tag{2.16}$$

for constant $C > 0$ independent of ρ^- and ρ^+.

Remark 2.9. Corollary 2.1 [71] is stated for problem (2.14) with non-homogeneous jump of the flux, i.e. $[\nabla u \cdot \boldsymbol{n}] = \beta$ with $\beta \in H^{1/2}(\Gamma)$. We consider homogeneous jumps for simplicity.

In addition, in order to state the error estimates of the numerical methods in terms of the data, we need some regularity results on semi-norms weighted with $\sqrt{\rho^{\pm}}$. We begin with an energy result direct consequence of the variational formulation of problem (2.14).

Proposition 2.4.1. *Let u solve* (2.14)*, then the following energy estimate holds*

$$\sqrt{\rho^+}\|\nabla u\|_{L^2(\Omega^+)} + \sqrt{\rho^-}\|\nabla u\|_{L^2(\Omega^-)} \leq \frac{C}{\sqrt{\rho^-}}\|f\|_{L^2(\Omega)}, \tag{2.17}$$

where $C > 0$ is a constant independent of ρ^- and ρ^+.

Proof. Consider variational formulation of problem (2.14), for $v \in H_0^1(\Omega)$

$$\int_{\Omega^-} \rho^- \nabla u \cdot \nabla v + \int_{\Omega^+} \rho^- \nabla u \cdot \nabla v = \int_{\Omega} f v, \tag{2.18}$$

implies that

$$\|\sqrt{\rho^-}\nabla u\|^2_{L^2(\Omega^-)} + \|\sqrt{\rho^+}\nabla u\|^2_{L^2(\Omega^+)} \leq \|f\|_{L^2(\Omega)}\|u\|_{L^2(\Omega)}.$$

By Poincare's inequality on Ω (see Prop. 5.3.5 in [27]) and $\rho^- \leq \rho^+$ it follows that

$$\sqrt{\rho^-}\|u\|_{L^2(\Omega)} \leq C_\Omega \left(\|\sqrt{\rho^-}\nabla u\|_{L^2(\Omega^-)} + \|\sqrt{\rho^+}\nabla u\|_{L^2(\Omega^+)}\right).$$

Hence, using last two inequalities we obtain the result. □

A better energy estimate, in terms of the independence of the constant with respect to the characteristic coefficients, weighted with $\rho^\pm$ holds as we proved in next proposition.

Proposition 2.4.2. *Let u solve (2.14), then the following energy estimate holds*

$$\rho^+\|\nabla u\|_{L^2(\Omega^+)} + \rho^-\|\nabla u\|_{L^2(\Omega^-)} \leq C\|f\|_{L^2(\Omega)}, \tag{2.19}$$

where $C > 0$ is a constant independent of ρ^- and ρ^+.

Proof. We prove this estimate in the case that Ω^+ is the inclusion (i.e. $\partial\Omega^+ = \Gamma$ does not intersect $\partial\Omega$). The proof of the other case is similar. First, from the previous proposition we have

$$\rho^- \|\nabla u\|_{L^2(\Omega^-)} \leq C\|f\|_{L^2(\Omega)}. \tag{2.20}$$

Let $w = u^+ - \frac{1}{|\Omega^+|}\int_{\Omega^+} u^+ dx$. Therefore, using Poincare's inequality (see equation 5.3.1 and Prop. 5.3.5 in [27]) we have

$$\|w\|_{L^2(\Omega^+)} \leq C\|\nabla u\|_{L^2(\Omega^+)}. \tag{2.21}$$

By means of an extension result (see Lemma 6.37 in [55]), there exists $v \in H_0^1(\Omega)$ such that $v|_{\Omega^+} = w|_{\Omega^+}$ and

$$\|v\|_{H^1(\Omega)} \leq C\|w\|_{H^1(\Omega^+)}. \tag{2.22}$$

Applying the variational formulation of problem (2.14) we have that

$$\int_{\Omega^-} \rho^- \nabla u \cdot \nabla v + \int_{\Omega^+} \rho^+ \nabla u \cdot \nabla v = \int_\Omega fv.$$

Multiplying last equation by ρ^+, it follows that

$$\|\rho^+ \nabla u\|^2_{L^2(\Omega^+)} = \rho^+ \int_{\Omega^+} \rho^+ \nabla u \cdot \nabla v = \rho^+ \int_\Omega fv - \rho^+ \int_{\Omega^-} \rho^- \nabla u \cdot \nabla v.$$

Therefore, we have

$$\|\rho^+ \nabla u\|^2_{L^2(\Omega^+)} \leq \|f\|_{L^2(\Omega)} \|\rho^+ v\|_{L^2(\Omega)} + \|\rho^- \nabla u\|_{L^2(\Omega^-)} \|\rho^+ \nabla v\|_{L^2(\Omega)}.$$

By (2.22) we have

$$\|\rho^+ \nabla u\|^2_{L^2(\Omega^+)} \leq C(\|f\|_{L^2(\Omega)} + \|\rho^- \nabla u\|_{L^2(\Omega^-)})\rho^+ \|w\|_{H^1(\Omega^+)}.$$

Hence, using (2.21) we get

$$\|\rho^+\nabla u\|^2_{L^2(\Omega^+)} \leq C(\|f\|_{L^2(\Omega)} + \|\rho^-\nabla u\|_{L^2(\Omega^-)})\|\rho^+\nabla u\|_{L^2(\Omega^+)}.$$

The proof is complete after applying (2.20). □

We will also need to state H^2 (semi-norm) regularity estimates which can essentially be proved if one combines results in [38] and [71]. Here we give an alternative argument using the results in [71] and classical regularity theory.

Proposition 2.4.3. *In addition to the assumptions already made on Ω and Γ, assume further that Ω is convex. Let u solve* (2.14)*. Then, the following regularity estimate holds*

$$\rho^+\|D^2u\|_{L^2(\Omega^+)} + \rho^-\|D^2u\|_{L^2(\Omega^-)} \ \leq \ C_{reg}\,\|f\|_{L^2(\Omega)}, \tag{2.23}$$

where C is independent of $\rho^\pm$.

The constant C_{reg} could depend on the geometry of the sub-domains $\Omega^\pm$.

Proof. We first assume that Ω^- is the inclusion (i.e. $\partial\Omega^- \cap \partial\Omega = \emptyset$). In this case, the result (2.23) follows directly from Lemma 2.4.1, estimate (2.15).

Now, assume that Ω^+ is the inclusion. From estimate (2.16) in Lemma 2.4.1 we have

$$\rho^-\|u\|_{H^2(\Omega^-)} \leq C\,\|f\|_{L^2(\Omega)}. \tag{2.24}$$

Let $\overline{u^+} = \frac{1}{|\Omega^+|}\int_{\Omega^+} u^+ dx$. Let $w = u^+ - \overline{u^+}$. Note that w satisfies

$$
\begin{aligned}
-\rho^+\Delta w &= f && \text{in } \Omega^+,\\
\rho^+\nabla w\cdot \boldsymbol{n} &= \rho^+\nabla u^+\cdot\boldsymbol{n} && \text{on } \partial\Omega^+.
\end{aligned}
$$

From a standard regularity result (see (2.3.3.1) in [60]) we have

$$\rho^+\|w\|_{H^2(\Omega^+)} \le C(\|f\|_{L^2(\Omega^+)} + \|\rho^+\nabla u^+\cdot\boldsymbol{n}\|_{H^{1/2}(\partial\Omega^+)} + \rho^+\|w\|_{H^1(\Omega^+)}).$$

Using the jump condition we have

$$\|\rho^+\nabla u^+\cdot\boldsymbol{n}\|_{H^{1/2}(\partial\Omega^+)} = \|\rho^-\nabla u^-\cdot\boldsymbol{n}\|_{H^{1/2}(\partial\Omega^+)}.$$

By a standard trace inequality we have

$$\|\rho^-\nabla u^-\cdot\boldsymbol{n}\|_{H^{1/2}(\partial\Omega^+)} \le \rho^-\|u^-\|_{H^2(\Omega^-)}.$$

Which by (2.24) gives

$$\|\rho^+\nabla u^+\cdot\boldsymbol{n}\|_{H^{1/2}(\partial\Omega^+)} \le C\,\|f\|_{L^2(\Omega)}.$$

Note that the estimate

$$\rho^+\|w\|_{H^1(\Omega^+)} \le C\|f\|_{L^2(\Omega)}$$

follows from Poincare's inequality and Proposition 2.4.2. Hence, we have

$$\rho^+\|w\|_{H^2(\Omega^+)} \le C\,\|f\|_{L^2(\Omega)}.$$

The result now follows after noting that $\|D^2u\|_{L^2(\Omega^+)} \le \|w\|_{H^2(\Omega^+)}$. $\square$

Remark 2.10. Note that, although the constant C in Lemma 2.4.3 (also 2.4.2) does not depend on the coefficients it could depend on the geometry of the sub-domains Ω^- and Ω^+.

2.4.2 Extensions results

Proposition 2.4.4. *(H^2 Extension) Consider $u^\pm \in H^2(\Omega^\pm)$ (with $u^\pm \equiv 0$ on $\partial\Omega^\pm \cap \partial\Omega$). Then, there exists a constant C and extensions $u_E^\pm \in H^2(\Omega)$ with the following properties*

$$u_E^\pm(x) = u^\pm(x) \qquad x \in \Omega^\pm, \tag{2.25}$$

$$\|Du_E^\pm\|_{L^2(\Omega)} + \|D^2 u_E^\pm\|_{L^2(\Omega)} \le C(\|Du^\pm\|_{L^2(\Omega^\pm)} + \|D^2 u^\pm\|_{L^2(\Omega^\pm)}). \tag{2.26}$$

Remark 2.11. This result follows from Theorem 7.25 in [55] (see also [51]) and applying Poincare's inequalities. Considering that we will only require the extensions $u_E^\pm$ to be defined on patches of elements on $\mathcal{T}_h^\Gamma$, in fact, we only need the following more *local* bound which could lead to a better geometric constant:

$$\|Du_E^\pm\|_{L^2(\Omega_E^\pm)} + \|D^2 u_E^\pm\|_{L^2(\Omega_E^\pm)} \le C_E(\|Du^\pm\|_{L^2(\Omega^\pm)} + \|D^2 u^\pm\|_{L^2(\Omega^\pm)}). \tag{2.27}$$

where $\Omega_E^\pm = \Omega^\pm \bigcup Tub(2h)$ are the local extension sets. For the sake of simplicity, we do not prove here how C_E depends on the geometric constants (e.g. κ and r).

Chapter Three

High order finite element method for interface problems in homogeneous media

3.1 Finite element methods for Poisson interface problem

In this chapter we analyze finite element methods for Poisson and Stokes problems in two dimensions with a one dimensional interface immersed in the domain, using triangulations that are non-fitted with the interface. The main goal of this chapter is to provide high order finite element methods approximating the respective interface problems.

3.1.1 Poisson interface problems

Let $\Omega \subset \mathbb{R}^2$ be a connected, open, bounded, polygonal domain with an immersed, smooth, and closed interface Γ such that $\overline{\Omega} = \overline{\Omega^-} \cup \overline{\Omega^+}$ and Γ encloses either Ω^- or Ω^+. Consider the problem

$$-\Delta u^\pm = f^\pm \qquad \text{in } \Omega^\pm, \tag{3.1a}$$

$$u = 0 \qquad \text{on } \partial\Omega, \tag{3.1b}$$

$$[u] = 0 \qquad \text{on } \Gamma, \tag{3.1c}$$

$$[\nabla u \cdot \boldsymbol{n}] = \beta \qquad \text{on } \Gamma, \tag{3.1d}$$

where we denote by $u^\pm \equiv u|_{\Omega^\pm}$, $\boldsymbol{n}^\pm$ is the unit outward pointing normal to $\Omega^\pm$, and the jumps across the interface Γ are defined as before, i.e.

$$[u] = u^+ - u^-, \quad [\nabla u \cdot \boldsymbol{n}] = \nabla u^- \cdot \boldsymbol{n}^- + \nabla u^+ \cdot \boldsymbol{n}^+.$$

In order to derive higher order finite element method for problem (3.1), higher order derivatives of u will be needed. With this aim we introduce the standard differential operator D and derivatives of order $k \in \mathbb{N}$

$$D^k u(x,y) := \left\{ D^{\boldsymbol{\alpha}} u := \frac{\partial^{|\boldsymbol{\alpha}|} u(x,y)}{\partial x^{\alpha_1} \partial y^{\alpha_2}} : \boldsymbol{\alpha} = (\alpha_1, \alpha_2),\ |\boldsymbol{\alpha}| = k \right\}.$$

For a vector $\boldsymbol{\nu}$ we denote the k-th order directional derivative

$$D^k_{\boldsymbol{\nu}} u(x) := \frac{\partial^k u(x)}{\partial^k \boldsymbol{\nu}}.$$

We now show how to derive the jumps of high order derivatives of u across Γ from the data, β and f. Similar ideas were used in [77, 87, 14].

Higher order derivatives jumps

Fix a point $x \in \Gamma$. Let $\boldsymbol{n}$ be the normal vector to Γ at x, and $\boldsymbol{t}$ the tangent vector to Γ at x. We clearly have $[(\nabla u \cdot \boldsymbol{n})(x)] = [D_{\boldsymbol{n}} u(x)] = \beta(x)$ and, thanks to (3.1c), we have that $[(\nabla u \cdot \boldsymbol{t})(x)] = [D_{\boldsymbol{t}} u(x)] = 0$. In fact, we also have the jump of higher tangential derivatives are zero, i.e. $\left[D^\ell_{\boldsymbol{t}} u(x)\right] = 0$ for any ℓ. Note that from the Poisson's equation (3.1a), we have

$$-D^2_{\boldsymbol{n}} u - D^2_{\boldsymbol{t}} u = f \quad \text{in } \Omega^\pm, \tag{3.2}$$

which implies that $[D^2_{\boldsymbol{n}} u(x)] = [f(x)]$. Moreover, we note that

$$[D_{\boldsymbol{t}} D_{\boldsymbol{n}} u(\,x)] = D_{\boldsymbol{t}} \left[D_{\boldsymbol{n}} u(x)\right] = D_{\boldsymbol{t}} \beta(x) \quad x \in \Gamma.$$

Now we proceed by induction. Suppose we have all jumps of the derivatives of order $\ell - 1$ in terms of β and f. Then, we will show how to get the jumps of derivatives of order ℓ. Let $i + j = \ell$. If $i \geq 1$ then

$$\left[D_{\boldsymbol{t}}^i D_{\boldsymbol{n}}^j u(x)\right] = D_{\boldsymbol{t}}\left[D_{\boldsymbol{t}}^{i-1} D_{\boldsymbol{n}}^j u(x)\right].$$

Otherwise, using Poisson's equation (3.2) in terms of the normal and tangential derivatives we have

$$\left[D_{\boldsymbol{n}}^{\ell} u(x)\right] = -\left[D_{\boldsymbol{n}}^{\ell-2} f(x)\right] - D_{\boldsymbol{t}}\left[D_{\boldsymbol{t}} D_{\boldsymbol{n}}^{\ell-2} u(x)\right].$$

Suppose that we would like the jump of u in a different direction, say $\boldsymbol{\eta}$. Then, we write $\boldsymbol{\eta} = a\boldsymbol{n} + b\boldsymbol{t}$, where $a = \boldsymbol{\eta} \cdot \boldsymbol{n}$ and $b = \boldsymbol{\eta} \cdot \boldsymbol{t}$, obtaining

$$\left[D_{\boldsymbol{\eta}}^{\ell} u(x)\right] = \sum_{j=0}^{\ell} \binom{l}{j} a^j b^{\ell-j} \left[D_{\boldsymbol{n}}^j D_{\boldsymbol{t}}^{\ell-j} u(x)\right]. \tag{3.3}$$

3.1.2 Higher order finite element methods

Let $\mathcal{T}_h$, $0 < h < 1$ be a sequence of triangulations of Ω (see Section 2.2), assumed to be shape-regular. Let h_T denote the diameter of the element $T \in \mathcal{T}_h$ and $h = \max_T h_T$. Consider Assumptions 1, 2 and 3. Let V_h^k be the finite element subspace of continuous piecewise polynomials of degree k, vanishing at $\partial\Omega$, i.e.

$$V_h^k := \{v \in C(\overline{\Omega}) \cap H_0^1(\Omega) \,:\, v|_T \in \mathbb{P}^k(T), \quad \forall T \in \mathcal{T}_h\}.$$

Let $T \in \mathcal{T}_h$ and define the local space $S^k(T)$, consisting of piecewise polynomials of degree k in T^+ and T^-, i.e.,

$$S^k(T) := \left\{ w \in L^2(T) : w|_{T^\pm} \in \mathbb{P}^k(T^\pm) \right\}. \tag{3.4}$$

Next, we define the Lagrange interpolation operator (see Definition 2.2.11) from the space of functions not necessarily continuous across the interface Γ onto the subspace V_h^k.

Definition 3.1.1. Given $v \in L^2(\Omega)$ with $v^- = v|_{\Omega^-} \in C(\overline{\Omega^-})$ and $v^+ = v|_{\Omega^+} \in C(\overline{\Omega^+})$, we define locally $I_h v \in V_h^k$ such that:

- if $T \in \mathcal{T}_h^\Gamma$, then nodal values of $(I_h v)$ are determined by

$$(I_h v)|_T(a_i) \;=\; \begin{cases} v^-(a_i), & \text{if } a_i \in \overline{\Omega^-}; \\ v^+(a_i), & \text{if } a_i \in \Omega^+, \end{cases} \tag{3.5}$$

  for all $a_i \in T$, $i = 1, \dots, n_{2,k}$, with $n_{2,k} = \dim(\mathbb{P}^k(T)) = (k+1)(k+2)/2$, the degree k Lagrange nodes of T;

- if $T \in \mathcal{T}_h \backslash \mathcal{T}_h^\Gamma$, then $(I_h v)|_T$ is imply the local Lagrange interpolant on T.

Remark 3.1. Note that if v is continuous $I_h v$ is simply the Lagrange interpolant of v. However, if v is discontinuous then $I_h v$ interpolates values of v on Lagrange points not intersecting Γ and for Lagrange points lying on Γ it takes the values of v coming from Ω^- (this is without loss of generality).

In terms of approximation, observe that for a function v with $v^\pm = v|_{\Omega^\pm} \in C(\overline{\Omega^\pm})$ the interpolant defined in Definition 3.1.1 has the same local approximation properties than the Lagrange interpolant defined in 2.2.11 on elements $T \in \mathcal{T}_h \backslash \mathcal{T}_h^\Gamma$, whilst for elements $T \in \mathcal{T}_h^\Gamma$ the local interpolant does not have optimal approximation properties. However, on the latter case we still have its stability. The following lemma states this result.

Lemma 3.1.1. *Let $v \in L^2(\Omega)$ with $v^\pm \in C(\overline{\Omega^\pm})$ and I_h the Lagrange interpolant defined above. Then, there exists a positive constant C such that*

$$\|I_h v\|_{L^\infty(T)} \leq C\|v\|_{L^\infty(T)}, \quad \forall T \in \mathcal{T}_h. \tag{3.6}$$

Remark 3.2. In order to prove L^2 based error estimates, shape regularity of the triangulation suffices. However, as is well known, some form of quasi-uniformity of the mesh is needed to prove max-norm estimates, even if there is no interface [43]. Since we will prove max-norm estimates of our method, and in order to avoid unnecessary details, we will assume that the meshes are quasi-uniform (see Definition 2.2.6).

The proposed finite element method

We now present our finite element method approximating the Poisson interface problem (3.1). Find $u_h \in V_h^k$, such that

$$\int_\Omega \nabla u_h \cdot \nabla v = \int_\Omega fv + \int_\Gamma \beta v - \sum_{T \in \mathcal{T}_h^\Gamma} \left(\int_{T^-} \nabla w_T^u \cdot \nabla v + \int_{T^+} \nabla w_T^u \cdot \nabla v \right) \tag{3.7}$$

for all $v \in V_h^k$, where w_T^u is a correction function to be defined in Section 3.1.2. Note the terms not involving the correction function are the standard variational formulation of problem (3.1) and they are separated in T^- and T^+ anticipating that w_T^u is discontinuous across the interface. We also remark that the left-hand side of the equations is the standard stiffness matrix for the Poisson problem.

The correction function

We now show how to construct the piecewise polynomial function $w_T^u \in S^k(T)$ that will help to correct the right-hand side of the natural finite element method ((3.7) without the correction term), in order to obtain a higher order approximation. First, we develop some notation. For each $T \in \mathcal{T}_h^\Gamma$ let y_T and z_T be the two endpoints of $T \cap \Gamma$, see Figure 3.1. Let L_T denote the line segment connecting y_T and z_T. Let $\boldsymbol{\eta}$ be the unit vector perpendicular to L_T and pointing outward T^-. Let also $\boldsymbol{\tau}$ be the unit vector parallel to the line L_T such that $\boldsymbol{\tau}$ is the clockwise rotation of $\boldsymbol{\eta}$ by ninety degrees.

For each $\ell = 0, 1, \ldots, k$, let $\{\bar{x}_i^{\ell,T}\}_{i=0}^{\ell}$ denote the Gauss points of the segment L_T. For each $\bar{x}_i^{\ell,T}$, let $Q_i^{\ell,T}$ be the line perpendicular to the line segment L_T that passes through the points $\bar{x}_i^{\ell,T}$. We then define $x_i^{\ell,T} = Q_i^{\ell,T} \cap \Gamma$, for $i = 0, \ldots, \ell$. Observe that the definition of the points $x_i^{\ell,T}$, for $i = 0, \ldots, \ell$, on the interface Γ is unique thanks to Assumption 2. Note here that the choice of Gauss points is a preference of the authors, related to the quadrature rules, but not essential in the proofs. We could also use, for instance, equally spaced points.

The correction functions w_T^u will be defined, for $T \in \mathcal{T}_h^\Gamma$, to be discontinuous across elements and satisfying jump conditions derived from (3.1c) and (3.1d) at points on T_Γ. Given a function u, with $u^- \in C(\overline{\Omega^-})$ and $u^+ \in C(\overline{\Omega^+})$, we define the *correction function* w_T^u to be the unique function in $S^k(T)$ (see Lemma 3.1.3) that

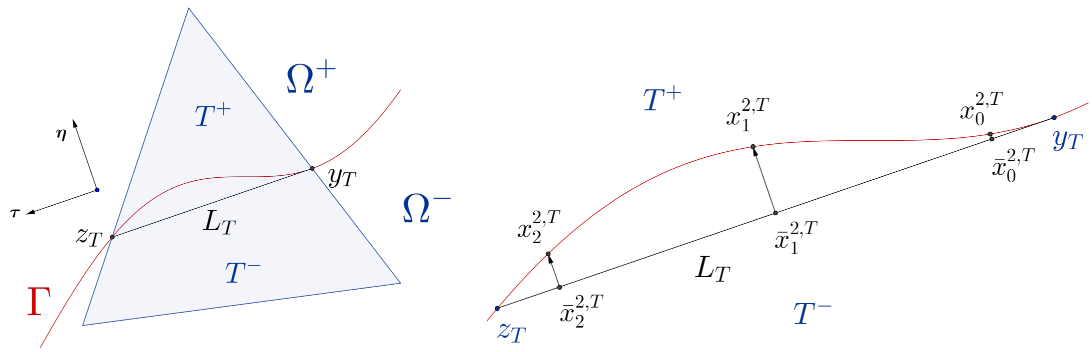

Figure 3.1: Illustration of notation on $T \in \mathcal{T}_h^\Gamma$. Left figure: T^+, T^-, vectors $\boldsymbol{\eta}$ and $\boldsymbol{\tau}$, line segment L_T and its extreme points y_T and z_T. Right figure: zoom in the region of T near the interface showing the Gaussian points $\bar{x}_i^{2,T}$ and their perpendicular projection onto Γ $x_i^{2,T}$, for $i = 0, 1, 2$.

satisfies

$$\left[D_{\boldsymbol{\eta}}^{k-\ell} w_u^T(x_i^{\ell,T})\right] = \left[D_{\boldsymbol{\eta}}^{k-\ell} u(x_i^{\ell,T})\right] \quad \text{for } 0 \le i \le \ell \text{ and } 0 \le \ell \le k, \tag{3.8}$$

$$\begin{cases} (w_T^u)^-(a_i) = 0, & \text{if } a_i \in \Omega^- \cup \Gamma; \\ (w_T^u)^+(a_i) = 0, & \text{if } a_i \in \Omega^+. \end{cases} \quad \text{for all } a_i \in T,\ i = 1, \ldots n_{2,k}, \tag{3.9}$$

where a_i are the degree k Lagrange nodes of T (see Definition 2.2.4) and $n_{2,k} = \dim(\mathbb{P}^k(T)) = (k+1)(k+2)/2$. We would like to stress that if u is the solution to (3.1) then we can derive all the jumps of u in terms of the data β and f so we can construct w_T^u a priori. It is important to notice that we impose directional derivatives jump conditions in the $\boldsymbol{\eta}$-direction (a fix direction for each $T \in \mathcal{T}_h^\Gamma$) rather than in the $\boldsymbol{n}$-direction. However, as it was shown in (3.3), we can easily transform the jump data described in $\boldsymbol{n}$-direction to jump data in the $\boldsymbol{\eta}$-direction. A reason for this choice is because we can show unisolvence, when Γ is curved, for any polynomial of degree k. Additionally, the construction of the correction functions can be made explicitly, that is, it does not require solving any local linear system. Such construction permits us to develop not only an elegant analysis for any polynomial degree k but also an analysis without imposing strong condition on how Γ intersects an element T (how small are the measures of T^- or T^+) in order to control the ill conditioning of this matrix.

Local approximation of the correction function

In this section we prove optimal local approximation of the interpolant (Definition 3.1.1) plus the correction function. We first introduce some crucial lemmas related to approximation on the space $S^k(T)$.

Lemma 3.1.2. *Let $T \in \mathcal{T}_h^\Gamma$ and define $r_T = |L_T|$. For any $v \in \mathbb{P}^k(T)$, we have*

$$h_T^j \|D^j v\|_{L^\infty(T)} \leq C\, h_T^k \sum_{\ell=0}^{k} \frac{1}{r_T^\ell} \max_{0\leq i\leq \ell} |D_{\boldsymbol{\eta}}^{k-\ell} v(x_i^{\ell,T})|, \quad j = 0, 1,$$

where the constant C depends only on the polynomial degree k.

Proof. Let L_T^E be the segment with length $|L_T^E| = 2h_T$, centered at $(y_T + z_T)/2$ and aligned with L_T. The size of L_T^E guarantees that any point $x \in T$ can be projected orthogonally on L_T^E. Then, using Taylor's expansion on T from L_T^E, we can easily show that

$$h_T^j \|D^j v\|_{L^\infty(T)} \leq C \sum_{\ell=0}^{k} h_T^{k-\ell} \|D_{\boldsymbol{\eta}}^{k-\ell} v\|_{L^\infty(L_T^E)}, \quad j = 0, 1.$$

Using Taylor's theorem on L_T^E from a point of L_T we get

$$\|D_{\boldsymbol{\eta}}^{k-\ell} v\|_{L^\infty(L_T^E)} \leq C \sum_{s=0}^{\ell} h_T^s \|D_{\boldsymbol{\tau}}^s D_{\boldsymbol{\eta}}^{k-\ell} v\|_{L^\infty(L_T)}.$$

The inverse inequality gives

$$\|D_{\boldsymbol{\tau}}^s D_{\boldsymbol{\eta}}^{k-\ell} v\|_{L^\infty(L_T)} \leq \frac{C}{r_T^s} \|D_{\boldsymbol{\eta}}^{k-\ell} v\|_{L^\infty(L_T)}.$$

We therefore have

$$\begin{aligned}
h_T^j \|D^j v\|_{L^\infty(T)} &\le C h_T^k \sum_{\ell=0}^{k} h_T^{-\ell} \sum_{s=0}^{\ell} \frac{h_T^s}{r_T^s} \|D_{\boldsymbol{\eta}}^{k-\ell} v\|_{L^\infty(L_T)} \\
&= C h_T^k \sum_{\ell=0}^{k} \sum_{s=0}^{\ell} \frac{1}{h_T^{\ell-s}} \frac{1}{r_T^s} \|D_{\boldsymbol{\eta}}^{k-\ell} v\|_{L^\infty(L_T)} \\
&\le C h_T^k \sum_{\ell=0}^{k} \sum_{s=0}^{\ell} \frac{1}{r_T^{\ell-s}} \frac{1}{r_T^s} \|D_{\boldsymbol{\eta}}^{k-\ell} v\|_{L^\infty(L_T)} \\
&= C\, h_T^k \sum_{\ell=0}^{k} \frac{1}{r_T^\ell} \|D_{\boldsymbol{\eta}}^{k-\ell} v\|_{L^\infty(L_T)},
\end{aligned}$$

where we used that $r_T \le h_T$. In order to bound the right-hand side above, we use induction on ℓ. First, using that $D_{\boldsymbol{\eta}}^k v$ is a constant we have

$$\|D_{\boldsymbol{\eta}}^k v\|_{L^\infty(L_T)} = |D_{\boldsymbol{\eta}}^k v(x_0^{0,T})|.$$

Assume that we have proved

$$\sum_{\ell=m+1}^{k} \frac{1}{r_T^\ell} \|D_{\boldsymbol{\eta}}^{k-\ell} v\|_{L^\infty(L_T)} \le C \sum_{\ell=m+1}^{k} \frac{1}{r_T^\ell} \max_{0\le i\le \ell} |D_{\boldsymbol{\eta}}^{k-\ell} v(x_i^{\ell,T})|, \tag{3.10}$$

then we want to prove that

$$\sum_{\ell=m}^{k} \frac{1}{r_T^\ell} \|D_{\boldsymbol{\eta}}^{k-\ell} v\|_{L^\infty(L_T)} \le C \sum_{\ell=m}^{k} \frac{1}{r_T^\ell} \max_{0\le i\le \ell} |D_{\boldsymbol{\eta}}^{k-\ell} v(x_i^{\ell,T})|. \tag{3.11}$$

Since $D_{\boldsymbol{\eta}}^{k-m} v$ is a polynomial of degree m, we have that

$$\|D_{\boldsymbol{\eta}}^{k-m} v\|_{L^\infty(L_T)} \le C \max_{0\le i\le m} |D_{\boldsymbol{\eta}}^{k-m} v(\bar{x}_i^{m,T})|.$$

Using Taylor's theorem we have

$$|D_{\boldsymbol{\eta}}^{k-m} v(\bar{x}_i^{m,T})| \leq |D_{\boldsymbol{\eta}}^{k-m} v(x_i^{m,T})| + \sum_{\ell=m+1}^{k} d^{\ell-m} \|D_{\boldsymbol{\eta}}^{k-\ell} v\|_{L^\infty(L_T)},$$

where $d = \max_{0 \leq i \leq \ell \leq k} |x_i^{\ell,T} - \bar{x}_i^{\ell,T}|$. Using Taylor expansion we could prove that $d \leq C r_T^2$, with a constant C depending on the second derivative of the parametrization of the curve Γ with respect to L_T. Instead we use the estimate $d \leq r_T/2$ resulting from the r-tubular neighborhood Assumption 2, $h < r/2$, see Lemma A.1.2. Hence, we have

$$\begin{aligned} \frac{1}{r_T^m} \max_{0 \leq i \leq m} |D_{\boldsymbol{\eta}}^{k-m} v(\bar{x}_i^{m,T})| \leq & \frac{1}{r_T^m} \max_{0 \leq i \leq m} |D_{\boldsymbol{\eta}}^{k-m} v(x_i^{m,T})| \\ & + \frac{1}{2^{\ell-m}} \sum_{\ell=m+1}^{k} \frac{1}{r_T^{2m-\ell}} \|D_{\boldsymbol{\eta}}^{k-\ell} v\|_{L^\infty(L_T)}. \end{aligned}$$

However, $\frac{1}{r_T^{2m-\ell}} \leq \frac{1}{r_T^{\ell}}$ for $\ell \geq m+1$ and so using (3.10) we arrive at (3.11). $\square$

The following is a fundamental result for the correction function w_T^u. Lemma below states the unisolvency of its construction (3.8) and (3.9), and the stability of $h_T^j \|D^j w_T^u\|_{L^\infty(T^\pm)}$ with respect to the data, when we choose $c_{i,\ell} = \left[D_{\boldsymbol{\eta}}^{k-\ell} u(x_i^{\ell,T})\right]$, see equation (3.8).

Lemma 3.1.3. *Given data $\{c_{i,\ell}\}$ for $0 \leq i \leq \ell$ and $0 \leq \ell \leq k$. There exists a unique function $w \in S^k(T)$, such that*

$$\left[D_{\boldsymbol{\eta}}^{k-\ell} w(x_i^{\ell,T})\right] = c_{i,\ell}, \quad \text{for } 0 \leq i \leq \ell \text{ and } 0 \leq \ell \leq k, \tag{3.12}$$

$$\begin{cases} (w_T^u)^-(a_i) = 0, & \text{if } a_i \in \Omega^- \cup \Gamma; \\ (w_T^u)^+(a_i) = 0, & \text{if } a_i \in \Omega^+. \end{cases} \quad \text{for all } a_i \in T,\ i = 1, \ldots n_{2,k}, \tag{3.13}$$

where a_i are the degree k Lagrange nodes of T (see Definition 2.2.4). In addition, *the solution $w \in S^k(T)$ satisfy the following stability bound*

$$h_T^j \|D^j w\|_{L^\infty(T^\pm)} \le C h_T^k \sum_{\ell=0}^{k} \frac{1}{r_T^\ell} \max_{0\le i\le \ell} |c_{i,\ell}|, \qquad \textit{for} \;\; j = 0, 1, \tag{3.14}$$

where C depends only on the polynomial degree k.

Proof. We will construct w of the form $w = z - I_h z$, where $z \in S^k(T)$ and I_h the Lagrange interpolant defined in Definition 3.1.1. Notice that, by definition of I_h, $z - I_h z$ vanishes on the $(k+1)(k+2)/2$ Lagrange points of T, satisfying (3.13). Moreover, since $I_h z$ is smooth on T

$$\left[D_{\boldsymbol{\eta}}^{k-\ell} w(x_i^{\ell,T})\right] = \left[D_{\boldsymbol{\eta}}^{k-\ell} z(x_i^{\ell,T})\right].$$

The function z will be given by

$$z = \begin{cases} 0 & \text{in } T^+, \\ v & \text{in } T^-, \end{cases}$$

where v is the unique polynomial on $\mathbb{P}^k$, such that

$$D_{\boldsymbol{\eta}^-}^{k-\ell} v(x_i^{\ell,T}) = \; c_{i,\ell} \qquad \text{for } 0 \le i \le \ell \text{ and } 0 \le \ell \le k.$$

The existence and uniqueness of v follow from representing $v = v(s,r)$ as a polynomial of degree k in r ($\boldsymbol{\tau}$-direction) and s ($\boldsymbol{\eta}$-direction), where $s = 0$ represents the straight line passing through y_T and z_T, then by decomposing

$$v(s,r) = p_k(r) + s p_{k-1}(r) + s^2 p_{k-2}(r) + \cdots + s^k p_0,$$

where p_ℓ, for $0 \le \ell \le k$, is a polynomial of degree ℓ in r. It is easy to see, by using interpolation at the Gauss point $\bar{x}_0^{0,T}$, that p_0 exists and is unique, then by using interpolation at the Gauss points $\bar{x}_1^{0,T}$ and $\bar{x}_1^{1,T}$ that $p_1(r)$ exists and is unique, and so on.

According to Lemma 3.1.2, we have the following bound

$$h_T^j \|D^j v\|_{L^\infty(T)} \le C\, h_T^k \sum_{\ell=0}^{k} \frac{1}{r_T^\ell} \max_{0\le i\le \ell} |c_{i,\ell}|. \tag{3.15}$$

Hence, w satisfies (3.12). Moreover,

$$h_T^j \|D^j w\|_{L^\infty(T^\pm)} = h_T^j \|D^j (z - I_h z)\|_{L^\infty(T^\pm)} \le h_T^j \|D^j v\|_{L^\infty(T^-)} + h_T^j \|D^j I_h z\|_{L^\infty(T)}.$$

Using an inverse estimate and stability of the interpolant Lemma 3.1.1, we have

$$h_T^j \|D^j I_h z\|_{L^\infty(T)} \le C \|I_h z\|_{L^\infty(T)} \le C\, \|z\|_{L^\infty(T)} \le C\, \|v\|_{L^\infty(T^-)}.$$

Then, it follows that

$$h_T^j \|D^j w\|_{L^\infty(T^\pm)} \le h_T^j \|D^j v\|_{L^\infty(T^-)} + \|v\|_{L^\infty(T^-)}.$$

Finally we arrive to (3.14) once we apply (3.15). $\square$

Let $T \in \mathcal{T}_h^\Gamma$. Consider a ball B_{2r_T} of radius $r_T = |L_T|$ such that encloses the piece of boundary T_Γ and $B_{2r_T} \subset \omega_T$, where ω_T is the patch of triangles of T introduced in Definition 2.2.7 equation (2.3). Let J_T be the local L^2 projection onto polynomials of degree k in B_{2r_T}, i.e. $J_T : L^2(B_{2r_T}) \to \mathbb{P}^k$ such that for $w \in L^2(B_{2r_T})$

$$\int_{B_{2r_T}} J_T(w)v = \int_{B_{2r_T}} wv, \quad \forall v \in \mathbb{P}^k,$$

By definition $J_T w \in \mathbb{P}^k$ is defined in the ball B_{2r_T}. However consider its natural extension to all of ω_T. Then, we can prove the following lemma.

Lemma 3.1.4. *Let $w \in C^{k+1}(\omega_T)$, then we have*

$$r_T^j \|D^j(J_T w - w)\|_{L^\infty(B_{2r_T})} \leq C\, r_T^{k+1} \|w\|_{C^{k+1}(B_{2r_T})} \quad \textit{for } 0 \leq j \leq k, \tag{3.16}$$

and

$$h_T^j \|D^j(J_T w - w)\|_{L^\infty(\omega_T)} \leq C\, h_T^{k+1} \|w\|_{C^{k+1}(\omega_T)} \quad \textit{for } 0 \leq j \leq k. \tag{3.17}$$

Proof. The inequality (3.16) is a standard approximation of the L^2 projection. To prove (3.17) we apply Taylor's theorem to get

$$h_T^j \|D^j(J_T w - w)\|_{L^\infty(\omega_T)} \leq h_T^j \sum_{\ell=1}^{k-j} h_T^\ell \|D^{j+\ell}(J_T w - w)\|_{L^\infty(B_{2r_T})} + h_T^{k+1} \|w\|_{C^{k+1}(\omega_T)}.$$

The result follows after applying (3.16) and using that $r_T \leq h_T$, which is trivial since L_T is a segment contained in T. □

Now we are in position to establish the approximation result for the correction function w_T^u defined in Section 3.1.2. One interpretation of the result below is that $(I_h u + w_T^u)$ approximates the function u on elements cut by the interface. In this sense, w_T^u "corrects" the approximation of the interpolant I_h on these elements.

Lemma 3.1.5. *Let I_h be the interpolant defined in Definition 3.1.1. Suppose the so-*

lution u to problem (3.1) *satisfies* $u^{\pm} \in C^{k+1}(\Omega^{\pm})$, *and* w_T^u *is the correction function defined by* (3.12) *and* (3.13)*. Then, we have*

$$h_T^j \|D^j(u - I_h u - w_T^u)\|_{L^\infty(T^\pm)} \leq C\, h_T^{k+1} \left(\|u_E^+\|_{C^{k+1}(\omega_T)} + \|u_E^-\|_{C^{k+1}(\omega_T)}\right), \quad \textit{for}\ \ j = 0, 1,$$

and C depends only on the shape regularity of T, the polynomial degree k.

Proof. We will define $v \in S^k(T)$ (see (3.4)) as follows

$$v = \begin{cases} J_T u_E^+ & \text{on } T^+, \\ J_T u_E^- & \text{on } T^-. \end{cases}$$

Clearly $v - I_h v = w_T^v$ by Lemma 3.1.3. Hence, we have

$$\begin{aligned} h_T^j \|D^j(u - I_h u - w_T^u)\|_{L^\infty(T^\pm)} &= h_T^j \|D^j \left((u - v) + v - I_h(u) - w_T^u\right)\|_{L^\infty(T^\pm)} \\ &= h_T^j \|D^j \left((u - v) + (v - I_h v) + I_h(v - u) - w_T^u\right)\|_{L^\infty(T^\pm)} \\ &= h_T^j \|D^j \left((u - v) - I_h(u - v) - w_T^{u-v}\right)\|_{L^\infty(T^\pm)} \\ &\leq C\, h_T^j \left(\|D^j(u - v)\|_{L^\infty(T^\pm)} + \|D^j w_T^{u-v}\|_{L^\infty(T^\pm)}\right) \\ &\quad + C\, \|u - v\|_{L^\infty(T)}, \end{aligned}$$

where we used $w_T^{u-v} = w_T^u - w_T^v$, an inverse estimate and the stability of I_h in the max-norm Lemma 3.1.1.

Using (3.17) we get

$$h_T^j \|D^j(u - v)\|_{L^\infty(T^\pm)} + \|u - v\|_{L^\infty(T^\pm)} \leq C h_T^{k+1} (\|u_E^-\|_{C^{k+1}(\omega_T)} + \|u_E^+\|_{C^{k+1}(\omega_T)}).$$

Estimate (3.14) implies

$$h_T^j \|w_T^{u-v}\|_{L^\infty(T)} \leq C\, h_T^k \sum_{\ell=0}^{k} \frac{1}{r_T^{k-\ell}} \| \left[D_{\boldsymbol{n}}^\ell (v-u) \right] \|_{L^\infty(T_\Gamma)}.$$

Applying (3.16) we obtain

$$\sum_{\ell=0}^{k} \frac{1}{r^{k-\ell}} \| \left[D_{\boldsymbol{n}}^\ell (v-u) \right] \|_{L^\infty(T_\Gamma)} \leq C\, r_T (\|u_E^+\|_{C^{k+1}(B_{2r_T})} + \|u_E^-\|_{C^{k+1}(B_{2r_T})}),$$

which completes the proof. □

3.1.3 A priori error analysis

The objective of this section is to prove rigorous pointwise error estimates for the finite element method (3.7), which shall be achieved in Theorems 3.1.1 and 3.1.2.

The next lemma will show that the correction term w_T^u in the finite element method (3.7) will allow us to compare $I_h u - u_h$.

Lemma 3.1.6. *Let $u^\pm \in C^{k+1}(\Omega^\pm)$ be the solution of (3.1) and u_h be its finite element approximation solution of (3.7). Let I_h be the interpolant defined in Definition 3.1.1. Then, it holds*

$$\int_\Omega \nabla (I_h u - u_h) \cdot \nabla v \, dx \leq C\, h^k \|\nabla v\|_{L^1(\Omega)} \left(\|u^+\|_{C^{k+1}(\Omega^+)} + \|u^-\|_{C^{k+1}(\Omega^-)} \right), \quad \forall v \in V_h^k,$$

where C depends only on the shape regularity of $\{\mathcal{T}_h\}_{h>0}$, the polynomial degree k.

Proof. Adding and subtracting u we have

$$\begin{aligned}
\int_\Omega \nabla(I_h u - u_h)\cdot\nabla v &= \int_\Omega \nabla(I_h u - u)\cdot\nabla v + \int_\Omega \nabla u\cdot\nabla v - \int_\Omega \nabla u_h\cdot\nabla v \\
&= \int_\Omega \nabla(I_h u - u)\cdot\nabla v + \sum_{T\in\mathcal{T}_h^\Gamma}\int_T \nabla w_T^u\cdot\nabla v \\
&= \sum_{T\in\mathcal{T}_h\backslash\mathcal{T}_h^\Gamma}\int_T \nabla(I_h u - u)\cdot\nabla v + \sum_{T\in\mathcal{T}_h^\Gamma}\int_T \nabla(I_h u + w_T^u - u)\cdot\nabla v
\end{aligned}$$

The result now easily follows from Lemma 3.1.5 and the fact that u is smooth on $T\in\mathcal{T}_h\backslash\mathcal{T}_h^\Gamma$. □

From the above lemma we can easily prove an optimal estimate in the H^1 semi-norm (only assuming shape-regularity of the triangulation):

$$\|\nabla(I_h u - u_h)\|_{L^2(\Omega)} \le C\, h^k \left(\|u^+\|_{C^{k+1}(\Omega^+)} + \|u^-\|_{C^{k+1}(\Omega^-)}\right).$$

However, are goal is to prove estimates in the maximum-norm as our next result states. A slightly sub-optimal (off by a log factor) can be proved if we use the above lemma directly. In order to prove the optimal estimate, we will give a more involved argument.

Theorem 3.1.1. *Suppose that Ω is convex and assume $\mathcal{T}_h$ is quasi-uniform. Let $u^\pm\in C^{k+1}(\Omega^\pm)$ be the solution of* (3.1) *and u_h be the solution of* (3.7)*, then*

$$\|\nabla(I_h u - u_h)\|_{L^\infty(\Omega)} \le C\, h^k(\|u^+\|_{C^{k+1}(\Omega^+)} + \|u^-\|_{C^{k+1}(\Omega^-)}),$$

where C depends only on the quasi-uniformity constant of $\{\mathcal{T}_h\}_{h>0}$ and the polynomial degree k.

Proof. Let $e_h = I_h u - u_h$ and suppose that the maximum of $|\partial_{x_i} e_h|$ occurs at $z\in\Omega$

(for some fixed $1 \leq i \leq 2$). Suppose $z \in T_z$, for some $T_z \in \mathcal{T}_h$. Consider now the regularized Dirac delta function $\delta_h^z = \delta_h \in C_0^1(T_z)$ (see [27]), which satisfies

$$r(z) = (r, \delta_h)_{T_z}, \qquad \forall r \in \mathbb{P}^k(T_z), \tag{3.18}$$

and has the following property

$$\|\delta_h\|_{W^{r,q}(T_z)} \leq Ch^{-r-2(1-1/q)}, \qquad 1 \leq q \leq \infty, \; r = 0, 1. \tag{3.19}$$

For each $i = 1, 2$, define the approximate Green's function $g \in H_0^1(\Omega)$, which solves the following equation:

$$-\Delta g = \partial_{x_i} \delta_h \qquad \text{in } \Omega, \tag{3.20a}$$

$$g = 0 \qquad \text{on } \partial\Omega. \tag{3.20b}$$

We also consider its finite element approximation $g_h \in V_h^k$ that satisfies

$$\int_\Omega \nabla g_h \cdot \nabla v = \int_\Omega v \, \partial_{x_i} \delta_h \quad \text{ for all } v \in V_h^k. \tag{3.21}$$

From the work of Rannacher and Scott [100] we have

$$\|\nabla (g - g_h)\|_{L^1(\Omega)} \leq C. \tag{3.22}$$

Moreover, using a dyadic decomposition one can show

$$\|\nabla g\|_{L^1(\Omega)} \leq C \log(1/h). \tag{3.23}$$

A log free estimate holds if we consider a smaller domain, i.e.

$$\|\nabla g\|_{L^1(S^\Gamma)} \leq C, \tag{3.24}$$

where $S^\Gamma = \{x \in \Omega : dist(x, \Gamma) \leq \kappa h\}$ for some fixed constant κ; see for instance [62]. Hence, combining (3.22) and (3.24) we have

$$\|\nabla g_h\|_{L^1(S^\Gamma)} \leq C. \tag{3.25}$$

We start by using the definition of δ_h and problem (3.21)

$$\|\partial_{x_i} e_h\|_{L^\infty(\Omega)} = |\partial_{x_i} e_h(z)| = |\int_\Omega \delta_h \partial_{x_i} e_h| = |\int_\Omega \partial_{x_i} \delta_h \, e_h|.$$

Then, we see that

$$\|\partial_{x_i} e_h\|_{L^\infty(\Omega)} = |\int_\Omega \nabla g \cdot \nabla e_h| = |\int_\Omega \nabla g_h \cdot \nabla e_h|.$$

If we follow the proof of Lemma 3.1.6 we see that

$$\int_\Omega \nabla g_h \cdot \nabla e_h = J_1 + J_2,$$

where

$$J_1 = \sum_{T\in\mathcal{T}_h\setminus\mathcal{T}_h^\Gamma} \int_T \nabla(I_h u - u)\cdot\nabla g_h, \quad J_2 = \sum_{T\in\mathcal{T}_h^\Gamma} \int_T \nabla(I_h u + w_T^u - u)\cdot\nabla g_h.$$

Applying Cauchy-Schwarz inequality to J_2 we get

$$J_2 \le C\,\|\nabla g_h\|_{L^1(S^\Gamma)} \max_{T\in\mathcal{T}_h^\Gamma} \|\nabla(I_h u + w_T^u - u)\|_{L^\infty(T)}.$$

Moreover, using (3.25) and Lemma 3.1.5 we have

$$J_2 \le C\,h^k(\|u^+\|_{C^{k+1}(\Omega^+)} + \|u^-\|_{C^{k+1}(\Omega^-)}).$$

To give an estimate for J_1 we define $R_h = \cup_{T\in\mathcal{T}_h\setminus\mathcal{T}_h^\Gamma} T$. Now, adding and subtracting ∇g, we obtain

$$J_1 = \sum_{T\in\mathcal{T}_h\setminus\mathcal{T}_h^\Gamma} \int_T \nabla(I_h u - u)\cdot\nabla g_h = \int_{R_h} \left(\nabla(I_h u - u)\cdot\nabla(g_h - g) + \nabla(I_h u - u)\cdot\nabla g\,\right).$$

Using (3.22), we have

$$\int_{R_h} \nabla(I_h u - u)\cdot\nabla(g_h - g)\,dx \le C\,h^k(\|u^+\|_{C^{k+1}(\Omega^+)} + \|u^-\|_{C^{k+1}(\Omega^-)}).$$

For the remaining term we integrate by parts to get

$$\int_{R_h} \nabla(I_h u - u)\cdot\nabla g = \int_{R_h} (I_h u - u)\partial_{x_i}\delta_h\,dx + \int_{\partial R_h\setminus\partial\Omega} (I_h u - u) D_{\boldsymbol{n}} g.$$

Here we used that, since Ω is convex, ∇g is continuous and so integration by parts makes sense.

Clearly we have by (3.19)

$$\int_{R_h} (I_h u - u)\partial_{x_i}\delta_h \leq Ch^k \left(\|u^+\|_{C^{k+1}(\Omega^+)} + \|u^-\|_{C^{k+1}(\Omega^-)}\right).$$

Finally, we have

$$\begin{aligned}\int_{\partial R_h\setminus\partial\Omega} (I_h u - u)D_{\boldsymbol{n}} g &\leq C\,\|I_h u - u\|_{L^\infty(R_h)}\|D_{\boldsymbol{n}} g\|_{L^1(\partial R_h\setminus\partial\Omega)} \\ &\leq Ch^{k+1}\|D_{\boldsymbol{n}} g\|_{L^1(\partial R_h\setminus\partial\Omega)}\left(\|u^+\|_{C^{k+1}(\Omega^+)} + \|u^-\|_{C^{k+1}(\Omega^-)}\right).\end{aligned}$$

In Appendix A.2 we prove the bound

$$\|D_{\boldsymbol{n}} g\|_{L^1(\partial R_h\setminus\partial\Omega)} \leq \frac{C}{h}, \tag{3.26}$$

which will then show that

$$J_1 \leq Ch^k(\|u^+\|_{C^{k+1}(\Omega^+)} + \|u^-\|_{C^{k+1}(\Omega^-)}),$$

and will complete the proof. □

Next, we will prove an estimate for the error in the maximum norm. In the case there is no interface a logarithmic factor is not present for $k \geq 2$ (see [27]), however, we do not see how to remove this factor in our setting.

Theorem 3.1.2. *Suppose that Ω is convex and that $\mathcal{T}_h$ is quasi-uniform. Let $u^\pm \in$*

$C^{k+1}(\Omega^{\pm})$ be the solution of (3.1) and u_h be the solution of (3.7), then

$$\|I_h u - u_h\|_{L^\infty(\Omega)} \leq Ch^{k+1}\log(1/h)\left(\|u^+\|_{C^{k+1}(\Omega^+)} + \|u^-\|_{C^{k+1}(\Omega^-)}\right). \tag{3.27}$$

where C depends only on the quasi-uniformity constant of $\{\mathcal{T}_h\}_{h>0}$ and the polynomial degree k.

Proof. Let $z \in \Omega$ be arbitrary and let $\delta_h = \delta_h^z$ be the Dirac delta function defined in proof of Theorem 3.1.1, equation (3.18). Let $\tilde{g}$ satisfy

$$-\Delta \tilde{g} = \delta_h \qquad \text{in } \Omega, \tag{3.28}$$

$$\tilde{g} = 0 \qquad \text{on } \partial\Omega, \tag{3.29}$$

and consider its continuous piecewise linear finite element approximation $\tilde{g}_h$, i.e.

$$\int_\Omega \nabla \tilde{g}_h \cdot \nabla v dx = \int_\Omega \delta_h v dx, \quad \forall v \in V_h^1.$$

Then, using definition of δ_z we have

$$\begin{aligned}
(I_h u - u_h)(z) &= \int_\Omega (I_h u - u_h)\delta_h \\
&= \int_\Omega \nabla(I_h u - u_h) \cdot \nabla \tilde{g}_h \\
&= \sum_{T \in \mathcal{T}_h \setminus \mathcal{T}_h^\Gamma} \int_T \nabla(I_h u - u) \cdot \nabla \tilde{g}_h + \sum_{T \in \mathcal{T}_h^\Gamma} \int_T \nabla(I_h u + w_T^u - u) \cdot \nabla \tilde{g}_h \\
&=: \quad J_1 \; + \; J_2.
\end{aligned}$$

We first give a bound for J_2.

$$
\begin{aligned}
J_2 \;&\leq\; \max_{T\in\mathcal{T}_h^\Gamma} \|\nabla(I_h u + w_T^u - u)\|_{L^\infty(T)}\|\nabla\tilde{g}_h\|_{L^1(S^\Gamma)}\\
&\leq\; Ch^k\left(\|u^+\|_{C^{k+1}(\Omega^+)} + \|u^-\|_{C^{k+1}(\Omega^-)}\right)\|\nabla\tilde{g}_h\|_{L^1(S^\Gamma)}\\
&\leq\; Ch^k\left(\|u^+\|_{C^{k+1}(\Omega^+)} + \|u^-\|_{C^{k+1}(\Omega^-)}\right)\left(\|\nabla\tilde{g}_h - \nabla\tilde{g}\|_{L^1(S^\Gamma)} + \|\nabla\tilde{g}\|_{L^1(S^\Gamma)}\right).
\end{aligned}
$$

The error of the piecewise linear finite element approximation of $\tilde{g}_h$ is a standard result. See for instance Scott [105] (also [102, 103]) provides the estimate for a similar problem. We state the estimate below.

$$
\|\nabla\tilde{g}_h - \nabla\tilde{g}\|_{L^1(\Omega)} \leq Ch\log(1/h).
$$

For $\nabla\tilde{g}$, the bound is proved for example in [62] for a similar problem (the techniques are standard see [102, 103]), here we obtain $\|\nabla\tilde{g}\|_{L^1(S^\Gamma)} \leq Ch\log(1/h)$. Therefore, we have

$$
J_2 \;\leq\; Ch^{k+1}\log(1/h)\left(\|u^+\|_{C^{k+1}(\Omega^+)} + \|u^-\|_{C^{k+1}(\Omega^-)}\right).
$$

Now, in order to bound J_1, we will introduce the Raviart-Thomas projection (see [101]) $\Pi : H^1(\Omega) \to \Phi_h^D$, defined locally for any $T \in \mathcal{T}_h$, $\Pi|_T : H^1(T) \to RT_0(T)$, where

$$
RT_0(T) = [\mathbb{P}^0(T)]^2 \oplus x\mathbb{P}^0(T), \quad \Phi_h^D = \left\{\boldsymbol{\phi} \in [L^2(\Omega)]^2 :\; \boldsymbol{\phi}|_T \in RT_0(T)\ \forall T \in \mathcal{T}_h\right\}.
$$

Then, adding and subtracting $\Pi\nabla\tilde{g}_h$

$$
J_1 = J_1(\nabla\tilde{g}_h) = J_1(\nabla\tilde{g}_h - \Pi(\nabla\tilde{g}_h)) + J_1(\Pi(\nabla\tilde{g}_h)).
$$

For the first term we have

$$J_1(\nabla \tilde{g}_h - \Pi \nabla \tilde{g}) \;\leq\; Ch^k \left(\|u^+\|_{C^{k+1}(\Omega^+)} + \|u^-\|_{C^{k+1}(\Omega^-)} \right) \|\nabla \tilde{g}_h - \Pi \nabla \tilde{g}\|_{L^1(\Omega)}.$$

Adding and subtracting $\nabla \tilde{g}$, using the triangle inequality, approximation of Π and $\tilde{g}_h$ we have

$$\begin{aligned} \|\nabla \tilde{g}_h - \Pi \nabla \tilde{g}\|_{L^1(\Omega)} &\leq \left(\|\nabla(\tilde{g}_h - \tilde{g})\|_{L^1(\Omega)} + \|\nabla \tilde{g} - \Pi \nabla \tilde{g}\|_{L^1(\Omega)} \right) \\ &\leq Ch \log(1/h), \end{aligned}$$

and hence

$$J_1(\nabla \tilde{g}_h - \Pi \nabla \tilde{g}) \;\leq\; Ch^{k+1} \log(1/h) \left(\|u^+\|_{C^{k+1}(\Omega^+)} + \|u^-\|_{C^{k+1}(\Omega^-)} \right).$$

For the second term we have using integration by parts

$$J_1(\Pi \nabla \tilde{g}) = \sum_{T \in \mathcal{T}_h \setminus \mathcal{T}_h^\Gamma} \left(-\int_T (I_h u - u) \nabla \cdot \Pi(\nabla \tilde{g}_h) + \int_{\partial T} (I_h u - u) \Pi(\nabla \tilde{g}_h) \cdot \boldsymbol{n} ds \right).$$

For the first term above we use the following well-known commutative property of the Raviart-Thomas projection, $\nabla \cdot \Pi v = P_0 \nabla \cdot v$, for $v \in H^1(T)$, where P_0 is the L^2 projection onto the space of piecewise constant polynomials. Then, it follows

$$\begin{aligned} -\sum_{T \in \mathcal{T}_h \setminus \mathcal{T}_h^\Gamma} \int_T (I_h u - u) \nabla \cdot \Pi(\nabla \tilde{g}_h) dx &= -\sum_{T \in \mathcal{T}_h \setminus \mathcal{T}_h^\Gamma} \int_T (I_h u - u) P_0(\Delta \tilde{g}) dx \\ &= \sum_{T \in \mathcal{T}_h \setminus \mathcal{T}_h^\Gamma} \int_T (I_h u - u) P_0(\delta_h) dx. \end{aligned}$$

Observing that the support of $P_0(\delta_h)$ is T_z, it follows that the expression above is 0 if $z \in T \in \mathcal{T}_h^\Gamma$, otherwise

$$\sum_{T \in \mathcal{T}_h \backslash \mathcal{T}_h^\Gamma} \int_T (I_h u - u) P_0(\delta_h) dx = \int_{T_z} (I_h u - u) P_0(\delta_h) dx.$$

Using stability of the L^2 projection and bound of δ_h we obtain

$$\int_{T_z} (I_h u - u) P_0(\delta_h) dx \leq C h^{k+1} \left(\|u^+\|_{C^{k+1}(\Omega^+)} + \|u^-\|_{C^{k+1}(\Omega^-)} \right).$$

We now bound the last term. Observe that, since the Raviart-Thomas projection has continuous normal components on the interior edges, $I_h u - u = 0$ on $\partial\Omega$

$$\sum_{T \in \mathcal{T}_h \backslash \mathcal{T}_h^\Gamma} \int_{\partial T} (I_h u - u) \Pi(\nabla \tilde{g}_h) \cdot \boldsymbol{n} ds = \sum_{e \in \mathcal{E}_h^{\Gamma,\partial}} \int_e (I_h u - u) \Pi \nabla \tilde{g} \cdot \boldsymbol{n} ds$$

where $\mathcal{E}_h^{\Gamma,\partial} = \{e \in \mathcal{E}_h : e = \partial T_1 \cap \partial T_2, \text{ with } T_1 \in \mathcal{T}_h^\Gamma \text{ and } T_2 \in \mathcal{T}_h \backslash \mathcal{T}_h^\Gamma\}$. Therefore, we see that

$$\begin{aligned} J_1(\Pi \nabla \tilde{g}) &= \sum_{e \in \mathcal{E}_h^{\Gamma,\partial}} \int_e (I_h u - u) \Pi \nabla \tilde{g} \cdot \boldsymbol{n} ds \\ &\leq C h^k \|\Pi \nabla \tilde{g}\|_{L^1(S^\Gamma)} \left(\|u^+\|_{C^{k+1}(\Omega^+)} + \|u^-\|_{C^{k+1}(\Omega^-)} \right) \\ &\leq C \log(1/h) h^{k+1} \left(\|u^+\|_{C^{k+1}(\Omega^+)} + \|u^-\|_{C^{k+1}(\Omega^-)} \right), \end{aligned}$$

where we used $\|\Pi \nabla \tilde{g}\|_{L^1(S^\Gamma)} \leq C h \log(1/h)$, which follows after adding and subtracting $\nabla \tilde{g}$, using the triangle inequality, approximation of Π and the bound for $\nabla \tilde{g}$. □

Remark 3.3. Since $u - (u_h + w_T^u) = (I_h u - u_h) + (u - w_T^u - I_h u)$, by using triangle inequality and Lemma 3.1.5, $u_h + w_T^u$ approximates u on T by the same estimates given in Theorems 3.1.1 and 3.1.2.

3.2 Stokes interface problem

In this section we consider the Stokes problem in two dimensions with an immersed boundary introduced in equation (1.6) and we aim to design higher order finite element methods using the correction techniques introduced earlier in this chapter. As in the Poisson problem, the first step is to formulate problem (1.6) in interface form. Then, consider the variational formulation:

$$\begin{aligned}\int_\Omega \nabla \boldsymbol{u} : \nabla \boldsymbol{v} - \int_\Omega p \, \nabla \cdot \boldsymbol{v} = \int_\Omega \boldsymbol{f} \cdot \boldsymbol{v} + \int_\Omega \boldsymbol{f} \cdot \boldsymbol{v} \\ \int_\Omega q \, \nabla \cdot \boldsymbol{u} = 0,\end{aligned} \tag{3.30}$$

for all $\boldsymbol{v} \in [H_0^1(\Omega)]^2$ and $q \in L_0^2(\Omega)$, where $L_0^2(\Omega) = \{q \in L^2(\Omega) : \int_\Omega q = 0\}$.

The singular force field $\boldsymbol{f}_b$ is expressed int terms of a boundary force $\boldsymbol{\beta}$ as follows

$$\boldsymbol{f}_b(x) = \int_0^{|\Gamma|} \boldsymbol{\beta}(s)\delta(x - \boldsymbol{X}(s))ds, \quad x \in \Omega,$$

with $\delta(x)$ the two dimensional Dirac delta function and $\boldsymbol{X}(s)$, for $0 < s < |\Gamma|$, the arc-length parametrization of the interface Γ.

As before, strategically choosing test function $\boldsymbol{v}$ with compact support on: Ω^+,

Ω^-, and a neighborhood of Γ, we derive the interface form of problem (1.6)

$$
\begin{aligned}
-\Delta \boldsymbol{u}^{\pm} + \nabla p^{\pm} &= \boldsymbol{f}^{\pm} && \text{in } \Omega^{\pm}, && (3.31a)\\
\nabla \cdot \boldsymbol{u}^{\pm} &= 0 && \text{in } \Omega^{\pm}, && (3.31b)\\
\boldsymbol{u} &= \boldsymbol{0} && \text{on } \partial\Omega, && (3.31c)\\
[(\nabla \boldsymbol{u} - pI)\boldsymbol{n}] &= \boldsymbol{\beta} && \text{on } \Gamma, && (3.31d)\\
[\boldsymbol{u}] &= \boldsymbol{0} && \text{on } \Gamma. && (3.31e)
\end{aligned}
$$

Remark 3.4. At first glance, the setting of equations (3.31) does not quite match the methodology introduced in the previous sections for the construction of the correction function. The data across the interface, $\boldsymbol{\beta}$, considers information of the two variables $\boldsymbol{u}$ and p, then if a correction function is constructed from $\boldsymbol{\beta}$ it shall "correct" the flux $\nabla \boldsymbol{u} - pI$. Although is possible to construct such a correction the analysis will not be clear since we would be mixing the two variables. Instead, we shall construct individual corrections function for each variable.

3.2.1 Derivation of jump conditions for each variable

Following the ideas of LeVeque and Li in [76], we can easily write individual jump conditions for the velocity and the pressure in terms of the tangential and normal component of the data $\boldsymbol{\beta}$. Let θ be the angle between the x-direction (x-axis) and $\boldsymbol{n}$-direction pointing outward the interface Γ at a point $\boldsymbol{X}(s)$. Then, we write the normal and tangential components

$$
\hat{\boldsymbol{\beta}}(s) = \begin{pmatrix} \hat{\beta}_1 \\ \hat{\beta}_2 \end{pmatrix} = \begin{pmatrix} \cos(\theta) & \sin(\theta) \\ -\sin(\theta) & \cos(\theta) \end{pmatrix} \boldsymbol{\beta}(s).
$$

The jumps conditions for the velocity and the pressure are given by

$$[p] = \hat{\beta}_1, \quad [D_{\boldsymbol{n}} p] = \frac{d}{ds}\hat{\beta}_2, \tag{3.32}$$

$$[\boldsymbol{u}] = 0, \quad [D_{\boldsymbol{n}} \boldsymbol{u}] = \boldsymbol{\beta} + \hat{\beta}_1 \boldsymbol{n}. \tag{3.33}$$

For the sake of completeness, we present the derivation of these jumps in Appendix A.3.

3.2.2 Higher order finite element methods

As before, we consider a family of triangulations of Ω, $\mathcal{T}_h$ with $0 < h < 1$. We assume that the triangulation is quasi-uniform. Next we define the finite element spaces. The idea is to consider standard inf-sup stable finite element subspaces for the Stokes problem, as for instance the Taylor-Hood elements [28] or $[\mathbb{P}^2]^2 - \mathbb{P}^0$ elements [41].

Assumption 3.1. *We consider a class of finite element subspaces $\boldsymbol{V}_h \subset [H^1_0(\Omega)]^2$ and $M_h \subset L^2_0(\Omega)$ satisfying the following assumptions:*

- *$\boldsymbol{V}_h$ and M_h are a pair of inf-sup stables subspaces, with $\boldsymbol{V}_h \subset [H^1_0(\Omega)]^2$.*
- *We let $k \geq 1$ as the maximum integer such that*

$$\boldsymbol{V}_h^k := \left\{ \boldsymbol{v} \in C(\Omega) \cap [H^1_0(\Omega)]^2 : \boldsymbol{v}|_T \in [\mathbb{P}^k(T)]^2, \ \forall T \in \mathcal{T}_h \right\} \subseteq \boldsymbol{V}_h,$$

and, if M_h contains the discontinuous pressure space of degree $k-1$ we let

$$M_h^{k-1} := \left\{ q \in L^2_0(\Omega) : q|_T \in \mathbb{P}^{k-1}(T), \ \forall T \in \mathcal{T}_h \right\} \subseteq M_h,$$

otherwise

$$M_h^{k-1} := \left\{ q \in C(\Omega) \cap L_0^2(\Omega) : q|_T \in \mathbb{P}^{k-1}(T), \ \forall T \in \mathcal{T}_h \right\} \subseteq M_h.$$

For instance, $k = 1$ for the pairs: $[\mathbb{P}^2]^2 - \mathbb{P}^0$, reduced $[\mathbb{P}^2]^2 - \mathbb{P}^0$, and mini element. Whilst $k = 2$ for the pair: Taylor-Hood elements $[\mathbb{P}^2]^2 - \mathbb{P}^1$.

We next define the interpolant onto these spaces. We let I_h be the interpolant defined componentwise in (3.5) onto the space $\boldsymbol{V}_h^k$, and J_h be the interpolant defined in (3.5) onto the space M_h^{k-1}, in the case of continuous pressure finite element spaces. Otherwise, if M_h contains discontinuous finite element pressure spaces we define J_h to be the L^2 projection onto M_h^{k-1}.

Find $(\boldsymbol{u}_h, p_h) \in \boldsymbol{V}_h \times M_h$, such that

$$\begin{aligned} \int_\Omega \nabla \boldsymbol{u}_h : \nabla \boldsymbol{v} - \int_\Omega p_h \nabla \cdot \boldsymbol{v} &= \int_\Omega \boldsymbol{f} \cdot \boldsymbol{v} + \int_\Gamma \boldsymbol{\beta} \cdot \boldsymbol{v} \\ &\quad - \sum_{T \in \mathcal{T}_h^\Gamma} \left(\int_T \nabla \boldsymbol{w}_T^{\boldsymbol{u}} : \nabla \boldsymbol{v} + \int_T w_T^p \nabla \cdot \boldsymbol{v} \right), \\ \int_\Omega q \nabla \cdot \boldsymbol{u}_h &= - \sum_{T \in \mathcal{T}_h^\Gamma} \int_T q \nabla \cdot \boldsymbol{w}_T^{\boldsymbol{u}}, \end{aligned} \tag{3.34}$$

for all $(\boldsymbol{v}, q) \in \boldsymbol{V}_h \times M_h$. Note that we are using short notation for the integrals of the correction functions, writing them over T instead of T^- and T^+, but as before they are discontinuous across the interface.

Using equations (3.33), the correction function $\boldsymbol{w}_T^{\boldsymbol{u}}$ is defined componentwise as in Section 3.1.2. The same is true for w_T^p when J_h is the Lagrange interpolant by using equations (3.32). In the case J_h is the L^2 projection we replace equation (3.9) with the condition $J_h(w_T^p) = 0$, i.e.

$$\left[D_{\boldsymbol{\eta}}^{k-\ell} w_T^p(x_i^{\ell,T})\right] = \left[D_{\boldsymbol{\eta}}^{k-\ell} p(x_i^{\ell,T})\right] \quad \text{for } 0 \le i \le \ell \text{ and } 0 \le \ell \le k, \tag{3.35}$$

$$J_h(w_T^p) = 0. \tag{3.36}$$

Note that each component of $\boldsymbol{w}_T^{\boldsymbol{u}}$ and w_T^p are obtained independently to each other, therefore, the Lemma 3.1.5 can be applied to each one separately.

Similarly to Lemma 3.1.5, we have the following estimate for the interpolant J_h and the correction function w_T^p

$$\|p - J_h p - w_T^p\|_{L^\infty(T^\pm)} \le C\, h_T^{k+1} \left(\|p^+\|_{C^{k+1}(T)} + \|p^-\|_{C^{k+1}(T)}\right) \quad \forall T \in \mathcal{T}_h^\Gamma,$$

where C is a constant depending on k. Then, the following result holds and can be proved similar to Lemma 3.1.6.

Lemma 3.2.1. *Let $(\boldsymbol{u}, p)$ be solution of* (3.31) *and assume that $\boldsymbol{u}^\pm \in [C^{k+1}(\Omega^\pm)]^2$ and $p^\pm \in C^k(\Omega^\pm)$. Let $\boldsymbol{V}_h$ and M_h be the finite element spaces satisfying Assumption 3.1 and consider the definitions above for k, I_h and J_h. Let $(\boldsymbol{u}_h, p_h) \in \boldsymbol{V}_h \times M_h$ be solution of* (3.34)*. Then, it holds*

$$\int_\Omega \nabla(I_h\boldsymbol{u} - \boldsymbol{u}_h) : \nabla \boldsymbol{v} \;-\; \int_\Omega (J_h p - p_h)\nabla\cdot\boldsymbol{v}$$
$$\le C\, h^k \|\nabla \boldsymbol{v}\|_{L^1(\Omega)} \left(\|\boldsymbol{u}^+\|_{C^{k+1}(\Omega^+)} + \|\boldsymbol{u}^-\|_{C^{k+1}(\Omega^-)} + \|p^+\|_{C^k(\Omega^+)} + \|p^-\|_{C^k(\Omega^-)}\right)$$

$$\int_\Omega q\nabla\cdot(\boldsymbol{u}_h - I_h\boldsymbol{u}) \;\le\; Ch^k\|q\|_{L^1(\Omega)} \left(\|\boldsymbol{u}^+\|_{C^{k+1}(\Omega^+)} + \|\boldsymbol{u}^-\|_{C^{k+1}(\Omega^-)}\right),$$

for all $(\boldsymbol{v}, q) \in \boldsymbol{V}_h \times M_h$.

Proof. For the first equation we use (3.31) and (3.34) to obtain

$$
\begin{aligned}
\int_\Omega \nabla(I_h\boldsymbol{u}-\boldsymbol{u}_h) : \nabla\boldsymbol{v} - \int_\Omega (J_hp-p_h)\nabla\cdot\boldsymbol{v}& \\
&= \int_\Omega \nabla(I_h\boldsymbol{u}-\boldsymbol{u}) : \nabla\boldsymbol{v} - \int_\Omega (J_hp-p)\nabla\cdot\boldsymbol{v} \\
&\quad + \sum_{T\in\mathcal{T}_h^\Gamma}\left(\int_T w_T^p\nabla\cdot\boldsymbol{v} + \int_T \nabla\boldsymbol{w}_T^{\boldsymbol{u}} : \nabla\boldsymbol{v}\right) \\
&= \sum_{T\in\mathcal{T}_h\backslash\mathcal{T}_h^\Gamma}\left(\int_T \nabla(I_h\boldsymbol{u}-\boldsymbol{u}) : \nabla\boldsymbol{v} - \int_T (J_hp-p)\nabla\cdot\boldsymbol{v}\right) \\
&\quad + \sum_{T\in\mathcal{T}_h^\Gamma}\left(\int_T \nabla(I_h\boldsymbol{u}-\boldsymbol{u}+\boldsymbol{w}_T^{\boldsymbol{u}}) : \nabla\boldsymbol{v} + \int_T (J_hp-p+w_T^p)\nabla\cdot\boldsymbol{v}\right).
\end{aligned}
$$

Similarly for the second equation we have

$$
\begin{aligned}
\int_\Omega q\nabla\cdot(I_h\boldsymbol{u}-\boldsymbol{u}_h) &= \int_\Omega q\nabla\cdot(I_h\boldsymbol{u}-\boldsymbol{u}) + \sum_{T\in\mathcal{T}_h^\Gamma}\int_T q\nabla\cdot\boldsymbol{w}_T^{\boldsymbol{u}} \\
&= \sum_{T\in\mathcal{T}_h\backslash\mathcal{T}_h^\Gamma}\int_T q\nabla\cdot(I_h\boldsymbol{u}-\boldsymbol{u}) + \sum_{T\in\mathcal{T}_h^\Gamma}\int_T q\nabla\cdot(I_h\boldsymbol{u}-\boldsymbol{u}+\boldsymbol{w}_T^{\boldsymbol{u}}).
\end{aligned}
$$

Therefore, the results follow from the properties of the correction functions $\boldsymbol{w}_T^{\boldsymbol{u}}$ and w_T^p Lemma 3.1.5, and the fact that $(\boldsymbol{u}, p)$ is smooth on $T\in\mathcal{T}_h\backslash\mathcal{T}_h^\Gamma$. □

Analogously to the proof of Theorem 3.1.1, we can prove the following result using approximate Green's function estimates for the Stokes problem. We give a sketch of the proof.

Theorem 3.2.1. *Let $(\boldsymbol{u}, p)$ be solution of* (3.31) *and assume that $\boldsymbol{u}^\pm \in [C^{k+1}(\Omega^\pm)]^2$ and $p^\pm \in C^k(\Omega^\pm)$. Let $\boldsymbol{V}_h$ and M_h be the finite element spaces satisfying Assumption 3.1 and consider the definitions above for k, I_h and J_h. Let $(\boldsymbol{u}_h, p_h) \in \boldsymbol{V}_h \times M_h$ be* *solution of* (3.34)*. Then, there exists a constant* $C > 0$*, such that*

$$\begin{aligned}\|\nabla(I_h\boldsymbol{u}-\boldsymbol{u}_h)\|_{L^\infty(\Omega)} + \|J_hp-p_h\|_{L^\infty(\Omega)} \quad\quad (3.37)\\ \leq Ch^k\left(\|\boldsymbol{u}^+\|_{C^{k+1}(\Omega^+)} + \|\boldsymbol{u}^-\|_{C^{k+1}(\Omega^-)} + \|p^+\|_{C^k(\Omega^+)} + \|p^-\|_{C^k(\Omega^-)}\right).\end{aligned}$$

Proof. Let $\boldsymbol{e}_h^{\boldsymbol{u}} = I_h\boldsymbol{u} - \boldsymbol{u}_h$ and suppose that the maximum of $\partial_{x_j}(\boldsymbol{e}_h)_i$ $(i, j = 1, 2)$ occurs at $z \in \Omega$. Suppose $z \in T \in \mathcal{T}_h$. Considering the definition and properties of the regularized Dirac delta function $\delta_h = \delta_h^z$ introduced in (3.18) and (3.19), we define the approximate Green's function $(\boldsymbol{g}, \lambda) \in [H_0^1(\Omega)]^2 \times L^2(\Omega)$ such that

$$\begin{aligned} -\Delta\boldsymbol{g} + \nabla\lambda = (\partial x_j\delta_h)\mathbf{e}_i \quad & \text{in } \Omega,\\ \nabla\cdot\boldsymbol{g} = 0 \quad & \text{in } \Omega,\\ \boldsymbol{g} = 0 \quad & \text{on } \partial\Omega,\end{aligned}$$

where $\mathbf{e}_i$ denotes the ith standard canonical basis vector of $\mathbb{R}^2$. We also consider its finite element approximation $(\boldsymbol{g}_h, \lambda_h) \in \boldsymbol{V}_h \times M_h$ that satisfies

$$\begin{aligned}\int_\Omega \nabla(\boldsymbol{g}-\boldsymbol{g}_h) : \nabla\boldsymbol{v} - \int_\Omega(\lambda-\lambda_h)\nabla\cdot\boldsymbol{v} = 0 \quad \forall\boldsymbol{v}\in\boldsymbol{V}_h,\\ \int_\Omega q\nabla\cdot(\boldsymbol{g}-\boldsymbol{g}_h) = 0 \quad \forall q \in M_h.\end{aligned}$$

Using the definition of δ_h we have

$$\|(\partial_{x_j}\boldsymbol{e}_h^{\boldsymbol{u}})_i\|_{L^\infty(\Omega)} = \left|(\partial_{x_j}\boldsymbol{e}_h^{\boldsymbol{u}}(z))_i\right| = \left|\int_\Omega \partial_{x_j}\delta_h e_i\cdot\boldsymbol{e}_h^{\boldsymbol{u}}\right|,$$

and then

$$\|(\partial_{x_j}\boldsymbol{e}_h^{\boldsymbol{u}})_i\|_{L^\infty(\Omega)} \;=\; \left|\int_\Omega \nabla\boldsymbol{g} : \nabla\boldsymbol{e}_h^{\boldsymbol{u}} - \int_\Omega \lambda\nabla\cdot\boldsymbol{e}_h^{\boldsymbol{u}}\right| \;=\; \left|\int_\Omega \nabla\boldsymbol{g}_h : \nabla\boldsymbol{e}_h^{\boldsymbol{u}} - \int_\Omega \lambda_h\nabla\cdot\boldsymbol{e}_h^{\boldsymbol{u}}\right|.$$

Following the proof of Lemma 3.2.1, we see that

$$\int_\Omega \nabla\boldsymbol{g}_h : \nabla\boldsymbol{e}_h^{\boldsymbol{u}} - \int_\Omega \lambda_h\nabla\cdot\boldsymbol{e}_h^{\boldsymbol{u}} \;=\; J_1 \;+\; J_2,$$

where

$$\begin{aligned} J_1 &= \sum_{T\in\mathcal{T}_h\setminus\mathcal{T}_h^\Gamma}\left(\int_T \nabla(I_h\boldsymbol{u}-\boldsymbol{u}) : \nabla\boldsymbol{g}_h + \int_T \lambda_h\nabla\cdot(I_h\boldsymbol{u}-\boldsymbol{u})\right)\\ J_2 &= \sum_{T\in\mathcal{T}_h^\Gamma}\left(\int_T \nabla(I_h\boldsymbol{u}-\boldsymbol{u}+\boldsymbol{w}_T^{\boldsymbol{u}}) : \nabla\boldsymbol{g}_h + \int_T \lambda_h\nabla\cdot(I_h\boldsymbol{u}-\boldsymbol{u}+\boldsymbol{w}_T^{\boldsymbol{u}})\right). \end{aligned}$$

As in the proof of Theorem 3.1.1, the estimates of J_1 and J_2 follows from the properties of the correction functions and bounds for the Green's functions that can be found for example in [56, 61]. The estimate for the error of the pressure follows from similar arguments, we leave the details to the reader. □

Remark 3.5. Using the same arguments as Remark 3.3, we can establish the same a priori error estimates given in Theorem 3.2.1 for $\boldsymbol{u}-(\boldsymbol{u}_h+\boldsymbol{w}_T^{\boldsymbol{u}})$ and for $p-(p_h+w_T^p)$. We note that the method (3.34) gives $p_h\in M_h$, therefore, if J_h is the L^2 projection, then $(p_h+w_T^p)\in L_0^2(\Omega)$, if J_h is the interpolation operator, $p_h+w_T^p$ might not have average zero and a constant $O(h^{k+1})$ must be added to make it in $L_0^2(\Omega)$.

3.3 Final discussion

3.3.1 Three dimensional problem

In this section we comment on the construction of the correction function for three-dimensional problems.

Consider problem (3.1) on a domain $\Omega \subset \mathbb{R}^3$ with an immersed interface Γ assumed to be simple and closed C^2 surface. Consider definitions given in Section 2.2 for a simplicial triangulation $\mathcal{T}_h$ and the set of all faces $\mathcal{E}_h$. Following definitions in Section 2.3.2 we can define the sets of elements intersecting the interface $\mathcal{T}_h^\Gamma$, and the edges of these elements $\mathcal{E}_h^\Gamma$. We will approximate the solution using the space of piecewise polynomials of degree less than or equal to k. Now, for $T \in \mathcal{T}_h^\Gamma$ we consider the 2-simplex L_T connecting the three points intersections of Γ with the edges (1-face) of T. Let $\boldsymbol{\eta}$ be the unit normal vector to L_T pointing outward T^- $(T \cap \Omega^-)$. For each $\ell = 0, 1, \dots, k$ let $\{\bar{x}_i^{\ell,T}\}_{i=1}^{n_\ell}$, be the Gaussian points (of order ℓ) on the 2-simplex L_T, where $n_{2,\ell} = \dim(\mathbb{P}^\ell(L_T)) = (\ell+1)(\ell+2)/2$. Consider the set $\{x_i^{\ell,T}\}_{i=1}^{n_\ell}$ obtained by the orthogonal projection (direction $\boldsymbol{\eta}$) of $\{\bar{x}_i^{\ell,T}\}_{i=1}^{n_\ell}$ onto the surface Γ. Considering the jump conditions on the interface of problem (3.1) we construct the correction function $w_T^u \in S^k(T)$ satisfying:

$$\left[D_{\boldsymbol{\eta}}^{k-\ell} w_u^T(x_i^{\ell,T})\right] = \left[D_{\boldsymbol{\eta}}^{k-\ell} u(x_i^{\ell,T})\right] \quad \text{for } 0 \le i \le n_\ell \text{ and } 0 \le \ell \le k, \tag{3.38}$$

$$\begin{cases} (w_T^u)^-(a_i) = 0, & \text{if } a_i \in \Omega^- \cup \Gamma; \\ (w_T^u)^+(a_i) = 0, & \text{if } a_i \in \Omega^+. \end{cases} \quad \text{for all } a_i \in T,\ i = 1, \dots n_{3,k}, \tag{3.39}$$

where a_i are the degree k Lagrange nodes of T (see Definition 2.2.4) and $n_{3,k} = \dim(\mathbb{P}^k(T)) = (k+3)(k+2)(k+1)/6$.

Therefore, the correction method is defined by (3.7) using w_T^u, defined by (3.38) and (3.39), correcting the load vector.

3.3.2 Concluding remarks

In this chapter we have developed higher-order finite element methods for Poisson interface problem (3.1) and Stokes interface problem (3.31). We have proved near optimal convergence results for the methods in the maximum norms: Theorem 3.1.1, Theorem 3.1.2 and Theorem 3.2.1, recovering the convergence of the finite element method for a problem without interface. The stiffness matrix remains the same (as for the problem without the interface) which is a desirable feature in time dependent problems. To the best of our knowledge, this is the first family of numerical methods that have provable higher-order accuracy (or arbitrary order) for these problems.

The algorithms and theory developed point to a number of promising research directions and opportunities. In the future, we plan to move in the direction of evolution problems, such as the time-dependent version of problem (3.31) with moving interfaces. We plan to develop time stepping methods where in each time step we used the methodology developed here to solve the resulting problem. For example the model problem (1.1). Navier-Stokes equations and more challenging problems such as fluid-structure interactions will be explored in the future.

Finally, more straightforward generalizations are possible. In this paper, for convenience, we used triangular meshes, but it is clear that rectangular or quadrilateral meshes can be used as well. Indeed, the correction function did not use the fact that the mesh is triangular.

3.4 Numerical examples

We illustrate the performance of our finite element methods with some numerical examples. We consider the square domain $\Omega = (-1,1)^2$, and we triangulate the domain with structured and non-structured triangular meshes. We use cris-cross meshes for structured and Triangle mesh generator (Delaunay triangulations), with an initial mesh of two triangles and recursive refinements with a minimum angle condition of 15°, for the non-structured meshes. We tabulate the L^2 norm and H^1 semi-norm errors as well as the L^∞ norm and $W^{1,\infty}$ semi-norm errors, with their respective order of convergence. Plots of approximate solutions and rate of convergence are also provided. For the case when the interface is not a straight line we need to integrate over curved region. We address this problem in Appendix A.4.1 giving explicit quadrature formulas. Computationally, we obtain the system as for the respective smooth problem (3.1) and (3.31) without interface. The extra work is in the computation of the correction functions, we perform this locally in each triangle intersecting the interface to then add them to the load vector.

3.4.1 Numerical example for Poisson interface problem

Let u be the exact solution of problem (3.1), u_h be the solution by the method defined in (3.7). We consider definition of correction function w_T^u (3.12) -(3.13), and consider the approximation $u_h^\star$ defined locally by

$$u_h^\star|_T = \begin{cases} u_h|_T, & \text{if } T \in \mathcal{T}_h \backslash \mathcal{T}_h^\Gamma; \\ u_h|_T + w_T^u, & \text{if } T \in \mathcal{T}_h^\Gamma. \end{cases}$$

We summarize our experimental results in tables, displaying the following errors and experimental orders of convergence (eoc):

$$e_h^0 := \|u - u_h^\star\|_{L^2(\Omega)}, \qquad e_h^\infty := \|u - u_h^\star\|_{L^\infty(\Omega)},$$
$$e_h^1 := \|\nabla(u - u_h^\star)\|_{L^2(\Omega)}, \qquad e_h^{1,\infty} := \|\nabla(u - u_h^\star)\|_{L^\infty(\Omega)},$$

$$\mathrm{eoc}(e) := \frac{\log(e_{h_{l+1}}/e_{h_l})}{\log(h_{l+1}/h_l)}.$$

We will illustrate our results with a numerical experiment using piecewise quadratic polynomials, i.e., $k = 2$. Note that I_h is then the piecewise quadratic Lagrange interpolant.

Example 3.1. Consider the model problem [77] with exact solution of problem (3.1) defined by on $\Omega = (-1, 1)^2$

$$u(x, y) \quad = \quad \begin{cases} 1, & \text{if } r \le 1/3 \\ 1 - \log(3r), & \text{if } r > 1/3 \end{cases} \qquad (x, y) \in \Omega,$$

where $r = \sqrt{x^2 + y^2}$. We summarize the errors and order of convergence in the following tables

h	e_h^0	eoc	e_h^∞	eoc	e_h^1	eoc	$e_h^{1,\infty}$	eoc
7.1e-1	1.7e-2	–	4.7e-2	–	1.8e-1	–	4.3e-1	–
3.5e-1	1.7e-3	3.29	5.0e-3	3.22	3.6e-2	2.37	1.2e-1	1.76
1.8e-1	1.4e-4	3.54	7.4e-4	2.78	5.6e-3	2.69	3.0e-2	2.08
8.8e-2	1.2e-5	3.61	6.8e-5	3.44	8.4e-4	2.74	5.9e-3	2.34
4.4e-2	1.1e-6	3.40	1.3e-5	2.29	1.5e-4	2.46	1.7e-3	1.75
2.2e-2	1.0e-7	3.41	2.0e-6	2.74	2.7e-5	2.51	5.0e-4	1.81
1.1e-2	9.1e-9	3.57	2.3e-7	3.12	4.7e-6	2.52	1.3e-4	1.90

Table 3.1: Example 3.1: errors and experimental orders of convergence (eoc) using method (3.7) on structured meshes.

In this example we are considering a curved interface, then quadrature rules over

h	e_h^0	eoc	e_h^∞	eoc	e_h^1	eoc	$e_h^{1,\infty}$	eoc
3.3e-1	1.7e-3	–	2.6e-3	–	6.7e-2	–	4.0e-1	–
1.8e-1	2.2e-4	3.37	4.0e-4	3.08	1.8e-2	2.15	2.1e-1	1.04
9.0e-2	2.6e-5	3.15	7.5e-5	2.49	4.4e-3	2.08	4.0e-2	2.46
4.7e-2	3.2e-6	3.22	1.1e-5	3.00	1.1e-3	2.11	1.3e-2	1.78
2.4e-2	4.1e-7	3.03	1.4e-6	2.95	2.8e-4	2.02	4.0e-3	1.69
1.2e-2	5.1e-8	3.12	2.2e-7	2.76	7.1e-5	2.07	1.2e-3	1.82
6.1e-3	6.4e-9	3.02	3.1e-8	2.85	1.8e-5	2.01	3.2e-4	1.90

Table 3.2: Example 3.1: errors and experimental orders of convergence (eoc) using method (3.7) on non-structured meshes.

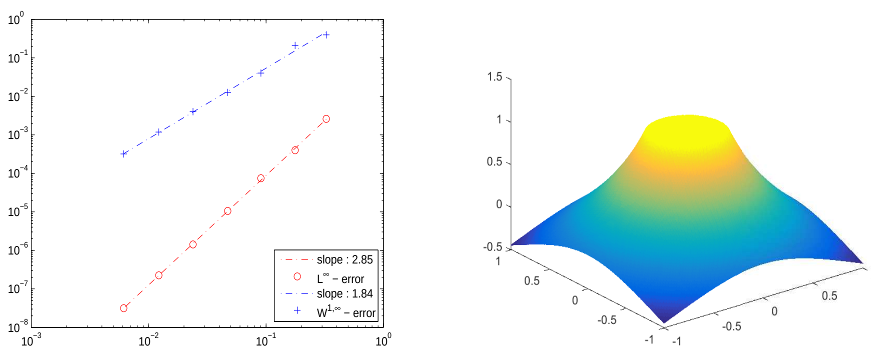

Figure 3.2: Example 3.1. Left figure: Plot on *Log* scale of e_h^∞ and $e_h^{1,\infty}$ errors vs h corresponding to Table 3.2. Right figure: approximate solution by method (3.7) of Poisson interface problem (3.1).

elements with one curved edge are needed. In Appendix A.4.1 we address this issue giving higher-order quadrature rules over this kind of elements. We observe in Tables 3.1 and 3.2 optimal convergence, confirming our results in Theorems 3.1.1 and 3.1.2. Super-convergence phenomenon is observed in the case of structured meshes Table 3.1 .

3.4.2 Numerical example for Stokes interface problem

In order to illustrate our method for the Stokes interface problem we consider the pair of inf-sup stable finite element spaces $\boldsymbol{V}_h$ and M_h, piecewise quadratic polynomial for the velocity and piecewise linear polynomials for the pressure (Taylor-Hood $[\mathbb{P}^2]^2 - \mathbb{P}_1$). Let $(\boldsymbol{u}, p)$ solution of problem (3.31) and $(\boldsymbol{u}_h, p_h)$ the finite element approximation of (3.34). We define the approximations using the definitions of the correction functions

$$\boldsymbol{u}_h^\star|_T = \begin{cases} \boldsymbol{u}_h|_T, & \text{if } T \in \mathcal{T}_h \backslash \mathcal{T}_h^\Gamma; \\ \boldsymbol{u}_h|_T + \boldsymbol{w}_T^{\boldsymbol{u}}, & \text{if } T \in \mathcal{T}_h^\Gamma. \end{cases} \qquad p_h^\star|_T = \begin{cases} p_h|_T, & \text{if } T \in \mathcal{T}_h \backslash \mathcal{T}_h^\Gamma; \\ p_h|_T + w_T^p, & \text{if } T \in \mathcal{T}_h^\Gamma. \end{cases}$$

We define the error function and the respective order of convergence (associated to the error and the norm) as follows

$$\begin{aligned} e_{\boldsymbol{u}}^0 &:= \|\boldsymbol{u} - \boldsymbol{u}_h^\star\|_{L^2(\Omega)}, & e_{\boldsymbol{u}}^\infty &:= \|\boldsymbol{u} - \boldsymbol{u}_h^\star\|_{L^\infty(\Omega)}, \\ e_{\boldsymbol{u}}^1 &:= \|\nabla(\boldsymbol{u} - \boldsymbol{u}_h^\star)\|_{L^2(\Omega)}, & e_{\boldsymbol{u}}^{1,\infty} &:= \|\nabla(\boldsymbol{u} - \boldsymbol{u}_h^\star)\|_{L^\infty(\Omega)}, \\ e_p^0 &:= \|p - p_h^\star\|_{L^2(\Omega)}, & e_p^\infty &:= \|p - p_h^\star\|_{L^\infty(\Omega)}, \end{aligned}$$

$$\operatorname{eoc}(e) := \frac{\log(e_{h_{l+1}}/e_{h_l})}{\log(h_{l+1}/h_l)}.$$

With these finite element spaces, the value of k is 2 (see assumption **A2**) , then I_h is the piecewise quadratic Lagrange interpolant and J_h is the piecewise linear Lagrange interpolant.

Example 3.2. Consider an exact solution of Stokes problem (3.31) on $\Omega = (-1,1)^2$

$$\boldsymbol{u}(x,y) = \begin{pmatrix} u_1(x,y) = \begin{cases} 3y & \text{if } r \leq \frac{1}{3}, \\ \frac{4y}{3r} - y & \text{if } r > \frac{1}{3} \end{cases} \\ \\ u_2(x,y) = \begin{cases} -3x, & \text{if } r \leq \frac{1}{3}, \\ x - \frac{4x}{3r} & \text{if } r > \frac{1}{3} \end{cases} \end{pmatrix},$$

$$p(x,y) = \begin{cases} 4 - \frac{\pi}{9} + 3x^2 - 3y^2 & \text{if } r \leq \frac{1}{3}, \\ \frac{\pi}{9} + 3x^2 - 3y^2 & \text{if } r > \frac{1}{3} \end{cases},$$

for $(x,y) \in \Omega$ and $r = \sqrt{x^2+y^2}$. In this case the interface is the circumference of radius 1/3, i.e. $\Gamma = \{(x,y) \in \Omega : r = 1/3\}$.

l	$e^0_{\boldsymbol{u}}$	eoc	$e^\infty_{\boldsymbol{u}}$	eoc	$e^1_{\boldsymbol{u}}$	eoc	$e^{1,\infty}_{\boldsymbol{u}}$	eoc
1	2.0e-3	–	3.5e-3	–	1.0e-1	–	3.9e-1	–
2	2.5e-4	2.98	4.2e-4	3.04	2.8e-2	1.87	1.5e-1	1.38
3	3.0e-5	3.06	8.6e-5	2.30	7.2e-3	1.94	4.2e-2	1.81
4	3.7e-6	3.03	1.1e-5	2.92	1.8e-3	1.97	1.3e-2	1.67
5	4.5e-7	3.04	1.7e-6	2.77	4.6e-4	1.99	3.6e-3	1.87

Table 3.3: Example 3.2: errors and experimental orders of convergence (eoc) for velocity approximate solution, using method (3.34) on structured meshes. $h = 2^{-(l+3/2)}$, for $l = 1, ..., 5$.

We observe optimal convergence for the velocity and pressure in Tables 3.3 and 3.4 respectively, confirming our result in Theorem 3.2.1. We also observe from the plot of the approximate pressure (see Figure 3.3) that there is no pollution beyond the interface.

l	e_p^0	eoc	e_p^∞	eoc
1	2.3e-2	–	6.3e-2	–
2	8.5e-3	1.46	3.3e-2	0.93
3	2.6e-3	1.68	1.6e-2	1.07
4	7.1e-4	1.89	5.1e-3	1.64
5	1.8e-4	1.95	1.5e-3	1.80

Table 3.4: Example 3.2: errors and experimental orders of convergence (eoc) for pressure approximate solution, using method (3.34) on structured meshes. $h = 2^{-(l+3/2)}$, for $l = 1, ..., 5$.

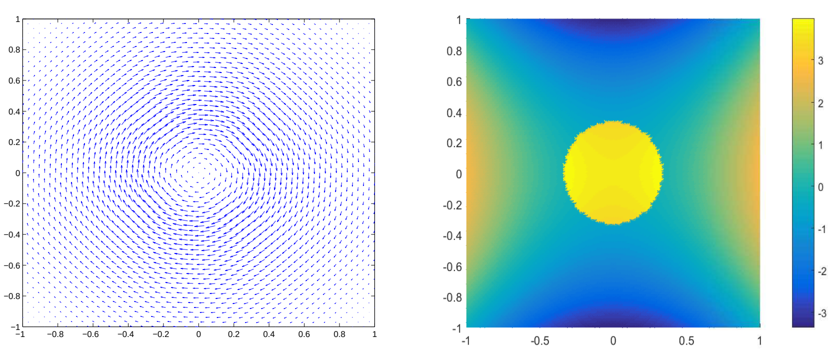

Figure 3.3: Example 3.2. Plots of approximate solution by method (3.34) of problem (3.31). Left figure: $\boldsymbol{u}_h$ velocity. Right figure: p_h pressure.

Chapter Four

High contrast interface problem I: analysis of an immersed finite element method

4.1 An immersed finite element method for Poisson interface problem

In this section we introduce an Immersed Finite Element Method approximating the Poisson interface problem with discontinuous constant coefficients $\rho^+ \gg \rho^-$, and using triangulations that are non-fitted with the interface.

4.1.1 Introduction

We consider the problem: Let $\Omega \subset \mathbb{R}^2$ be a polygonal domain with an immersed interface Γ such that $\overline{\Omega} = \overline{\Omega^-} \cup \overline{\Omega^+}$ with $\Omega^- \cap \Omega^+ = \emptyset$, and $\Gamma = \overline{\Omega^-} \cap \overline{\Omega^+}$. We assume that Γ does not intersect $\partial\Omega$, enclosing either Ω^- or Ω^+. Our numerical method will approximate a solution of the problem below.

$$-\nabla \cdot (\rho^{\pm} \nabla u^{\pm}) = f^{\pm} \qquad \text{in } \Omega^{\pm}, \tag{4.1a}$$

$$u = 0 \qquad \text{on } \partial\Omega, \tag{4.1b}$$

$$[u] = 0 \qquad \text{on } \Gamma, \tag{4.1c}$$

$$[\rho \nabla u \cdot \boldsymbol{n}] = 0 \qquad \text{on } \Gamma. \tag{4.1d}$$

where we denote by $u^{\pm} \equiv u|_{\Omega^{\pm}}$, $\boldsymbol{n}^{\pm}$ is the unit outward pointing normal to $\Omega^{\pm}$, and the jumps across the interface Γ are defined as before, i.e.

$$[\rho \nabla u \cdot \boldsymbol{n}] = \rho^- \nabla u^- \cdot \boldsymbol{n}^- + \rho^+ \nabla u^+ \cdot \boldsymbol{n}^+, \quad [u] = u^+ - u^-. \tag{4.2}$$

We furthermore assume that $\rho^+ \geq \rho^- > 0$ are constants and that the interface Γ is a closed, simple and regular $\mathcal{C}^2$ curve with an arc-length parameterization $\boldsymbol{X}$.

4.1.2 Notation

We consider a sequence of triangulation $\mathcal{T}_h$, $0 < h < 1$ of Ω (see Section 2.2), and we assume that $\mathcal{T}_h$ is shape-regular. Let h_T denote the diameter of the element $T \in \mathcal{T}_h$ and $h = \max_T h_T$. We also consider Assumptions 1, 2 and 3. We first need to build our local finite element space (on each element). With this aim we introduce some notation. To this end, we let x_0 be the midpoint with respect to the arc-length on the curve segment T_Γ. We note that the midpoint choice is a preference of the authors, the proofs below hold for any $x_0 \in T_\Gamma$. Let L_0 be the line segment inside T which is tangent to Γ at x_0.

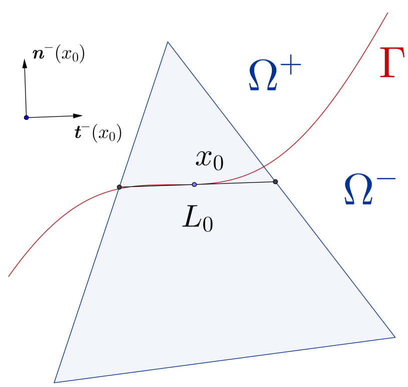

Figure 4.1: Illustration of notation on an element $T \in \mathcal{T}_h^\Gamma$, point x_0 and line segment L_0.

In order to define our finite element space, we will need the following lemma.

Lemma 4.1.1. *Consider the operator $\Upsilon : \mathbb{P}^1(T^+) \to \mathbb{P}^1(T^-)$ defined by*

$$\Upsilon(v)(x_0) := v(x_0), \tag{4.3}$$

$$(D_{\boldsymbol{t}_0^+}\Upsilon(v))(x_0) := (D_{\boldsymbol{t}_0^+}v)(x_0), \tag{4.4}$$

$$\rho^-(D_{\boldsymbol{n}_0^+}\Upsilon(v))(x_0) := \rho^+(D_{\boldsymbol{n}_0^+}v)(x_0), \tag{4.5}$$

where $\boldsymbol{n}_0^\pm = \boldsymbol{n}^\pm(x_0)$ and $\boldsymbol{t}_0^\pm = \boldsymbol{t}^\pm(x_0)$. Then, Υ is well defined.

Proof. We use the Taylor representation of a $w \in \mathbb{P}^1(T)$ at x_0 and the decomposition of the gradient into the directions $\boldsymbol{n}_0^+$ and $\boldsymbol{t}_0^+$ (normal and tangent at x_0), i.e.

$$w(x) = w(x_0) + (x - x_0) \cdot \boldsymbol{n}_0^+ D_{\boldsymbol{n}_0^+} w + (x - x_0) \cdot \boldsymbol{t}_0^+ D_{\boldsymbol{t}_0^+} w.$$

Therefore, with this representation of a function $w \in \mathbb{P}^1(T^-)$, equations (4.3), (4.4) and (4.5) uniquely define a function $w = \Upsilon(v) \in \mathbb{P}^1(T^-)$. $\square$

Note that the exact solution $u^\pm$ satisfies the transmission conditions (4.3), (4.4) and (4.5) on all points over Γ.

Next, given $T \in \mathcal{T}_h^\Gamma$ and for each $v \in \mathbb{P}^1(T^+)$ we can consider the unique corresponding function

$$G(v) = \begin{cases} v, & \text{on } T^+; \\ \Upsilon(v), & \text{on } T^-. \end{cases}$$

Let span $\{v_1, v_2, v_3\}$ be a basis for $\mathbb{P}^1(T)$ restricted to T^+. Then we define the local finite element space

$$S(T) = \begin{cases} \text{span } \{G(v_1), G(v_2), G(v_3)\}, & \text{if } T \in \mathcal{T}_h^\Gamma; \\ \mathbb{P}^1(T), & \text{if } T \in \mathcal{T}_h \backslash \mathcal{T}_h^\Gamma. \end{cases} \tag{4.6}$$

An explicit construction of basis functions of the local space $S(T)$ is given in Appendix A.4.2. The global finite element space is defined by

$$V_h := \{v : v|_T \in S(T),\ \forall T \in \mathcal{T}_h,\ v \text{ is continuous across all edges in } \mathcal{E}_h \backslash \mathcal{E}_h^\Gamma\}. \tag{4.7}$$

Remark 4.1. The local space $S(T)$ introduced in this chapter can be seen as a restriction of the local space $S^k(T)$ for $k = 1$ introduced in (3.4), satisfying the jump conditions (4.3), (4.4) and (4.5).

4.1.3 Finite element method

Next we introduce the finite element approximation to problem (4.1). Find $u_h \in V_h$ such that

$$a_h(u_h, v) \;=\; (f, v), \qquad \text{for all } v \in V_h, \tag{4.8}$$

where the bilinear $a_h : V \times V \to \mathbb{R}$ and the linear functional $(f, \cdot) : V \to \mathbb{R}$ are defined by

$$\begin{aligned} a_h(w, v) \;:=\; & \int_\Omega \rho \nabla_h w \cdot \nabla_h v - \sum_{e \in \mathcal{E}_h^\Gamma} \int_e \left(\{\rho \nabla_h v\} \cdot [\![w]\!] + \{\rho \nabla_h w\} \cdot [\![v]\!] \right) \\ & + \sum_{e \in \mathcal{E}_h^\Gamma} \left(\frac{\gamma}{|e^-|} \int_{e^-} \rho^- [\![w]\!] \cdot [\![v]\!] + \frac{\gamma}{|e^+|} \int_{e^+} \rho^+ [\![w]\!] \cdot [\![v]\!] \right) \\ & + \sum_{e \in \mathcal{E}_h^\Gamma} \left(|e^-| \int_{e^-} \rho^- [\![\nabla_h v]\!] \, [\![\nabla_h w]\!] + |e^+| \int_{e^+} \rho^+ [\![\nabla_h v]\!] \, [\![\nabla_h w]\!] \right), \end{aligned} \tag{4.9}$$

$$(f, v) \;:=\; \sum_{T \in \mathcal{T}_h} \left(\int_{T^-} f^- v \;+\; \int_{T^+} f^+ v \right),$$

for a penalty parameter $\gamma > 0$ to be chosen in order to prove coercivity of the bilinear form. The discrete gradient operator ∇_h is piecewise defined on $T^\pm$ for an element $T \in \mathcal{T}_h$ by

$$\nabla_h v|_{T^\pm} = \nabla v.$$

The space V is defined as the union of the broken Sobolev spaces

$$V := H_h^2(\Omega^+) \cup H_h^2(\Omega^-), \tag{4.10}$$

where

$$H_h^2(\Omega^\pm) := \{v : v|_{T^\pm} \in H^2(T^\pm), \text{ for all } T \in \mathcal{T}_h\}. \tag{4.11}$$

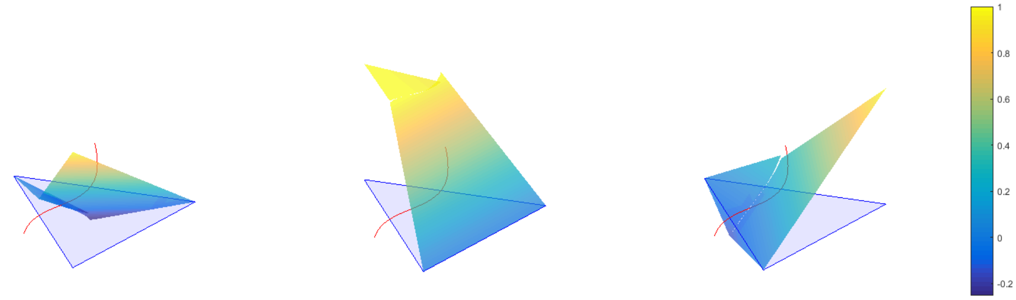

Figure 4.2: Illustration of basis functions of the local space $S(T)$ with $\rho^- = 1$ and $\rho^+ = 100$, where the element T and the interface are given by the configuration displayed in Figure 4.1.

Bilinear form a_h is based on the symmetric interior penalty discontinuous Galerkin method [2, 3, 4] applied to the edges $\mathcal{E}_h^\Gamma$ where we allow discontinuity of the numerical approximation. Note that in (4.9) we not only penalize the jumps of the function but also the normal jumps of the first derivatives across edges. This will allow us to prove coerciveness and a priori error estimates independent of the contrast of the coefficients and also independent of how small T^+ or T^- might be. Finally, we like to stress that in (4.9) only the normal derivative jumps are penalized, not the tangential derivative jumps.

4.2 Local approximation on the finite element sub-space

In this section we show that our finite element space V_h (4.7) has optimal local approximation properties. Henceforth we will keep track, as much as possible, on how constants depend on the maximum curvature κ, and in general in the geometry of sub-domains. When we use standard results (e.g. regularity and extensions lemmas) we just state that the constants depend on the geometry without explicitly saying how they scale with quantities such as curvature and the radius of the tubular neighborhood r. In order to define an interpolation operator onto V_h we consider the extension results given in Chapter 2.

Definition 4.2.1. Let u such that $u^- \in H^2(\Omega^-)$ and $u^+ \in H^2(\Omega^+)$. Consider the extension $u_E^\pm$ of $u^\pm$ given in Section 2.4.2. We define the interpolation operator I_h onto the finite element subspace V_h by

$$I_h u|_T = I_T(u)|_T, \qquad \text{for all } T \in \mathcal{T}_h, \tag{4.12}$$

where the local interpolation operator $I_T(u)$ is defined as follows: Let $T \in \mathcal{T}_h$ then

- If $T \in \mathcal{T}_h^\Gamma$ we define $I_T u \in S(T)$. In fact, we define $I_T u$ on all ω_T

$$I_T u = \begin{cases} I_T^+ u, & \text{in } \omega_T^+ \\ I_T^- u, & \text{in } \omega_T^-, \end{cases}$$

where $I_T^\pm$ are defined satisfying the following conditions

$$\left\{ \begin{array}{rcccl} (I_T^- u)(x_0) & := & (J_T u_E^+)(x_0) & =: & (I_T^+ u)(x_0) \\ (D_{\boldsymbol{t}_0^+} I_T^- u)(x_0) & := & (D_{\boldsymbol{t}_0^+}(J_T u_E^+))(x_0) & =: & (D_{\boldsymbol{t}_0^+} I_T^+ u)(x_0) \\ \rho^-(D_{\boldsymbol{n}_0^+} I_T^- u)(x_0) & := & \rho^-(D_{\boldsymbol{n}_0^+} J_T u_E^-)(x_0) & =: & \rho^+(D_{\boldsymbol{n}_0^+} I_T^+ u)(x_0). \end{array} \right. \tag{4.13}$$

Here J_T denotes the L^2 projection operator onto $\mathbb{P}^1(\omega_T)$ (note that $\omega_T \subset Tub(r)$ thanks to Assumption 2, $2h \le r$).

- If T does not belong to $\mathcal{T}_h^\Gamma$, we consider the sets $\Omega_{-h}^\pm \subset \Omega^\pm$ defined as follows:

$$\Omega_{-h}^\pm := \operatorname{int}\Big(\bigcup_{T \in \mathcal{T}_h^\pm \setminus \mathcal{T}_h^\Gamma} \overline{T} \Big). \tag{4.14}$$

We define $I_{\rm sz}u^{\pm}$ to be the Scott-Zhang interpolant (see Definition 2.2.12 of Scott-Zhang interpolant) of $u^{\pm}$ defined on $\Omega^{\pm}_{-h}$. However, we need to modify the interpolant at every vertex x (if one exists) that is an endpoint of an edge e satisfying $e \subset \partial\Omega^{+}_{-h} \cap \partial\Omega^{-}_{-h}$ (e.g. $e \subset \Gamma$). In this case, we define $I_{sz}u^{\pm}(x)$ to be the average of $u^{\pm}$ on the edge e . Note that such an x might correspond to two edges. Either edge will work for the definition of $I_{sz}u^{\pm}(x)$. This will give $I_{sz}u^{+} = I_{sz}u^{-}$ for every edge $e \subset \partial\Omega^{+}_{-h} \cap \partial\Omega^{-}_{-h}$ since $u^{+} = u^{-}$ on such an edge. Then, for $T \subset \Omega^{+}$ (or $T \subset \Omega^{-}$) we define $I_T(u)|_T = I_{\rm sz}u^{+}|_T$ (or $I_{\rm sz}u^{-}|_T$).

The motivation of the definition of the local interpolant $I_T u$ on triangles intersecting the interface is because we can bound

$$\rho^{-}\|D_{\boldsymbol{t}_0^+} I_T^- u\|^2_{L^2(\omega_T^-)} \le c\rho^{+}\|D_{\boldsymbol{t}_0^+} I_T^+ u\|^2_{L^2(\omega_T^+)}$$

and

$$\rho^{+}\|D_{\boldsymbol{n}_0^+} I_T^+ u\|^2_{L^2(\omega_T^+)} \le c\rho^{-}\|D_{\boldsymbol{n}_0^+} I_T^- u\|^2_{L^2(\omega_T^-)}$$

with c independent of ρ^- and ρ^+, this allows us to prove estimates for I_h independent of the contrast.

Lemma 4.2.1. *Consider $T \in \mathcal{T}_h^{\Gamma}$. Then, for every $v \in \mathbb{P}^1(\omega_T)$ the following bound holds*

$$h_T^j \|D^j v\|_{L^2(\omega_T)} \ \le \ C\left(h_T|v(x_0)| + h_T^2|D_{\boldsymbol{n}_0^+}v(x_0)| + h_T^2|D_{\boldsymbol{t}_0^+}v(x_0)|\right),$$

for $j = 0, 1$.

Proof. Using the Cauchy-Schwarz inequality one has, for $j = 0, 1$

$$h_T^j \|D^j v\|_{L^2(\omega_T)} \;\leq\; C\, h_T^{j+1} \|D^j v\|_{L^\infty(\omega_T)}.$$

Then, the lemma follows from the fact that v is a linear function. $\square$

We next prove a fundamental result of this chapter, a local approximation property on the space $S(T)$.

Lemma 4.2.2. *Let u such that $u^\pm \in H^2(\Omega^\pm)$ and satisfies the interface conditions $[u] = 0$ and $[\rho D_{\boldsymbol{n}} u] = 0$. Then, for any $T \in \mathcal{T}_h^\Gamma$ and $j = 0, 1$, the following bounds hold:*

$$h_T^j \|D^j(u^- - I_T^- u)\|_{L^2(\omega_T^-)} \;\leq\; C(1+\kappa)\, h_T^2 \left(|u_E^-|_{H^1(\omega_T)} + |u_E^-|_{H^2(\omega_T)} + |u_E^+|_{H^2(\omega_T)}\right) \tag{4.15}$$

and

$$\begin{aligned} h_T^j \|D^j(u^+ - I_T^+ u)\|_{L^2(\omega_T^+)} \;\leq C\,(1+\kappa) h_T^2 \Big(& |u_E^+|_{H^1(\omega_T)} + |u_E^+|_{H^2(\omega_T)} \\ & + \frac{\rho^-}{\rho^+} |u_E^-|_{H^2(\omega_T)}\Big). \end{aligned} \tag{4.16}$$

Proof. First note that by adding and subtracting $J_T u_E^\pm$ to $u_E^\pm - I_T^\pm u$, using the triangle inequality, and by means of the following well known approximation property for $\varphi \in H^2(\omega_T)$

$$h_T^j \|D^j(\varphi - J_T\varphi)\|_{L^2(\omega_T)} \;\leq\; C\, h_T^2 \|D^2\varphi\|_{L^2(\omega_T)} \quad \text{for } j \,=\, 0,\, 1, \tag{4.17}$$

the proof of the lemma reduces to estimate

$$h_T^j \|D^j w_T^\pm\|_{L^2(\omega_T^\pm)}, \quad \text{where} \quad w_T^\pm := J_T u_E^\pm - I_T^\pm u, \quad \text{for} \quad w_T^\pm \in \mathbb{P}^1(\omega_T).$$

According to the definition of I_T (4.13), and denoting $\boldsymbol{n}_0^\pm = \boldsymbol{n}^\pm(x_0)$ and $\boldsymbol{t}_0^\pm = \boldsymbol{t}^\pm(x_0)$, we have

$$\begin{cases} w_T^-(x_0) & = \; J_T u_E^-(x_0) - J_T u_E^+(x_0), \\ (D_{\boldsymbol{t}_0^+} w_T^-)(x_0) & = \; (D_{\boldsymbol{t}_0^+} J_T u_E^-)(x_0) - (D_{\boldsymbol{t}_0^+} J_T u_E^+)(x_0), \\ (D_{\boldsymbol{n}_0^+} w_T^-)(x_0) & = \; 0, \end{cases}$$

and

$$\begin{cases} w_T^+(x_0) & = \; 0, \\ (D_{\boldsymbol{t}_0^+} w_T^+)(x_0) & = \; 0, \\ \rho^+(D_{\boldsymbol{n}_0^+} w_T^+)(x_0) & = \; \rho^+(D_{\boldsymbol{n}_0^+} J_T u_E^+)(x_0) - \rho^-(D_{\boldsymbol{n}_0^+} J_T u_E^-)(x_0). \end{cases}$$

Then, using Lemma 4.2.1 and the values derived for $w_T^\pm$ we have

$$h_T^j \|D^j w_T^-\|_{L^2(\omega_T^-)} \; \leq \; C\left(h_T |w_T^-(x_0)| + h_T^2 |D_{\boldsymbol{t}_0^+} w_T^-(x_0)| \right), \tag{4.18}$$

and

$$h_T^j \|D^j w_T^+\|_{L^2(\omega_T^+)} \; \leq \; C h_T^2 |D_{\boldsymbol{n}_0^+} w_T^+(x_0)|. \tag{4.19}$$

We proceed by bounding the two terms in (4.18) and the term in (4.19), separately. For the first term in (4.18), we use that u is continuous on the interface (4.1c), in particular on ω_T^Γ, and we apply the triangle inequality

$$\begin{aligned} |w_T^-(x_0)| \; = \; |(J_T u_E^- - J_T u_E^+)(x_0)| \; &\leq \|J_T u_E^- - J_T u_E^+\|_{L^\infty(\omega_T^\Gamma)} \\ &\leq \|J_T u_E^- - u_E^-\|_{L^\infty(\omega_T^\Gamma)} + \|J_T u_E^+ - u_E^+\|_{L^\infty(\omega_T^\Gamma)}. \end{aligned}$$

Note that $ch_T \leq |\omega_T^\Gamma| \leq Ch_T$, where the second inequality follows from Lemma

A.1.4. By means of a Sobolev inequality in one dimension, we have

$$\|J_T u_E^- - u_E^-\|_{L^\infty(\omega_T^\Gamma)} \;\le\; C\left(\frac{1}{\sqrt{h_T}}\|J_T u_E^- - u_E^-\|_{L^2(\omega_T^\Gamma)} + \sqrt{h_T}\|D(J_T u_E^- - u_E^-)\|_{L^2(\omega_T^\Gamma)}\right),$$

consequently, using a trace inequality we obtain

$$\begin{aligned}\|J_T u_E^- - u_E^-\|_{L^\infty(\omega_T^\Gamma)} &\le C\left(h_T^{-1}\|J_T u_E^- - u_E^-\|_{L^2(\omega_T)} + \|D(J_T u_E^- - u_E^-)\|_{L^2(\omega_T)}\right)\\ &\quad + C\,h_T\|D^2 u_E^-\|_{L^2(\omega_T)}.\end{aligned}$$

Hence, using the approximation property (4.17), we get

$$\|J_T u_E^- - u_E^-\|_{L^\infty(\omega_T^\Gamma)} \le C h_T \|D^2 u_E^-\|_{L^2(\omega_T)}.$$

Analogously, we can show that

$$\|J_T u_E^+ - u_E^+\|_{L^\infty(\omega_T^\Gamma)} \le C h_T \|D^2 u_E^+\|_{L^2(\omega_T)}.$$

Therefore, we have the bound for the first term in (4.18)

$$h_T|w_T^-(x_0)| \;\le\; C\,h_T^2\left(\|D^2 u_E^-\|_{L^2(\omega_T)} + \|D^2 u_E^+\|_{L^2(\omega_T)}\right). \tag{4.20}$$

We now turn to the second term in (4.18). We use the fact that $D_{\boldsymbol{t}_0^-} w_T^-$ is constant on ω_T^Γ to obtain

$$|D_{\boldsymbol{t}_0^+} w_T^-(x_0)| \;=\; |\omega_T^\Gamma|^{-1/2}\|D_{\boldsymbol{t}_0^+} w_T^-\|_{L^2(\omega_T^\Gamma)} \;\le\; C h_T^{-1/2}\|D_{\boldsymbol{t}_0^+}(J_T u_E^- - J_T u_E^+)\|_{L^2(\omega_T^\Gamma)}.$$

Using the identities, denoting $\boldsymbol{t}^+ = \boldsymbol{t}^+(x)$ and $\boldsymbol{n}^+ = \boldsymbol{n}^+(x)$, for $x \in \omega_T^\Gamma$

$$\begin{aligned} D_{\boldsymbol{t}_0^+} u_E^\pm &= (\boldsymbol{t}_0^+ \cdot \boldsymbol{t}^+) D_{\boldsymbol{t}^+} u_E^\pm + (\boldsymbol{t}_0^+ \cdot \boldsymbol{n}^+) D_{\boldsymbol{n}^+} u_E^\pm, && (4.21)\\ D_{\boldsymbol{t}^+} u_E^+ &= D_{\boldsymbol{t}^+} u_E^-, && (4.22)\\ D_{\boldsymbol{n}^+} u_E^+ &= \frac{\rho^-}{\rho^+} D_{\boldsymbol{n}^+} u_E^-, && (4.23) \end{aligned}$$

we have

$$\begin{aligned} \|D_{\boldsymbol{t}_0^+} w_T^-\|_{L^2(\omega_T^\Gamma)} =& \Big\| D_{\boldsymbol{t}_0^+}(J_T u_E^- - u_E^- + u_E^+ - J_T u_E^+) + (1 - \frac{\rho^-}{\rho^+})(\boldsymbol{t}_0^+ \cdot \boldsymbol{n}^+) D_{\boldsymbol{n}^+} u_E^- \Big\|_{L^2(\omega_T^\Gamma)} \\ \le& \|D(J_T u_E^- - u_E^-)\|_{L^2(\omega_T^\Gamma)} + \|D(J_T u_E^+ - u_E^+)\|_{L^2(\omega_T^\Gamma)} \\ &+ (1 - \frac{\rho^-}{\rho^+}) \|(\boldsymbol{t}_0^+ \cdot \boldsymbol{n}^+) D u_E^-\|_{L^2(\omega_T^\Gamma)}. \end{aligned}$$

For the first two terms in the previous bound we use a trace inequality to obtain

$$\begin{aligned} \|D(J_T u_E^\pm - u_E^\pm)\|_{L^2(\omega_T^\Gamma)} \le& \frac{C}{\sqrt{h_T}} \|D(J_T u_E^\pm - u_E^\pm)\|_{L^2(\omega_T)} \\ &+ C\sqrt{h_T} \|D^2(J_T u_E^\pm - u_E^\pm)\|_{L^2(\omega_T)}, \end{aligned}$$

and for the third term we use that $|\boldsymbol{t}_0^- \cdot \boldsymbol{n}^-| \le \|\boldsymbol{X}''\|_{L^\infty} |\omega_T^\Gamma| = \mathcal{O}(\kappa h_T)$ on ω_T^Γ, $\rho^- \le \rho^+$, and a trace inequality to obtain

$$(1 - \frac{\rho^-}{\rho^+}) \|(\boldsymbol{t}_0^+ \cdot \boldsymbol{n}^+) D u_E^-\|_{L^2(\omega_T^\Gamma)} \le C\,\kappa \left(\sqrt{h_T} \|D u_E^-\|_{L^2(\omega_T)} + h_T^{3/2} \|D^2 u_E^-\|_{L^2(\omega_T)} \right).$$

Hence, applying approximation property (4.17) we obtain

$$h_T^2 |D_{\boldsymbol{t}_0^+} w_T^-(x_0)| \le C(1+\kappa) h_T^2 \left(\|D u_E^-\|_{L^2(\omega_T)} + \|D^2 u_E^-\|_{L^2(\omega_T)} + \|D^2 u_E^+\|_{L^2(\omega_T)} \right). \tag{4.24}$$

If we combine the inequalities (4.20) and (4.24) with (4.18), we arrive at the first result of the lemma, inequality (4.15).

Now we estimate the term in (4.19). We need to bound

$$|D_{\boldsymbol{n}_0^+} w_T^+(x_0)| = |\omega_T^\Gamma|^{-1/2} \|D_{\boldsymbol{n}_0^+} w_T^+\|_{L^2(\omega_T^\Gamma)} \le C h_T^{-1/2} \|D_{\boldsymbol{n}_0^+}(J_T u_E^+ - \frac{\rho^-}{\rho^+} J_T u_E^-)\|_{L^2(\omega_T^\Gamma)}.$$

Similarly to the previous bound, we note that

$$D_{\boldsymbol{n}_0^+} u_E^\pm = (\boldsymbol{n}_0^+ \cdot \boldsymbol{t}^+) D_{\boldsymbol{t}^+} u_E^\pm + (\boldsymbol{n}_0^+ \cdot \boldsymbol{n}^+) D_{\boldsymbol{n}^+} u_E^\pm,$$

and then using (4.22) and (4.23) we obtain

$$\|D_{\boldsymbol{n}_0^+} w_T^+\|_{L^2(\omega_T^\Gamma)} = \\ \Big\|D_{\boldsymbol{n}_0^+}\big(J_T u_E^+ - u_E^+ - \frac{\rho^-}{\rho^+}(J_T u_E^- - u_E^-)\big) + (1 - \frac{\rho^-}{\rho^+})(\boldsymbol{n}_0^+ \cdot \boldsymbol{t}^+) D_{\boldsymbol{t}^+} u_E^+\Big\|_{L^2(\omega_T^\Gamma)}.$$

The remaining of the proof is similar as above and we obtain

$$h_T^2 |D_{\boldsymbol{n}_0^+} w_T^+(x_0)| \le C(1+\kappa) h_T^2 \left(\frac{\rho^-}{\rho^+} \|D^2 u_E^-\|_{L^2(\omega_T)} + \|D u_E^+\|_{L^2(\omega_T)} + \|D^2 u_E^+\|_{L^2(\omega_T)} \right).$$

If we combine this inequality with (4.19), we arrive at our second result (4.16). $\square$

4.3 A priori error estimates

The purpose of this section is to prove a priori error estimates for the method defined in (4.8)-(4.9) in the energy and L^2 norm. We have commented on the similarities of the bilinear form (4.9) with the symmetric interior penalty method. Consequently, the proofs presented below follow the same arguments than the classical discontinuous Galerkin theory with emphasis on the contrast independency of the constants in the estimates.

4.3.1 Coercivity of the bilinear form

We define the following energy norm $\|\cdot\|_V : V \to \mathbb{R}_0^+$

$$\|v\|_V^2 = \|\sqrt{\rho}\nabla_h v\|_{L^2(\Omega)}^2 + \sum_{e\in\mathcal{E}_h^\Gamma}\left(\frac{\rho^-}{|e^-|}\|[\![v]\!]\|_{L^2(e^-)}^2 + \frac{\rho^+}{|e^+|}\|[\![v]\!]\|_{L^2(e^+)}^2\right) \qquad (4.25)$$
$$+ \sum_{e\in\mathcal{E}_h^\Gamma}\left(\rho^-|e^-|\|[\![\nabla_h v]\!]\|_{L^2(e^-)}^2 + \rho^+|e^+|\|[\![\nabla_h v]\!]\|_{L^2(e^+)}^2\right).$$

In order to prove coercivity we will need the following lemma.

Lemma 4.3.1. *Let $e = \operatorname{int}(\partial T_1 \cap \partial T_2) \in \mathcal{E}_h^\Gamma$, for $T_1, T_2 \in \mathcal{T}_h$. Then, there exists a constant $\theta > 0$ such that*

$$|e^\pm|^2 \leq \theta \max_{i=1,2} |T_i^\pm|.$$

The constant θ depends on the shape regularity of the triangulation.

Proof. See Appendix A.1.1. □

Lemma 4.3.2. *(Coercivity) If γ is large enough (depending on shape regularity of triangulation) there exists a constant $c > 0$, independent of h, ρ^- and ρ^+, such that*

$$c\|v\|_V^2 \leq a_h(v,v), \quad \textit{for all } v \in V_h. \qquad (4.26)$$

Proof. Let $v \in V_h$, then

$$\begin{aligned} a_h(v,v) &= \|\sqrt{\rho}\nabla_h v\|^2_{L^2(\Omega)} - 2\sum_{e\in\mathcal{E}_h^\Gamma}\int_e \{\rho\nabla_h v\}\cdot[\![v]\!] \\ &+ \sum_{e\in\mathcal{E}_h^\Gamma}\left(\frac{\gamma}{|e^-|}\rho^-\|[\![v]\!]\|^2_{L^2(e^-)} + \frac{\gamma}{|e^+|}\rho^+\|[\![v]\!]\|^2_{L^2(e^+)}\right) \\ &+ \sum_{e\in\mathcal{E}_h^\Gamma}\left(\rho^-|e^-|\|[\![\nabla_h v]\!]\|^2_{L^2(e^-)} + \rho^+|e^+|\|[\![\nabla_h v]\!]\|^2_{L^2(e^+)}\right). \end{aligned}$$

To prove the lemma, it is enough to bound the non-symmetric term

$$\int_e \{\rho\nabla_h v\}\cdot[\![v]\!] = \int_{e^-}\{\rho\nabla_h v\}\cdot[\![v]\!] + \int_{e^+}\{\rho\nabla_h v\}\cdot[\![v]\!].$$

Let $T_1, T_2 \in \mathcal{T}_h$ be such that $e = \mathrm{int}\,(\partial T_1 \cap \partial T_2)$ and set $T_e = T_1 \cup T_2$. Without loss of generality assume $T_2^- = \max_{i=1,2}|T_i^-|$. Then, according to Lemma 4.3.1

$$|e^-|^2 \le \theta |T_2^-|. \tag{4.27}$$

Then, we see that

$$\begin{aligned} \int_{e^-}\{\rho\nabla v\}\cdot[\![v]\!] &= \int_{e^-}\frac{\rho^-}{2}\Big((D_{\boldsymbol{n}_1}v)\,(v|_{T_1} - v|_{T_2}) + (D_{\boldsymbol{n}_2}v)\,(v|_{T_2} - v|_{T_1})\Big) \\ &= \int_{e^-}\rho^-(D_{\boldsymbol{n}_2}v)\,(v|_{T_2} - v|_{T_1}) + \frac{\rho^-}{2}(D_{\boldsymbol{n}_1}v + D_{\boldsymbol{n}_2}v)(v|_{T_1} - v|_{T_2}) \\ &= \int_{e^-}\rho^-(D_{\boldsymbol{n}_2}v)\,(v|_{T_2} - v|_{T_1}) + \frac{\rho^-}{2}([\![\nabla_h v]\!])\,(v|_{T_1} - v|_{T_2}). \end{aligned}$$

Using the fact that v is a linear function on T_2^- and using (4.27) we have

$$\Big|2\int_{e^-}\rho^-(D_{\boldsymbol{n}_2}v)\,(v|_{T_2} - v|_{T_1})\Big| \le C\,\|\rho^- Dv\|_{L^2(T_2^-)}\frac{1}{|e^-|^{1/2}}\|[\![v]\!]\|_{L^2(e^-)}, \tag{4.28}$$

where C depends on θ. Therefore, we have

$$\big|2\int_{e^-} \rho^-(D_{\boldsymbol{n}_2} v)\,(v|_{T_2} - v|_{T_1})\big| \le \epsilon\rho^- \|\nabla_h v\|^2_{L^2(T_e^-)} + \frac{\rho^- C^2}{\epsilon|e^-|}\|[\![v]\!]\|^2_{L^2(e^-)},$$

for any $\epsilon > 0$. Furthermore, we have

$$\big|\int_{e^-} \rho^-([\![\nabla_h v]\!])\,(v|_{T_1} - v|_{T_2})\big| \le \epsilon\rho^-|e^-|\|[\![\nabla_h v]\!]\|^2_{L^2(e^-)} + \frac{\rho^-}{\epsilon|e^-|}\|[\![v]\!]\|^2_{L^2(e^-)}.$$

Collecting the last two estimates gives

$$\big|2\int_{e^-} \{\rho\nabla_h v\}\cdot[\![v]\!]\big| \le \epsilon\rho^-(|e^-|\|[\![\nabla_h v]\!]\|^2_{L^2(e^-)} + \|\nabla_h v\|^2_{L^2(T_e^-)}) + \frac{(C^2+1)\rho^-}{\epsilon|e^-|}\|[\![v]\!]\|^2_{L^2(e^-)}.$$

Likewise, we can bound the integral over e^+ to get a combined result

$$\begin{aligned}\big|2\int_e \{\rho\nabla_h v\}\cdot[\![v]\!]\big| \le &\epsilon(\|\sqrt{\rho}\nabla_h v\|^2_{L^2(T_e)} + \rho^-|e^-|\|[\![\nabla_h v]\!]\|^2_{L^2(e^-)} + \rho^+|e^+|\|[\![\nabla_h v]\!]\|^2_{L^2(e^+)}) \\ &+ \frac{(C^2+1)\rho^-}{\epsilon|e^-|}\|[\![v]\!]\|^2_{L^2(e^-)} + \frac{(C^2+1)\rho^+}{\epsilon|e^+|}\|[\![v]\!]\|^2_{L^2(e^+)}.\end{aligned}$$

Summing over all edges $e \in \mathcal{E}_h^\Gamma$ we get

$$\begin{aligned}\big|2\sum_{e\in\mathcal{E}_h^\Gamma}\int_e \{\rho\nabla_h v\}\cdot[\![v]\!]\big| \le &\sum_{e\in\mathcal{E}_h^\Gamma} \epsilon(\|\sqrt{\rho}\nabla_h v\|^2_{L^2(T_e)} + \rho^-|e^-|\|[\![\nabla_h v]\!]\|^2_{L^2(e^-)} \\ &+ \rho^+|e^+|\|[\![\nabla_h v]\!]\|^2_{L^2(e^+)}) + \sum_{e\in\mathcal{E}_h^\Gamma} \frac{(C^2+1)\rho^-}{\epsilon|e^-|}\|[\![v]\!]\|^2_{L^2(e^-)} + \frac{(C^2+1)\rho^+}{\epsilon|e^+|}\|[\![v]\!]\|^2_{L^2(e^+)}.\end{aligned}$$

Finally, the result follows by choosing $\epsilon = 1/2$ and then choosing $\gamma = \frac{(C^2+1)}{\epsilon} + 1$. $\square$

4.3.2 Continuity of the bilinear form

Next we prove continuity of the bilinear form. To do this we define the augmented norm

$$\|v\|_W^2 \;=\; \|v\|_V^2 + \sum_{e\in\mathcal{E}_h^\Gamma} (\rho^- \|\{\nabla_h v\}\cdot \boldsymbol{n}\|^2_{L^2(e^-)}|e^-| + \rho^+ \|\{\nabla_h v\}\cdot \boldsymbol{n}\|^2_{L^2(e^+)}|e^+|). \quad (4.29)$$

Lemma 4.3.3. *(Continuity) Suppose that v, $w \in V$. Then, there exists a constant $C > 0$, independent of h, ρ^- and ρ^+, such that*

$$a_h(w,v) \;\le\; C\,\|w\|_W\,\|v\|_W.$$

Additionally, if $w \in V$ and $v \in V_h$ we have

$$a_h(w,v) \;\le\; C\,\|w\|_W\,\|v\|_V. \quad (4.30)$$

Proof. We give a sketch of the proof by bounding each term of $a_h(\cdot,\cdot)$ in (4.9) separately. The first term can easily be bounded by Cauchy-Schwarz inequality

$$\int_\Omega \rho\,\nabla_h v\cdot\nabla_h w \;\le\; \|\sqrt{\rho}\nabla_h v\|_{L^2(\Omega)}\,\|\sqrt{\rho}\nabla_h w\|_{L^2(\Omega)}.$$

The first part of the second term can be written as

$$\int_e \{\rho\nabla_h v\}\cdot [\![w]\!] \;=\; \int_{e^-} \{\rho^-\nabla_h v\}\cdot [\![w]\!] + \int_{e^+} \{\rho^+\nabla_h v\}\cdot [\![w]\!].$$

Using the Cauchy-Schwarz inequality one has

$$\int_{e^\pm} \{\rho^\pm\nabla_h v\}\,[\![w]\!] \;\le\; \left(\sqrt{|e^\pm|}\sqrt{\rho^\pm}\|\{\nabla_h v\}\cdot\boldsymbol{n}\|_{L^2(e^\pm)}\right)\frac{\sqrt{\rho^\pm}}{\sqrt{|e^\pm|}}\|[\![w]\!]\|_{L^2(e^\pm)}.$$

Let $e = \operatorname{int}(\partial T_1 \cap \partial T_2)$. If $v \in V_h$ then $\nabla_h v|_{T_i^\pm}$ is constant for each $i = 1, 2$. Then, we can use Lemma 4.3.1 to get

$$\sqrt{|e^\pm|}\sqrt{\rho^\pm}\|\{\nabla_h v\}\cdot \boldsymbol{n}\|_{L^2(e^\pm)} \leq \\ \sqrt{|e^\pm|}\sqrt{\rho^\pm}\|[\![\nabla_h v]\!]\|_{L^2(e^\pm)} + C\sqrt{\rho^\pm}(\|\nabla_h v\|_{L^2(T_1^\pm)} + \|\nabla_h v\|_{L^2(T_2^\pm)})$$

where C here depends on θ. The third term can be bounded by

$$\int_{e^\pm} \rho^\pm [\![w]\!]\cdot[\![v]\!] \;\leq\; \rho^\pm \|[\![w]\!]\|_{L^2(e^\pm)}\|[\![v]\!]\|_{L^2(e^\pm)}.$$

Finally, the fourth term can be bounded by Cauchy-Schwarz inequality

$$\int_{e^\pm} \rho^\pm [\![\nabla_h w]\!]\,[\![\nabla_h v]\!] \;\leq\; \rho^\pm \|[\![\nabla_h v]\!]\|_{L^2(e^\pm)}\|[\![\nabla_h w]\!]\|_{L^2(e^\pm)}.$$

The proof is complete summing over the edges, using finite overlapping of the elements associated to the edges and using arithmetic-geometric mean inequality. $\square$

4.3.3 Energy error estimates

Theorem 4.3.1. *(A priori energy error estimate) Let u be the solution to problem* (4.1) *and $u_h \in V_h$ be its finite element approximation solution of* (4.8). *Then, there exists $C > 0$, independent of h, ρ^- and ρ^+, such that*

$$\|u - u_h\|_V \leq C\, h(1+\kappa)\Big(\sqrt{\rho^-}(||Du||_{L^2(\Omega^-)} + \|D^2 u\|_{L^2(\Omega^-)}) + \\ \sqrt{\rho^+}(||Du||_{L^2(\Omega^+)} + ||D^2 u||_{L^2(\Omega^+)})\Big).$$

The constant C depends on C_E from (2.27).

Proof. Note that $\|u-u_h\|_V \leq \|u-I_hu\|_V + \|I_hu-u_h\|_V$. Since $d_h := I_hu - u_h \in V_h$, coercivity of $a_h(\cdot,\cdot)$ (see (4.26)) gives

$$c\|d_h\|_V^2 \;\leq\; a_h(d_h,d_h) \;=\; a_h(I_hu-u,d_h) + a_h(u-u_h,d_h). \tag{4.31}$$

Using (4.30) we obtain, for $\epsilon > 0$

$$a_h(I_hu-u,d_h) \;\leq\; C\,\|I_hu-u\|_W\|d_h\|_V \leq C\left(\frac{\epsilon}{2}\|d_h\|_V^2 + \frac{1}{2\epsilon}\|I_hu-u\|_W^2\right). \tag{4.32}$$

Choosing ϵ sufficiently small we have

$$\|d_h\|_V^2 \;\leq\; C\,\|I_hu-u\|_W^2 + a_h(u-u_h,d_h). \tag{4.33}$$

The proof of the theorem follows by checking below Lemma 4.3.5 (approximation error in W-norm) and Lemma 4.3.7 (inconsistency error). □

We next prove the missing parts of Theorem 4.3.1. We need an estimate for interpolant I_h (see (4.12)) in the augmented norm W, and to do so, we first need to prove a trace inequality that goes from a part of boundary to the interior of the domain.

Lemma 4.3.4. *Let $T \in \mathcal{T}_h^\Gamma$ and let e be an edge of T. Suppose that $w \in H^2(\omega_T^-) \cup H^2(\omega_T^+)$ and $|e^\pm| > 0$. Then, there exists a constant such that*

$$\frac{1}{|e^\pm|}\|w\|_{L^2(e^\pm)}^2 \;\leq\; C\left(\frac{1}{h_T^2}\|w\|_{L^2(\omega_T^\pm)}^2 + \|Dw\|_{L^2(\omega_T^\pm)}^2 + h_T^2\|D^2w\|_{L^2(T^\pm)}^2\right).$$

Proof. Consider the case where $e\cap\Gamma \neq \emptyset$. Let e_1 be an interior edge of ω_T, contained in ω_T^- and connected by one node to e^-. Edge e_1 exists thanks to the r-tubular neighborhood assumption with $2h < r$. Note that $ch_T \leq |e_1|$ for a constant c that only depends on the shape regularity of the mesh. Using the fundamental theorem of calculus we can show (see Lemma 3 of [47] for a similar two dimensional result)

$$\frac{1}{|e^-|}\|w\|^2_{L^2(e^-)} \;\leq\; C(|e^-|\,\|Dw\|^2_{L^2(e^-)} + \frac{1}{h_T}\|w\|^2_{L^2(e_1)} + h_T\|Dw\|^2_{L^2(e_1)}).$$

Noting that $|\omega_T^-| \geq Ch_T^2$, and using standard trace inequalities gives the result. The exact same argument would apply for e^+. If $e \cap \Gamma = \emptyset$, $e^- = e$ we apply trace inequality from e to ω_T^-. $\square$

Lemma 4.3.5. *(Interpolation error estimate) It holds,*

$$\|I_h u - u\|_W \leq C\, h\, (1+\kappa) \left(\sqrt{\rho^-}(\|Du\|_{L^2(\Omega^-)} + \|D^2 u\|_{L^2(\Omega^-)}) + \sqrt{\rho^+}(\|Du\|_{L^2(\Omega^+)} + \|D^2 u\|_{L^2(\Omega^+)})\right).$$

Here the constant C depends on the constant C_E from (2.27)*.*

Proof. We bound each term of $\|u - I_h u\|_W$, see ((4.29)) and (4.25), separately. Using Lemma 4.2.2 we easily have

$$\begin{aligned}
\|\sqrt{\rho}\nabla_h(u - I_h u)\|^2_{L^2(\Omega)} \;&\leq\; C \sum_{T\in\mathcal{T}_h\setminus\mathcal{T}_h^\Gamma} h_T^2 \left(\rho^-\|D^2 u_E^-\|^2_{L^2(T)} + \rho^+\|D^2 u_E^+\|^2_{L^2(T)}\right)\\
&+ C \sum_{T\in\mathcal{T}_h^\Gamma} h_T^2(1+\kappa)^2\,\rho^-(\|Du_E^-\|^2_{L^2(\omega_T)} + \|D^2 u_E^-\|^2_{L^2(\omega_T)})\\
&+ C \sum_{T\in\mathcal{T}_h^\Gamma} h_T^2(1+\kappa)^2\,\rho^+(\|Du_E^+\|^2_{L^2(\omega_T)} + \|D^2 u_E^+\|^2_{L^2(\omega_T)})\\
&\leq Ch^2(1+\kappa)^2 \left(\rho^-(\|Du\|^2_{L^2(\Omega^-)} + \|D^2 u\|^2_{L^2(\Omega^-)}) + \rho^+(\|Du\|^2_{L^2(\Omega^+)} + \|D^2 u\|^2_{L^2(\Omega^+)})\right)
\end{aligned}$$

where we used (2.27) in the last inequality. We also have used finite overlapping of the sets ω_T. We next estimate the term

$$\sum_{e\in\mathcal{E}_h^\Gamma}\left(\frac{\rho^-}{|e^-|}\|[\![u-I_hu]\!]\|^2_{L^2(e^-)}+\frac{\rho^+}{|e^+|}\|[\![u-I_hu]\!]\|^2_{L^2(e^+)}\right).$$

Suppose that $e=\operatorname{int}(\partial T_1\cap\partial T_2)$. Then, using Lemma 4.3.4 we have

$$\begin{aligned}
\frac{\rho^-}{|e^-|}\|[\![u-&I_hu]\!]\|^2_{L^2(e^-)}+\frac{\rho^+}{|e^+|}\|[\![u-I_hu]\!]\|^2_{L^2(e^+)}\\
&\le C\frac{\rho^-}{|e^-|}(\|u-I_{T_1}u\|^2_{L^2(e^-)}+\|u-I_{T_2}u\|^2_{L^2(e^-)})\\
&+C\frac{\rho^+}{|e^+|}(\|u-I_{T_1}\|^2_{L^2(e^+)}+\|u-I_{T_2}\|^2_{L^2(e^+)})\\
&\le C\rho^-\sum_{i=1}^2\left(\frac{1}{h_{T_i}^2}\|u-I_{T_i}u\|^2_{L^2(\omega_{T_i}^-)}+\|D(u-I_{T_i}u)\|^2_{L^2(\omega_{T_i}^-)}\right.\\
&\qquad\qquad\left.+\,h_{T_i}^2\|D^2(u-I_{T_i}u)\|^2_{L^2(\omega_{T_i}^-)}\right)\\
&+C\rho^+\sum_{i=1}^2\left(\frac{1}{h_{T_i}^2}\|u-I_{T_i}u\|^2_{L^2(\omega_{T_i}^+)}+\|D(u-I_{T_i}u)\|^2_{L^2(\omega_{T_i}^+)}\right.\\
&\qquad\qquad\left.+\,h_{T_i}^2\|D^2(u-I_{T_i}u)\|^2_{L^2(\omega_{T_i}^+)}\right).
\end{aligned}$$

If we now apply Lemma 4.2.2 and use (2.27), we get

$$\begin{aligned}
&\sum_{e\in\mathcal{E}_h^\Gamma}(\frac{\rho^-}{|e^-|}\|[\![u-I_hu]\!]\|^2_{L^2(e^-)}+\frac{\rho^+}{|e^+|}\|[\![u-I_hu]\!]\|^2_{L^2(e^+)})\le\\
&Ch^2(1+\kappa)^2\left(\rho^-(\|Du\|^2_{L^2(\Omega^-)}+\|D^2u\|^2_{L^2(\Omega^-)})+\rho^+(\|Du\|^2_{L^2(\Omega^+)}+\|D^2u\|^2_{L^2(\Omega^+)})\right).
\end{aligned}$$

We next bound

$$\sum_{e\in\mathcal{E}_h^\Gamma}\left(\rho^-|e^-|\,\|[\![D(u-I_hu)]\!]\|^2_{L^2(e^-)}+\rho^+|e^+|\,\|[\![D(u-I_hu)]\!]\|^2_{L^2(e^+)}\right).$$

Using a trace inequality to obtain

$$
\begin{aligned}
&\rho^-|e^-|\,\|[\![\nabla_h(u-I_hu)]\!]\|^2_{L^2(e^-)} + \rho^+|e^+|\,\|[\![\nabla_h(u-I_hu)]\!]\|^2_{L^2(e^+)}\\
&\qquad\qquad \le \rho^-|e|\,\|[\![\nabla_h(u-I_hu)]\!]\|^2_{L^2(e^-)} + \rho^+|e|\,\|[\![\nabla_h(u-I_hu)]\!]\|^2_{L^2(e^+)}\\
&\qquad\qquad \le \rho^-|e|\left(\|D(u-I_{T_1}u)\|^2_{L^2(e^-)} + \|D(u-I_{T_2}u)\|^2_{L^2(e^-)}\right)\\
&\qquad\qquad\quad + \rho^+|e|\left(\|D(u-I_{T_1}u)\|^2_{L^2(e^+)} + \|D(u-I_{T_2}u)\|^2_{L^2(e^+)}\right)\\
&\qquad\qquad \le C\rho^-\sum_{i=1}^{2}\left(\|D(u-I_{T_i}u)\|^2_{L^2(\omega^-_{T_i})} + h^2_{T_i}\|D^2(u-I_{T_i}u)\|^2_{L^2(\omega^-_{T_i})}\right)\\
&\qquad\qquad\quad + C\rho^+\sum_{i=1}^{2}\left(\|D(u-I_{T_i}u)\|^2_{L^2(\omega^+_{T_i})} + h^2_{T_i}\|D^2(u-I_{T_i}u)\|^2_{L^2(\omega^+_{T_i})}\right).
\end{aligned}
$$

Again, if we apply Lemma 4.2.2 and (2.27) we obtain

$$
\begin{aligned}
&\sum_{e\in\mathcal{E}_h^\Gamma}\left(\rho^-|e^-|\|[\![\nabla_h(u-I_hu)]\!]\|^2_{L^2(e^-)} + \rho^+|e^+|\|[\![\nabla_h(u-I_hu)]\!]\|^2_{L^2(e^+)}\right) \le\\
&Ch^2(1+\kappa)^2\left(\rho^-(\|Du\|^2_{L^2(\Omega^-)} + \|D^2u\|^2_{L^2(\Omega^-)}) + \rho^+(\|Du\|^2_{L^2(\Omega^+)} + \|D^2u\|^2_{L^2(\Omega^+)})\right).
\end{aligned}
$$

Finally, the last term is estimated by

$$
\begin{aligned}
&\sum_{T\in\mathcal{E}_h}(|e^-|\rho^-\|\{\nabla_h(u-I_hu)\}\cdot\boldsymbol{n}\|^2_{L^2(e^-)} + |e^+|\rho^+\|\{\nabla_h(u-I_hu)\}\cdot\boldsymbol{n}\|^2_{L^2(e^+)}) \le\\
&Ch^2(1+\kappa)^2\left(\rho^-(\|Du\|^2_{L^2(\Omega^-)} + \|D^2u\|^2_{L^2(\Omega^-)}) + \rho^+(\|Du\|^2_{L^2(\Omega^+)} + \|D^2u\|^2_{L^2(\Omega^+)})\right),
\end{aligned}
$$

exactly in the same way as it was done above. $\square$

In order to bound the inconsistency term we need a technical lemma.

Lemma 4.3.6. *Let $T\in\mathcal{T}_h^\Gamma$ and enumerate the three edges of T by e_1, e_2, e_3. Then,* *there exists a constant m such that*

$$|T_\Gamma| \;\le\; m \max_{i=1,2,3} |e_i^-| \quad \textit{and} \quad |T_\Gamma| \;\le\; m \max_{i=1,2,3} |e_i^+|.$$

The constant m is independent of r, depends only on the shape regularity of the triangulation.

Proof. See Appendix A.1.2. $\square$

Now we are able to establish the inconsistency estimate. The constant will be independent of the contrast of the coefficients ρ^- and ρ^+.

Lemma 4.3.7. *(Inconsistency estimate) Let u be the solution to (4.1) and $u_h \in V_h$ be its finite element approximation solution to (4.8). Then for any $d_h \in V_h$, it holds*

$$\begin{aligned} a_h(u-u_h,d_h) \le Ch\kappa\Big(\sqrt{\rho^-}\left(||Du||_{L^2(\Omega^-)} + h\|D^2u\|_{L^2(\Omega^-)}\right) \\ + \sqrt{\rho^-}h\|D^2u\|_{L^2(\Omega^+)}\Big)\,\|d_h\|_V. \end{aligned} \tag{4.34}$$

The constant C depends on the constant C_E from (2.27).

Proof. First note that $a_h(u-u_h,d_h) = a_h(u,d_h) - (f,d_h)$. The inconsistency term is then given by

$$a_h(u-u_h,d_h) \;=\; \sum_{T\in\mathcal{T}_h^\Gamma} \int_{T_\Gamma} (\rho^- D_{\boldsymbol{n}^-}u^-)[d_h],$$

where we have used that $\rho^- D_{\boldsymbol{n}^-}u^- = \rho^+ D_{\boldsymbol{n}^+}u^+$ on Γ. We also have used the notation $[d_h] = d_h^+ - d_h^-$. Note that $[d_h](x) = 0$ on the segment line $L_0 \subset T$ tangent to Γ at x_0. Since the distance between this line segment and the curve T_Γ is $O(s^2)$, where we set $s = |T_\Gamma|$, we have that $|[d_h](x)| \le C\|\boldsymbol{X}''\|_{L^\infty}\, s^2|D[d_h](x)|$ on T_Γ. Hence, we have

$$\int_{T_\Gamma} (\rho^- D_{\boldsymbol{n}^-} u^-)[d_h] \;\le\; C\,\kappa\, s^2 \|\sqrt{\rho^-} D_{\boldsymbol{n}^-} u_E^-\|_{L^2(T_\Gamma)} \sqrt{\rho^-}\|D[d_h]\|_{L^2(T_\Gamma)}.$$

For the moment, let us assume that following inequality holds

$$\sqrt{\rho^-}\sqrt{s}\|D[d_h]\|_{L^2(T_\Gamma)} \;\le\; C\, M_T, \tag{4.35}$$

where

$$M_T \;=\;$$
$$\sum_{e\subset\partial T}\left(\sqrt{|e^+|}\|\sqrt{\rho^+}[\![\nabla_h d_h]\!]\|_{L^2(e^+)} + \frac{1}{\sqrt{|e^+|}}\|\sqrt{\rho^+}\, d_h\|_{L^2(e^+)} + \|\sqrt{\rho^+}\nabla_h d_h\|_{L^2(\omega_T^+)}\right)$$
$$+ \sum_{e\subset\partial T}\left(\sqrt{|e^-|}\|\sqrt{\rho^-}[\![\nabla_h d_h]\!]\|_{L^2(e^-)} + \frac{1}{\sqrt{|e^-|}}\|\sqrt{\rho^-}\, d_h\|_{L^2(e^-)} + \|\sqrt{\rho^-}\nabla_h d_h\|_{L^2(\omega_T^-)}\right).$$

Then,

$$\int_{T_\Gamma} (\rho^- D_{\boldsymbol{n}^-} u^-)[d_h] \;\le\; C\,\kappa\, s^{3/2} \|\sqrt{\rho^-} D u_E^-\|_{L^2(T_\Gamma)} M_T.$$

Letting B_s be the ball of radius s centered at x_0 we can use the trace inequality to get

$$\|\sqrt{\rho^-} D u_E^-\|_{L^2(T_\Gamma)} \;\le\; C(\frac{1}{\sqrt{s}}\|\sqrt{\rho^-} D u_E^-\|_{L^2(B_s)} + \sqrt{s}\|\sqrt{\rho^-} D^2 u_E^-\|_{L^2(B_s)}).$$

Hence,

$$\int_{T_\Gamma} (\rho^- D_{\boldsymbol{n}^-} u^-)[d_h] \;\le\; Cs(\|\sqrt{\rho^-} D u_E^-\|_{L^2(B_s)} + s\|\sqrt{\rho^-} D^2 u_E^-\|_{L^2(B_s)}) M_T.$$

We see that (4.34) follows after using that

$$\sum_{T \in \mathcal{T}_h^\Gamma} M_T^2 \;\leq\; C \, \|d_h\|_V^2,$$

the inequality (2.27) and the fact that $s \leq C\, h_T$ (see Lemma A.1.4).

In order to complete the proof we need to prove (4.35). Firstly, by using the triangle inequality we have

$$\sqrt{\rho^-}\sqrt{s}\|D[d_h]\|_{L^2(T_\Gamma)} \;\leq\; \sqrt{\rho^-}\sqrt{s}\left(\|Dd_h^-\|_{L^2(T_\Gamma)} + \|Dd_h^+\|_{L^2(T_\Gamma)}\right).$$

Then by Lemma 4.3.6, there exists an edge e of T such that

$$s \;\leq\; m|e^+|. \tag{4.36}$$

Now let $e = \operatorname{int}(\partial T \cap \partial K)$, for a $K \in \mathcal{T}_h$. Using that Dd_h^+ is constant we get

$$\|Dd_h^+\|_{L^2(T_\Gamma)} \;=\; \sqrt{s}|Dd_h^+| \;=\; \frac{\sqrt{s}}{\sqrt{|e^+|}}\|Dd_h^+\|_{L^2(e^+)} \;\leq\; \sqrt{m}\|Dd_h^+\|_{L^2(e^+)}.$$

According to Lemma 4.3.1

$$|e^+|^2 \;\leq\; \theta \max\{|T^+|, |K^+|\}. \tag{4.37}$$

First, suppose that $|T^+| = \max\{|T^+|, |K^+|\}$. Then,

$$\|\nabla_h d_h^+\|_{L^2(e^+)} \;=\; \frac{\sqrt{|e^+|}}{\sqrt{|T^+|}}\|Dd_h^+\|_{L^2(T^+)}.$$

Hence,

$$\|\nabla_h d_h^+\|_{L^2(e^+)} \;\leq\; \frac{\sqrt{\theta m}}{\sqrt{s}}\|Dd_h^+\|_{L^2(T^+)}.$$

On the other hand, if $|K^+| = \max\{|T^+|, |K^+|\}$ then we have

$$\|\nabla_h d_h^+\|_{L^2(e^+)} \;\leq\; \|D(d_h^+|_T - d_h^+|_K)\|_{L^2(e^+)} + \frac{\sqrt{\theta m}}{\sqrt{s}}\|Dd_h^+\|_{L^2(K^+)}.$$

We write $D(d_h|_T - d_h|_K)$ as its normal part and tangential part, then, use an inverse inequality for the tangential part on e^+, and have

$$\|\nabla_h(d_h^+|_T - d_h^+|_K)\|_{L^2(e^+)} \;\leq\; \|[\![\nabla_h d_h]\!]\|_{L^2(e^+)} + \frac{C}{|e^+|}\|[\![d_h]\!]\|_{L^2(e^+)},$$

therefore,

$$\|\nabla_h d_h^+\|_{L^2(e^+)} \;\leq\; \|[\![\nabla_h d_h]\!]\|_{L^2(e^+)} + \frac{\sqrt{\theta m}}{\sqrt{s}}\|Dd_h^+\|_{L^2(K^+)} + \frac{C}{|e^+|}\|[\![d_h]\!]\|_{L^2(e^+)}.$$

Combining the above inequalities we obtain

$$\begin{aligned}\sqrt{\rho^- s}\|Dd_h^+\|_{L^2(T_\Gamma)} \;\leq\; & \sqrt{m|e^+|}\sqrt{\rho^+}\|[\![\nabla_h d_h]\!]\|_{L^2(e^+)} + \frac{C\sqrt{\rho^+}\sqrt{m}}{\sqrt{|e^+|}}\|[\![d_h]\!]\|_{L^2(e^+)} \\ & + Cm\sqrt{\theta}(\|\sqrt{\rho^+}Dd_h\|_{L^2(T^+)} + \|\sqrt{\rho^+}Dd_h\|_{L^2(K^+)}),\end{aligned}$$

where we have used $\rho^- \leq \rho^+$, so

$$\begin{aligned}\sqrt{\rho^- s}\|Dd_h^+\|_{L^2(T_\Gamma)} \;\leq\; & C\sum_{e\subset\partial T}(\sqrt{m|e^+|}\sqrt{\rho^+}\|[\![\nabla_h d_h]\!]\|_{L^2(e^+)} + \frac{\sqrt{\rho^+}\sqrt{m}}{\sqrt{|e^+|}}\|[\![d_h]\!]\|_{L^2(e^+)}) \\ & + m\sqrt{\theta}\|\sqrt{\rho^+}\nabla_h d_h\|_{L^2(\omega_T^+)}.\end{aligned}$$

Using the same argument we can prove

$$(\rho^- s)^{1/2}\|Dd_h^-\|_{L^2(T_\Gamma)} \;\leq C \sum_{e\subset\partial T}\big(\sqrt{m|e^-|}\sqrt{\rho^-}\|[\![Dd_h]\!]\|_{L^2(e^-)} + \frac{\sqrt{\rho^-}\sqrt{m}}{\sqrt{|e^-|}}\|[\![d_h]\!]\|_{L^2(e^-)}\big)$$
$$+\, Cm\sqrt{\theta}\|\sqrt{\rho^-}\nabla_h d_h\|_{L^2(\omega_T^-)}.$$

Combining the two last inequalities we obtain (4.35). □

Now we would like to state a corollary of Theorem 4.3.1 using regularity of the solution to give error estimates in terms of the data of problem (4.1). We first need some regularity results. We start with a standard energy estimate.

Combining Theorem 4.3.1 and the regularity results for a solution of problem (4.1) studied in Section (2.4.1) we have the following corollary.

Corollary 4.3.1. *Let u be the solution to* (4.1) *and $u_h \in V_h$ be its finite element approximation. If Ω is convex, we have*

$$\|u - u_h\|_V \;\leq\; \frac{C\, h(1+\kappa)}{\sqrt{\rho^-}}\|f\|_{L^2(\Omega)}. \tag{4.38}$$

The constant C depends on the constant C_E from (2.27) *and the constant C_{reg} from* (2.23)*.*

Proof. The result is obtained combining: a priori error estimate in Theorem (4.3.1), estimate (2.17) in Proposition (2.4.1) for the H^1 semi-norm weighted with $\sqrt{\rho^{\pm}}$, and estimate (2.23) in Proposition 2.4.3 (observing that $\rho^- \leq \rho^+$). □

4.3.4 L^2-error estimates

We now prove an L^2 error estimate using standard duality techniques for discontinuous Galerkin methods [26].

Theorem 4.3.2. *Let u be the solution to problem* (4.1) *and $u_h \in V_h$ be its finite element approximation solution to* (4.8). *Assume that Ω is convex. Then, there exists a constant $C > 0$ independent of h, ρ^- and $\rho+$, such that*

$$\|u - u_h\|_{L^2(\Omega)} \ \le \ \frac{C\, h^2(1+\kappa)^2}{\rho^-}\|f\|_{L^2(\Omega)}. \tag{4.39}$$

The constant C depends on C_E from (2.27) *and C_{reg} from* (2.23)

Proof. Let ϕ be a solution of the problem

$$-\rho^{\pm}\Delta\phi^{\pm} = (u-u_h)^{\pm} \qquad \text{in } \Omega^{\pm}, \tag{4.40a}$$

$$\phi = 0 \qquad \text{on } \partial\Omega, \tag{4.40b}$$

$$[\phi] = 0 \qquad \text{on } \Gamma, \tag{4.40c}$$

$$[\rho D_{\boldsymbol{n}}\phi] = 0 \qquad \text{on } \Gamma. \tag{4.40d}$$

We have

$$\|u-u_h\|^2_{L^2(\Omega)} = \int_\Omega (u-u_h)u - \int_\Omega (u-u_h)u_h = a_h(\phi, u) - a_h(\phi_h, u_h),$$

where ϕ_h is the finite element approximation of ϕ. Therefore, we see that

$$\begin{aligned}
\|u-u_h\|^2_{L^2(\Omega)} &= a_h(\phi, u-u_h) + a_h(\phi-\phi_h, u_h) \qquad (4.41)\\
&= a_h(\phi-\phi_h, u-u_h) + a_h(u-u_h, \phi_h) + a_h(\phi-\phi_h, u_h)\\
&= a_h(\phi-\phi_h, u-u_h) + a_h(u-u_h, \phi_h - I_h\phi) + a_h(u-u_h, I_h\phi)\\
&\quad + a_h(\phi-\phi_h, u_h - I_hu) + a_h(\phi-\phi_h, I_hu).
\end{aligned}$$

Using continuity of the bilinear form we have

$$a_h(\phi-\phi_h, u-u_h) \;\le\; C\|\phi-\phi_h\|_W \, \|u-u_h\|_W.$$

Using the triangle inequality we have

$$\|u-u_h\|_W \;\le\; \|u-I_hu\|_W + \|I_hu-u_h\|_W.$$

It is not difficult to show that

$$\|I_hu-u_h\|_W \;\le\; C\|I_hu-u_h\|_V.$$

Hence,

$$\|u-u_h\|_W \;\le\; \|u-I_hu\|_W + \|u-u_h\|_V.$$

Now using Theorem 4.3.5, Theorem 4.3.1, (2.23) and (2.17) we get

$$\|u-u_h\|_W \;\le\; \frac{C\,h(1+\kappa)}{\sqrt{\rho^-}}\|f\|_{L^2(\Omega)}.$$

Similarly,

$$\|\phi-\phi_h\|_W \;\le\; \frac{C\,h(1+\kappa)}{\sqrt{\rho^-}}\|u-u_h\|_{L^2(\Omega)},$$

and hence we have a bound for the first term in (4.41)

$$a_h(\phi - \phi_h, u - u_h) \;\leq\; \frac{C\,h^2(1+\kappa)^2}{\rho^-}\|f\|_{L^2(\Omega)}\,\|u - u_h\|_{L^2(\Omega)}.$$

Using Lemma 4.3.7, (2.23) and (2.17) we have

$$a_h(u - u_h, \phi_h - I_h\phi) \;\leq\; \frac{C\,h(1+\kappa)}{\sqrt{\rho^-}}\|f\|_{L^2(\Omega)}\|I_h\phi - \phi_h\|_V,$$

which implies the following bound for the second term in (4.41)

$$a_h(u - u_h, \phi_h - I_h\phi) \;\leq\; \frac{C\,h^2(1+\kappa)^2}{\rho^-}\|f\|_{L^2(\Omega)}\|u - u_h\|_{L^2(\Omega)}.$$

Analogously, for the fourth term in (4.41)we have

$$a_h(\phi - \phi_h, u_h - I_h u) \;\leq\; \frac{C\,h^2(1+\kappa)^2}{\rho^-}\|f\|_{L^2(\Omega)}\|u - u_h\|_{L^2(\Omega)}.$$

For the third term in (4.41) we have

$$a_h(u - u_h, I_h\phi) \;=\; \sum_{T\in\mathcal{T}_h^\Gamma}\int_{T_\Gamma}(\rho^- D_{\boldsymbol{n}^-}u^-)[I_h\phi]. \tag{4.42}$$

Using the Cauchy-Schwarz inequality we obtain

$$a_h(u - u_h, I_h\phi) \;\leq\; \|\sqrt{\rho^-}D_{\boldsymbol{n}^-}u^-\|_{L^2(\Gamma)}\sqrt{\rho^-}\Big(\sum_{T\in\mathcal{T}_h^\Gamma}\|[I_h\phi]\|^2_{L^2(T_\Gamma)}\Big)^{1/2},$$

For the first term in (4.3.4) we apply a trace inequality to obtain

$$\|\sqrt{\rho^-}D_{\boldsymbol{n}}u^-\|_{L^2(\Gamma)} \;\leq\; C\sqrt{\rho^-}(\|D^2u\|_{L^2(\Omega^-)} + \|Du\|_{L^2(\Omega^-)}) \leq \frac{C}{\sqrt{\rho^-}}\|f\|_{L^2(\Omega)}.$$

where we used (2.23), (2.17) and the fact that $\rho^- \leq \rho^+$. Now for the second term in (4.3.4), we note that $[I_h\phi] = 0$ on L_0 and that L_0 is at most distance $\mathcal{O}(s^2)$ from T_Γ where $s = |T_\Gamma|$. Therefore we can use, Taylor's theorem to show that

$$[I_h\phi](x) \;\leq\; C\|\boldsymbol{X}''\|_{L^\infty} s^2 |D[I_h\phi]|(x) \quad \forall x \in T_\Gamma.$$

Hence,

$$\|[I_h\phi]\|_{L^2(T_\Gamma)} \;\leq\; C\kappa r^2 \|D[I_h\phi]\|_{L^2(T_\Gamma)} \leq C\kappa h_T^2 \|D[I_h\phi]\|_{L^2(T_\Gamma)},$$

where we used that $s \leq C\, h_T$. Consequently, adding and subtracting $D[\phi]$

$$\begin{aligned}\Big(\sum_{T\in\mathcal{T}_h^\Gamma} \|[I_h\phi]\|^2_{L^2(T_\Gamma)}\Big)^{1/2} \;&\leq C\kappa\Big(\sum_{T\in\mathcal{T}_h^\Gamma} h_T^4 \|D[I_h\phi - \phi]\|^2_{L^2(T_\Gamma)}\Big)^{1/2} \\ &\quad + C\kappa\Big(\sum_{T\in\mathcal{T}_h^\Gamma} h_T^4 \|D[\phi]\|^2_{L^2(T_\Gamma)}\Big)^{1/2}.\end{aligned}$$

Observe that

$$h^2\|D[\phi]\|_{L^2(\Gamma)} \leq Ch^2(\|D\phi^+\|_{L^2(\Gamma)} + \|D\phi^-\|_{L^2(\Gamma)}).$$

Application of trace inequality gives

$$\begin{aligned}&\Big(\sum_{T\in\mathcal{T}_h^\Gamma} \|D[\phi]\|^2_{L^2(T_\Gamma)}\Big)^{1/2} \\ &\qquad \leq Ch^2\Big(\|D^2\phi\|_{L^2(\Omega^-)} + \|D\phi\|_{L^2(\Omega^-)} + \|D^2\phi\|_{L^2(\Omega^+)} + \|D\phi\|_{L^2(\Omega^+)}\Big).\end{aligned}$$

For the other term we use that $I_h\phi|_T = I_T\phi$ and use a trace inequality to bound

$$
\begin{aligned}
\|D[I_h\phi-\phi]\|_{L^2(T_\Gamma)} &= \|D[I_T\phi-\phi]\|_{L^2(T_\Gamma)}\\
&\le \frac{C}{\sqrt{h_T}}(\|D(I_T\phi-\phi)\|_{L^2(\omega_T^-)}+\|D(I_T\phi-\phi)\|_{L^2(\omega_T^+)})\\
&\quad + C\sqrt{h_T}(\|D^2\phi\|_{L^2(\omega_T^-)}+\|D^2\phi\|_{L^2(\omega_T^+)}).
\end{aligned}
$$

From (4.15) and (4.16) (using that $\rho^- \le \rho^+$) we obtain

$$
\|D(I_T\phi-\phi)\|_{L^2(\omega_T^-)}+\|D(I_T\phi-\phi)\|_{L^2(\omega_T^+)} \le Ch_T(\|D^2\phi\|_{L^2(\omega_T^-)}+\|D^2\phi\|_{L^2(\omega_T^+)}).
$$

Therefore,

$$
\begin{aligned}
\Big(\sum_{T\in\mathcal{T}_h^\Gamma} h_T^4\|D[I_h\phi-\phi]\|^2_{L^2(T_\Gamma)}\Big)^{1/2} &\le C\,h^2\kappa(\|D^2\phi\|_{L^2(\Omega^-)}+\|D\phi\|_{L^2(\Omega^-)})\\
&\quad + C\,h^2(\|D^2\phi\|_{L^2(\Omega^+)}+\|D\phi\|_{L^2(\Omega^+)}).
\end{aligned}
$$

Hence, using the regularity result (2.23) and (2.17) we have

$$
\sqrt{\rho^-}\Big(\sum_{T\in\mathcal{T}_h^\Gamma}\|[I_h\phi]\|^2_{L^2(T_\Gamma)}\Big)^{1/2} \le \frac{Ch^2\kappa}{\sqrt{\rho^-}}\|u-u_h\|_{L^2(\Omega)}.
$$

Thus, we obtain the bound for the third term in (4.41)

$$
a_h(u-u_h, I_h\phi) \le \frac{Ch^2\kappa}{\rho^-}\|f\|_{L^2(\Omega)}\|u-u_h\|_{L^2(\Omega)}.
$$

In a similar fashion we can prove

$$
a_h(\phi-\phi_h, I_hu) \le \frac{Ch^2\kappa}{\rho^-}\|f\|_{L^2(\Omega)}\|u-u_h\|_{L^2(\Omega)}.
$$

The proof is complete after combining the above inequalities for the terms in (4.41).

□

4.4 Final discussion

4.4.1 Extension to three dimensions

We now show that the space $S(T)$, introduced in (4.6), can easily be extended in three dimensions. We consider the problem (4.1) where Ω is a three dimensional domain and Γ is a simple, closed, $\mathcal{C}^2$ surface. Let now $\mathcal{T}_h$ be a simplicial triangulation of Ω. Let $\mathcal{E}^h$ be all the faces of the mesh $\mathcal{T}_h$. Finally, let $\mathcal{E}_h^\Gamma$ be the set of all faces that belong to a tetrahedron that intersects Γ.

We now define the local finite element space. Let $T \in \mathcal{T}_h$ be a tetrahedron. Let x_0 be a fixed point on $\Gamma \cap T$. Let $\boldsymbol{n}_0^+$ be the outward pointing unit vector normal to Ω^+ at x_0. Let $\boldsymbol{t}_0^+, \boldsymbol{s}_0^+$ be such that $\{\boldsymbol{n}_0^+, \boldsymbol{t}_0^+, \boldsymbol{s}_0^+\}$ forms an orthonormal system.

Given $v \in \mathbb{P}^1(T^+)$ there exists a unique $\Upsilon(v) \in \mathbb{P}^1(T^-)$ satisfying

$$\begin{aligned}
\Upsilon(v)(x_0) &= v(x_0), \\
\left(D_{\boldsymbol{t}_0^+}\Upsilon(v)\right)(x_0) &= \left(D_{\boldsymbol{t}_0^+}v\right)(x_0), \\
\left(D_{\boldsymbol{s}_0^+}\Upsilon(v)\right)(x_0) &= \left(D_{\boldsymbol{s}_0^+}v\right)(x_0), \\
\rho^-\left(D_{\boldsymbol{n}_0^+}\Upsilon(v)\right)(x_0) &= \rho^+\left(D_{\boldsymbol{n}_0^+}v\right)(x_0).
\end{aligned}$$

Given $T \in \mathcal{T}_h^\Gamma$ and for each $v \in \mathbb{P}^1(T^+)$ we can consider the unique corresponding function

$$G(v) = \begin{cases} v & \text{in } T^+, \\ \Upsilon(v) & \text{in } T^-. \end{cases}$$

Let span $\{v_1, v_2, v_3, v_4\}$ be a basis for $\mathbb{P}^1(T)$ restricted to T^+. Then we define the local finite element space

$$S(T) \;=\; \begin{cases} \text{span } \{G(v_1), G(v_2), G(v_3), G(v_4)\} & , \text{ if } T \in \mathcal{T}_h^\Gamma; \\ \mathbb{P}^1(T) & , \text{ if } T \in \mathcal{T}_h \backslash \mathcal{T}_h^\Gamma. \end{cases}$$

Consequently, the global finite element space is given by

$$V_h \;:=\; \left\{ v \,:\, v|_T \in S(T),\, \forall T \in \mathcal{T}_h,\, v \text{ is continuous across all faces in } \mathcal{E}_h \backslash \mathcal{E}_h^\Gamma \right\}.$$

The numerical method is now given by (4.8), where $e^\pm = e \cap \Omega^\pm$ are pieces of e a face of a tetrahedra.

4.4.2 Alternative local spaces

An alternative approach to enforce weak continuity of our local space $S(T)$ is normally used in the literature (see [38]). Instead of enforcing continuity of function and tangential derivative at x_0 one imposes continuity at two distinct points x_1, x_2. More precisely, define x_1, x_2 be the two points in Γ that intersect ∂T. Then, one can define $\Upsilon(v)$ (in contrast to the definition in Lemma 4.1.1) by

$$\begin{aligned}
\Upsilon(v)(x_i) &= v(x_i) \qquad \text{for } i = 1,2 \\
\rho^-(D_{\boldsymbol{n}_0^+}\Upsilon(v))(x_0) &= \rho^+(D_{\boldsymbol{n}_0^+}v)(x_0).
\end{aligned}$$

Subsequently, $I_T u$ is now defined by

$$\begin{aligned}
(I_T^- u)(x_i) &:= \quad (J_T u_E^+)(x_i) \quad =: (I_T^+ u)(x_i) \qquad \text{for } i = 1,2 \\
\rho^-(D_{\boldsymbol{n}_0^+} I_T^- u)(x_0) &:= \rho^+(D_{\boldsymbol{n}_0^+} J_T u_E^+)(x_0) =: \rho^+(D_{\boldsymbol{n}_0^+} I_T^+ u)(x_0).
\end{aligned}$$

Defining the finite element method using these local spaces, we can prove all the a-priori estimates above.

Another alternative is to enforce the matching conditions by averaging on T_Γ. More precisely, one can redefine $\Upsilon(v)$ in Lemma 4.1.1 by

$$\begin{aligned}
\int_{T_\Gamma} \Upsilon(v)\, ds &:= \int_{T_\Gamma} v, \\
\int_{T_\Gamma} \Upsilon(v)\, s\ ds &:= \int_{T_\Gamma} v\, s, \\
\int_{T_\Gamma} \rho^+ D_{\boldsymbol{n}^+}\Upsilon(v) &:= \int_{T_\Gamma} \rho^- D_{\boldsymbol{n}^+} v,
\end{aligned}$$

or alternatively, one can replace the second equation by

$$\int_{T_\Gamma} D_{\boldsymbol{t}^+}\Upsilon(v)\, ds := \int_{T_\Gamma} D_{\boldsymbol{t}^+}\, v ds.$$

Even though their numerical implementation is more complicated and require numerical integrations, these alternatives have the advantage that the analysis is shorter especially for the consistency error, and also can be formulated using Lagrange multipliers [5].

4.4.3 Extension to Cartesian grids

We note that the analysis and methods developed here can be easily extended to Cartesian grids and $\mathbb{Q}^1$ elements. One possibility would be to use same local spaces $S(T)$ defined before for quadrangular elements $T \in \mathcal{T}_h^\Gamma$, that is, one has three degrees of freedom for $T \in \mathcal{T}_h^\Gamma$ and four degrees otherwise. In case one wants to have four degrees of freedom for $T \in \mathcal{T}_h^\Gamma$, let the space $S(T)$ then be a piecewise bilinear function under the coordinates $\boldsymbol{n}_0, \boldsymbol{t}_0$ and impose

$$\begin{aligned}
\Upsilon(v)(x_0) &:= v(x_0)\\
(D_{\boldsymbol{t}_0^+}\Upsilon(v))(x_0) &:= (D_{\boldsymbol{t}_0^+}v)(x_0)\\
\rho^-(D_{\boldsymbol{n}_0^+}\Upsilon(v))(x_0) &:= \rho^+(D_{\boldsymbol{n}_0^+}v)(x_0)\\
\rho^-(D_{\boldsymbol{n}_0^+}D_{\boldsymbol{t}_0^+}\Upsilon(v))(x_0) &:= \rho^+(D_{\boldsymbol{n}_0^+}D_{\boldsymbol{t}_0^+}v)(x_0)
\end{aligned}$$

4.4.4 Alternative bilinear forms

In this section we discuss alternative bilinear forms. We will point out what are the theoretical difficulties in analyzing these alternative methods. When we provide numerical experiments in the following section we will also see that, although we cannot prove stability for some methods, they sometimes do well experimentally in some of the norms.

Firstly, formulation without flux stabilization has been used for example in [84].

Methods (4.43) and (4.44) experiment this direction.

$$a_h(w,v) := \int_\Omega \rho\nabla_h w\cdot\nabla_h v - \sum_{e\in\mathcal{E}_h^\Gamma}\int_e \left(\{\rho\nabla_h v\}\cdot[\![w]\!] + \{\rho\nabla_h w\}\cdot[\![v]\!]\right) \tag{4.43}$$
$$+\,\gamma\sum_{e\in\mathcal{E}_h^\Gamma}\frac{1}{|e|}\left(\int_{e^-}\rho^-[\![w]\!]\cdot[\![v]\!] + \int_{e^+}\rho^+[\![w]\!]\cdot[\![v]\!]\right).$$

$$a_h(w,v) := \int_\Omega \rho\nabla_h w\cdot\nabla_h v - \sum_{e\in\mathcal{E}_h^\Gamma}\int_e \left(\{\rho\nabla_h v\}\cdot[\![w]\!] + \{\rho\nabla_h w\}\cdot[\![v]\!]\right) \tag{4.44}$$
$$+\,\gamma\sum_{e\in\mathcal{E}_h^\Gamma}\left(\frac{1}{|e^-|}\int_{e^-}\rho^-[\![w]\!]\cdot[\![v]\!] + \frac{1}{|e^+|}\int_{e^+}\rho^+[\![w]\!]\cdot[\![v]\!]\right).$$

The problem with these methods is that we cannot establish neither the optimal inconsistency error nor the coercivity independent of the contrast and the mesh. This is due since in our proofs the presence of the flux stabilization terms, not appearing in (4.44) nor (4.43), allows us to transfer estimates in an element with a small portion in $\Omega^\pm$ to a neighbor element with a larger portion in the sub-domain, avoiding mixing of the estimates in the different sub-domains.

We note that methods (4.43) and (4.44) seem to do well numerically in the L^2 and energy norms, however, they are mesh dependent in the L^∞ norm and they do not converge in the weighted $W^{1,\infty}$ norm.

The method that seems to do the best numerically, slightly better than the proposed method, is the following one:

$$
\begin{aligned}
a_h(w,v) \;:=\; & \int_\Omega \rho \nabla_h w \cdot \nabla_h v - \sum_{e \in \mathcal{E}_h^\Gamma} \int_e \left(\{\rho \nabla_h v\} \cdot [\![w]\!] + \{\rho \nabla_h w\} \cdot [\![v]\!] \right) \qquad (4.45)\\
& + \gamma \sum_{e \in \mathcal{E}_h^\Gamma} \left(\frac{1}{|e^-|} \int_{e^-} \rho^- [\![w]\!] \cdot [\![v]\!] + \frac{1}{|e^+|} \int_{e^+} \rho^+ [\![w]\!] \cdot [\![v]\!] \right)\\
& \gamma_F \sum_{e \in \mathcal{E}_h^\Gamma} |e| \left(\int_{e^-} \rho^- [\![\nabla_h v]\!]\, [\![\nabla_h w]\!] + \int_{e^+} \rho^+ [\![\nabla_h v]\!]\, [\![\nabla_h w]\!] \right).
\end{aligned}
$$

The difference between this method and the one analyzed in this paper is that we are using a stronger flux stabilization (i.e. we replace $|e^{\pm}|$ by $|e|$ and we introduce a flux stabilization parameter γ_F). It is not difficult to see, that we can prove all the error estimates contained in this paper for this method. In particular, the coercivity of the bilinear form is obvious since we are adding even more stabilization. Clearly, now we would have to redefine our V and W norms but the approximation properties will still hold. In summary, Theorem 4.3.1 and Corollaries 4.3.1 and 4.3.2 hold for this formulation.

A very natural question would be if we can penalize the jump terms with $1/|e|$ instead of $1/|e^{\pm}|$ and get a stable and optimally convergent method independent of contrast. The answer is yes, as long as we penalize the jump of the full gradient instead of the flux.

$$
\begin{aligned}
a_h(w,v) \;:=\; & \int_\Omega \rho \nabla_h w \cdot \nabla_h v - \sum_{e \in \mathcal{E}_h^\Gamma} \int_e \left(\{\rho \nabla_h v\} \cdot [\![w]\!] + \{\rho \nabla_h w\} \cdot [\![v]\!] \right) \qquad (4.46)\\
& + \gamma \sum_{e \in \mathcal{E}_h^\Gamma} \frac{1}{|e|} \left(\int_{e^-} \rho^- [\![w]\!] \cdot [\![v]\!] + \int_{e^+} \rho^+ [\![w]\!] \cdot [\![v]\!] \right)\\
& \gamma_F \sum_{e \in \mathcal{E}_h^\Gamma} |e| \left(\int_{e^-} \rho^- \left[\nabla v\right]_\otimes \cdot \left[\nabla w\right]_\otimes + \int_{e^+} \rho^+ \left[\nabla v\right]_\otimes \cdot \left[\nabla w\right]_\otimes \right),
\end{aligned}
$$

where the jumps in the last line are defined by

$$[\nabla v]_{\otimes} = \nabla v^{-} \otimes \boldsymbol{n}^{-} + \nabla v^{+} \otimes \boldsymbol{n}^{+}.$$

and the symbol $\otimes$ denotes the outer product between vectors.

We note that in the coercivity and inconsistency error analysis proofs, we have used the inverse inequality $|e^-| \, \|D_{\boldsymbol{n}} v\|_{L^2(e^-)} \leq C \, \|\nabla v\|_{L^2(T^-)}$ (where T^- is a triangle with edge e, and similar result for e^+) in particular in the estimation of the left-hand side of (4.28). For method (4.46) we want to avoid using this inverse estimate and the factor $1/|e^-|$ (also $1/|e^+|$). Let x be the vertex of e belonging to Ω^-. Using the ideas in the proof of Lemma 4.3.1, we can find a sequence of elements $\{T_2, T_3, \cdots, T_N\}$ in the patch of x, and common edges $\{e_2, e_3, \cdots, e_{N-1}\}$ with $\bar{e}_i = \overline{T}_i \cap \overline{T}_{i+1}$ and $e_i^- := e_i \cap \Omega^-$, such that, $|e^-| \leq \sigma |e_2^-| \leq \sigma^2 |e_3^-| \leq \sigma^{N-2} |e_{N-1}^-| = \sigma^{N-1} |e|$ where σ a positive constant bounded uniformly from below by zero and N is bounded depending on the shape regularity of the mesh. Then, we bound the left-hand side of (4.28) by using recursively

$$\|\nabla v|_{T_{i-1}}\|^2_{L^2(e_i^-)} \leq 2 \left(\| \, [\nabla v]_{\otimes} \, \|^2_{L^2(e_i^-)} + \|\nabla v|_{T_i}\|^2_{L^2(e_i^-)} \right),$$

and

$$\|\nabla v|_{T_i}\|^2_{L^2(e_i^-)} \leq 1/\sigma \|\nabla v|_{T_i}\|^2_{L^2(e_{i+1}^-)},$$

and then use that

$$\|\nabla v|_{T_N}\|^2_{L^2(e_{N-1}^-)} \leq (C/|e|) \, \|\nabla v\|^2_{L^2(T_N^-)}.$$

Hence,

$$|e| \, \|\nabla v\|^2_{L^2(e^-)} \leq C \sum_{i=2}^{N} |e| \, \| \, [\nabla v]_{\otimes} \, \|^2_{L^2(e_i^-)} + \frac{C}{|e|} \, \|\nabla v\|^2_{L^2(T_N^-)}.$$

4.4.5 Concluding remarks

In this chapter rigorous error estimates independent of contrast were derived. However, many interesting research questions remain. Firstly, we kept track, as much as possible, of how the constants depend on the geometry (e.g. curvature). However, there are two constants, C_E and C_{reg}, that we did not investigate in detail how they scale with geometric quantities such as maximum curvature and the radius r of the tubular neighborhood. We believe it is possible to prove a bound for C_E in terms of geometric quantities, but for the sake of simplicity we did not investigate it here. In addition, the regularity constant C_{reg} appearing in (2.23) depends on the geometry. Addressing these issues will lead to error estimates that are completely explicit on their dependence on the curvature and radius r of the tubular neighborhood.

Secondly, our method and error estimates do not consider problems with high curvature. An interesting line of research would be to investigate problems with interfaces of arbitrary curvature. In this direction, perhaps a combination of the method presented here and the multicale method by Chu et al. in [38] could be a possible approach.

Thirdly, rigorous error analysis for higher order Immersed Finite Element methods ($k > 1$) remains open. It would be interesting to study this, in particular, for high-contrast problems.

Finally, we would like to study the sharpness of our assumptions in Assumption 2.1. For instance, we observe that our method is still well-defined without assumption 3.

4.5 Numerical examples

In this section we explore the properties of the methods presented in sections above applied to the two dimensional interface problem (4.1). In particular, we are interested in the computation of the following errors and their respective ratio of convergence

$$
\begin{aligned}
e_h^0 &:= \|u-u_h\|_{L^2(\Omega)}, & e_h^\infty &:= \|u-u_h\|_{L^\infty(\Omega)},\\
e_{h,\sqrt{\rho}}^1 &:= \|\sqrt{\rho}\nabla_h(u-u_h)\|_{L^2(\Omega)}, & e_{h,\sqrt{\rho}}^{1,\infty} &:= \|\sqrt{\rho}\nabla_h(u-u_h)\|_{L^\infty(\Omega)},\\
e_{h,\rho}^1 &:= \|\rho\nabla_h(u-u_h)\|_{L^2(\Omega)}, & e_{h,\rho}^{1,\infty} &:= \|\rho\nabla_h(u-u_h)\|_{L^\infty(\Omega)},\\
e_{h,\rho}^{\boldsymbol{n},\infty} &:= \|\rho D_{\boldsymbol{n}}(u-u_h)\|_{L^\infty(\Gamma)}, & \tilde{e}_{h,\rho}^{1,\infty} &:= \|\rho\nabla_h(u-u_h)\|_{L^\infty(\Omega\setminus(\cup\{T:T\in\mathcal{T}_h^\Gamma\}))}
\end{aligned}
$$

$$
\operatorname{eoc}(e) := \frac{\log(e_{h_{l+1}}/e_{h_l})}{\log(h_{l+1}/h_l)}.
$$

Computation (or approximation) of the L^∞ norms are performed evaluating the error at the following set of points: if an element does not intersect the interface then the set of points are the nodes and the centroid of the element, if the element does intersect the interface we evaluate at the nodes and at the two points intersections of the interface with the edges of the element. We observe that the errors corresponding to the L^2 norm and $W^{1,2}$ weighted with $\sqrt{\rho}$ semi-norm correspond to the only results proved in this paper, Theorem 4.3.2 and 4.3.1 respectively. We expect optimal convergence, second order in the L^2 norm and first order in the weighted $W^{1,2}$ semi-norm. We also compute the analogous in the L^∞ norm and $W^{1,\infty}$ weighted with $\sqrt{\rho}$ semi-norm. In addition, we compute the errors in the $W^{1,2}$ and $W^{1,\infty}$ semi-norm weighted with ρ. Note that the estimate for the interpolation error is also achieved in this semi-norm. Indeed, this is a consequence of Lemma 4.2.2 and Proposition

2.4.3 and 2.4.2

$$\|\rho\nabla_h(u - I_h u)\|_{L^2(\Omega)} \leq Ch\|f\|_{L^2(\Omega)}.$$

A revealing result of our experiments is that the ratio of convergence of the error is optimal when we compute using the triangles non intersecting the interface. Error $\tilde{e}^{1,\infty}_{h,\rho}$ illustrates this observation. Finally, error $e^{\boldsymbol{n},\infty}_{h,\rho}$ is a standard error for interface problems, illustrating the approximation of the normal derivative on the interface.

The experiment presented below shows that method (4.8)-(4.45) produces the best results. This method (and all the others) does not seem optimal for the $W^{1,\infty}$ error weighted with ρ. However, it is optimal when we do not consider the elements in $\mathcal{T}_h^\Gamma$. We highlight that this result was not remotely addressed in this paper, and this kind of estimates appear to be more difficult. For the method that we analyzed (4.8)-(4.9) we observe an uncertain behavior in the error $e^{1,\infty}_{h,\rho}$ for the last mesh, not achieving the optimal convergence as in the previous method. We also present tables for one of the method without flux stabilization, method (4.8)-(4.44). We observe non convergence so far for the error $e^{1,\infty}_{h,\sqrt{\rho}}$ and in the last mesh a deterioration in the L^∞ norm. Moreover, optimal convergence for the normal flux error $e^{\boldsymbol{n},\infty}_{h,\rho}$ is not observed.

In our numerical experiments we consider the two dimensional domain $\Omega = (-1,1)^2$ with the immersed interface $\Gamma = \{\boldsymbol{x} \in \Omega : x^2 + y^2 = (1/3)^2\}$. We define $\Omega^- := \{(x,y) \in \Omega : x^2 + y^2 < (1/3)^2\}$ and $\Omega^+ = \Omega\backslash(\Omega^- \cup \Gamma)$. Numerical examples 4.1 and 4.2 consider the following exact solution

$$u(x,y) = \begin{cases} \frac{r^\alpha}{\rho^-} & , \text{ if } (x,y) \in \Omega^-, \\ \frac{r^\alpha}{\rho^+} + \left(\frac{1}{3}\right)^\alpha \left(\frac{1}{\rho^-} - \frac{1}{\rho^+}\right) & , \text{ if } (x,y) \in \Omega^+, \end{cases} \tag{4.47}$$

where $r = \sqrt{x^2 + y^2}$ and $\alpha = 2$. Example 4.1 considers the configuration $\Gamma = \partial\Omega^-$ (Ω^- as the inclusion), whilst Example 4.2 considers $\Gamma = \partial\Omega^+$ (Ω^+ as the inclusion). We provide plots of the approximate solution for both cases.

Finite element uniform triangular meshes $\mathcal{T}_h$ that are non-fitted with the interface were used. In the tables we compute with $h = 2^{-(l+3/2)}$, for $l = 1, ..., 7$.

All the computations were performed in MATLAB, including solution of the linear system by means of "\".

Example 4.1. Case $\Gamma = \partial\Omega^-$ (i.e. Ω^- is the inclusion), $\rho^+ = 10^4$ and $\rho^- = 1$. Tables 4.1 and 4.2 show the results obtained by method (4.8)-(4.45) with stabilization parameters $\gamma = 10$ and $\gamma_F = 10$. Note that this method has a stronger flux stabilization that the method analyzed in the paper.

The results in Table 4.1 show optimal convergence for the errors e_h^1 and e_h^0 validating the theoretical results Theorem 4.3.1 and 4.3.2. In addition, we observe optimal convergence for the error e_h^∞ and $e_{h,\sqrt{\rho}}^{1,\infty}$. The error $e_{h,\rho}^1$, weighted with ρ instead of $\sqrt{\rho}$, converges optimally. However, the rate of convergence of the error $e_{h,\rho}^{1,\infty}$ is not optimal. An interesting observation is that the error $\tilde{e}_{h,\rho}^{1,\infty}$ converges optimally, indicating that is only a couple of elements where the error does not converge. Another appealing feature of the method is the optimal order of convergence for the error $e_{h,\rho}^{\boldsymbol{n},\infty}$.

In addition, in order to test the independence of the coefficient $\rho^\pm$ of our estimate

l	e_h^0	eoc	e_h^∞	eoc	$e^1_{h,\sqrt{\rho}}$	eoc	$e^{1,\infty}_{h,\sqrt{\rho}}$	eoc
1	8.2e-3	–	2.5e-2	–	1.1e-1	–	3.7e-1	–
2	1.7e-3	2.28	5.7e-3	2.12	4.4e-2	1.30	2.1e-1	0.86
3	2.7e-4	2.63	1.3e-3	2.19	1.8e-2	1.29	9.7e-2	1.08
4	4.6e-5	2.57	3.2e-4	1.97	8.3e-3	1.12	5.2e-2	0.90
5	9.0e-6	2.34	7.2e-5	2.15	3.9e-3	1.07	2.5e-2	1.08
6	2.0e-6	2.19	1.8e-5	2.01	1.9e-3	1.03	1.3e-2	0.92
7	4.7e-7	2.08	4.6e-6	1.94	9.5e-4	1.02	6.8e-3	0.94

l	$e^1_{h,\rho}$	eoc	$e^{1,\infty}_{h,\rho}$	eoc	$\tilde{e}^{1,\infty}_{h,\rho}$	eoc	$e^{\boldsymbol{n},\infty}_{h,\rho}$	eoc
1	3.9e-1	–	7.0e-1	–	7.0e-1	–	3.7e-1	–
2	1.6e-1	1.32	6.1e-1	0.19	4.0e-1	0.81	2.1e-1	0.86
3	6.4e-2	1.29	1.9e-1	1.68	1.9e-1	1.07	9.7e-2	1.08
4	2.9e-2	1.15	2.2e-1	-0.20	1.0e-1	0.91	4.9e-2	1.00
5	1.4e-2	1.09	1.4e-1	0.65	5.0e-2	1.01	2.5e-2	0.98
6	6.6e-3	1.04	6.6e-2	1.09	2.5e-2	0.99	1.2e-2	1.00
7	3.2e-3	1.02	5.1e-1	-2.95	1.3e-2	0.98	6.2e-3	1.00

Table 4.1: Example 4.1: errors and experimental orders of convergence (eoc) with $\rho^- = 1$ and $\rho^+ = 10^4$, using method (4.8)-(4.45) with stabilization parameters $\gamma = 10$ and $\gamma_F = 10$.

ρ^+	e_h^0	$e^1_{h,\rho}$	$e^1_{h,\sqrt{\rho}}$
10^1	2.3e-6	6.5e-3	2.8e-3
10^2	2.0e-6	6.6e-3	2.0e-3
10^3	2.0e-6	6.6e-3	1.9e-3
10^4	2.0e-6	6.6e-3	1.9e-3
10^5	2.0e-6	6.6e-3	1.9e-3
10^6	2.0e-6	6.6e-3	1.9e-3

Table 4.2: Example 4.1: errors with $\rho^- = 1$ and $h = 2^{-(6+3/2)}$, using method (4.8)-(4.45) with stabilization parameters $\gamma = 10$ and $\gamma_F = 10$.

in Theorem 4.3.1, we consider the exact solution (4.47) with a fix mesh corresponding to $h = 2^{-(5+3/2)}$. We compute errors e_h^0, $e_{h,\rho}^1$ and $e_{h,\sqrt{\rho}}^1$ for $\rho^- = 1$ and increasing values of ρ^+. We summarize the results in Table 4.2. We observe that although we increase ρ^+ the errors remain constant, showing the contrast independency of our estimates.

We present in Table 4.3 the errors and convergence orders for the method analyzed in the paper (4.8)-(4.9).

l	e_h^0	eoc	e_h^∞	eoc	$e_{h,\sqrt{\rho}}^1$	eoc	$e_{h,\sqrt{\rho}}^{1,\infty}$	eoc
1	8.6e-3	–	2.6e-2	–	1.1e-1	–	3.7e-1	–
2	1.7e-3	2.31	6.0e-3	2.14	4.5e-2	1.30	2.0e-1	0.90
3	2.8e-4	2.63	1.3e-3	2.18	1.8e-2	1.31	9.3e-2	1.09
4	4.7e-5	2.57	3.4e-4	1.97	8.4e-3	1.12	5.5e-2	0.76
5	9.2e-6	2.35	7.6e-5	2.16	4.0e-3	1.08	2.6e-2	1.09
6	2.0e-6	2.20	1.9e-5	2.01	1.9e-3	1.03	1.4e-2	0.91
7	4.7e-7	2.09	5.1e-6	1.88	9.5e-4	1.02	7.1e-2	-2.37

l	$e_{h,\rho}^1$	eoc	$e_{h,\rho}^{1,\infty}$	eoc	$\tilde{e}_{h,\rho}^{1,\infty}$	eoc	$e_{h,\rho}^{\boldsymbol{n},\infty}$	eoc
1	4.0e-1	–	7.4e-1	–	7.4e-1	–	3.7e-1	–
2	1.6e-1	1.33	2.5e+0	-1.79	4.0e-1	0.90	2.0e-1	0.90
3	6.4e-2	1.31	2.8e-1	3.20	1.9e-1	1.07	9.2e-2	1.11
4	2.9e-2	1.15	1.6e+0	-2.56	9.7e-2	0.96	4.5e-2	1.01
5	1.4e-2	1.09	4.8e-1	1.76	4.7e-2	1.04	2.3e-2	0.96
6	6.6e-3	1.05	4.8e-1	0.01	2.4e-2	1.00	1.1e-2	1.05
7	3.2e-3	1.02	7.1e+0	-3.88	1.8e-2	0.42	5.9e-3	0.93

Table 4.3: Example 4.1: errors and experimental orders of convergence (eoc) with $\rho^- = 1$ and $\rho^+ = 10^4$, using method (4.8)-(4.9) with stabilization parameter $\gamma = 10$.

The results in Table 4.3 show optimal convergence for the errors $e_{h,\sqrt{\rho}}^1$ and e_h^0 validating the theoretical results Theorem 4.3.1 and 4.3.2. In addition we observe optimal convergence for the error e_h^∞. The error $e_{h,\sqrt{\rho}}^{1,\infty}$ seems to converge optimal up to mesh $l = 6$, and then for the last mesh the rate can possibly be affected by the choice of the flux stabilization parameter. As in the previous test the error $\bar{e}_h^1$ converges optimally, however for the rest of the errors the convergence is not as clear as in the previous method. We suspect that this phenomena is related to the weights $|e^{\pm}|$ in the flux stabilization.

Finally, Table 4.4 displays error and convergence orders for the method without flux stabilization (4.8)-(4.44).

l	e_h^0	eoc	e_h^∞	eoc	$e^1_{h,\sqrt{\rho}}$	eoc	$e^{1,\infty}_{h,\sqrt{\rho}}$	eoc
1	1.7e-3	–	7.0e-3	–	5.8e-2	–	2.2e-1	–
2	4.5e-3	1.88	2.9e-3	1.29	3.1e-2	0.89	1.6e-1	0.51
3	3.6e-4	0.31	6.1e-3	-1.08	1.2e-1	-1.89	1.3e+1	-6.37
4	2.8e-5	3.69	2.1e-4	4.87	7.7e-3	3.92	2.0e-1	5.98
5	7.3e-6	1.96	5.0e-5	2.05	3.8e-3	1.02	1.5e-1	0.40
6	1.7e-6	2.06	1.2e-5	2.05	1.9e-3	1.01	2.5e-2	-0.70
7	4.5e-7	1.95	4.0e-6	1.60	9.5e-4	0.99	1.1e-1	0.23

l	$e^1_{h,\rho}$	eoc	$e^{1,\infty}_{h,\rho}$	eoc	$\tilde{e}^{1,\infty}_{h,\rho}$	eoc	$e^{\boldsymbol{n},\infty}_{h,\rho}$	eoc
1	2.1e-1	–	5.8e-1	–	2.2e-1	–	1.5e-1	–
2	1.3e-1	0.69	1.4e+1	-4.58	1.5e-1	0.49	1.1e-1	0.39
3	7.3e-1	-2.46	1.3e+2	0.10	8.9e-1	-2.5	1.3e+1	-6.83
4	2.8e-2	4.70	7.2e+0	0.84	5.3e-2	4.07	2.0e-1	6.00
5	1.3e-2	1.07	2.6e+0	1.50	2.9e-2	0.86	1.5e-1	0.39
6	7.0e-3	0.93	2.1e+0	0.27	3.7e-2	-0.35	2.5e-1	-0.71
7	3.3e-3	0.99	8.6e+0	-2.10	2.1e-2	0.86	1.1e-3	0.23

Table 4.4: Example 4.1: errors and experimental orders of convergence (eoc) with $\rho^- = 1$ and $\rho^+ = 10^4$, using method (4.8)-(4.44) with stabilization parameter $\gamma = 10$.

The results in Table 4.4 show optimal asymptotical convergence for the errors $e^1_{h,\sqrt{\rho}}$ and e^0_h. In addition we observe a slightly sub-optimal convergence for the error e^∞_h, approximately 1.8. The error $e^{1,\infty}_{h,\sqrt{\rho}}$ does not seem to converge. As in the previous test the error $e^1_{h,\rho}$ converges asymptotically to 1, however for the rest of the errors we do not observe convergence.

Example 4.2. Case $\Gamma = \partial\Omega^+$ (i.e. Ω^+ is the inclusion), $\rho^+ = 10^4$ and $\rho^- = 1$. Table 4.5 show the results obtained by method (4.8)-(4.45) with stabilization parameters $\gamma = 10$ and $\gamma_F = 10$.

l	e_h^0	eoc	e_h^∞	eoc	$e_{h,\sqrt{\rho}}^1$	eoc	$e_{h,\sqrt{\rho}}^{1,\infty}$	eoc
1	2.2e-2		2.4e-2		4.1e-1		7.4e-1	
2	5.3e-3	2.06	6.2e-3	1.95	2.0e-1	1.01	3.8e-1	0.97
3	1.3e-3	2.02	1.6e-3	1.98	1.0e-1	1.01	1.9e-1	0.98
4	3.2e-4	2.01	4.0e-4	1.99	5.1e-2	1.00	9.6e-2	0.99
5	8.1e-5	2.00	1.0e-4	1.99	2.5e-2	1.00	4.8e-2	1.00
6	2.0e-5	2.00	2.5e-5	2.00	1.3e-2	1.00	2.4e-2	1.00
7	5.1e-6	2.00	6.3e-6	2.00	6.4e-3	1.00	1.2e-2	1.00

Table 4.5: Example 4.2: errors and experimental orders of convergence (eoc) with $\rho^- = 1$ and $\rho^+ = 10^4$, using method (4.8)-(4.45) with stabilization parameters $\gamma = 10$ and $\gamma_F = 10$.

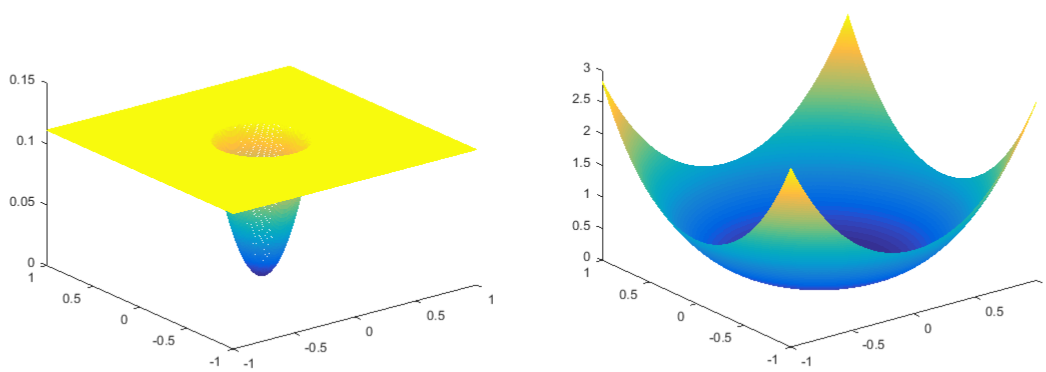

Figure 4.3: Approximate solutions by method (4.8)-(4.45) of problem (4.1). Left figure: Example 4.1 case $\Gamma = \partial\Omega^-$. Right figure: Example 4.2 case $\Gamma = \partial\Omega^+$.

Chapter Five

High contrast interface problem II: analysis of a Nitsche finite element method

5.1 Unfitted Nitsche finite element method

This chapter is devoted to the analysis of an stabilized Nitsche finite element method based on piecewise linear polynomials, applied to the Poisson interface problem with constant discontinuous coefficients (4.1), and using triangulations that are non-fitted with the interface.

5.1.1 Introduction

We begin rewriting the equations of the model problem. Let $\Omega \subset \mathbb{R}^2$ be an open polygonal domain with an immersed smooth interface Γ such that $\overline{\Omega} = \overline{\Omega}^- \cup \overline{\Omega}^+$ and Γ encloses either Ω^- or Ω^+. Consider the problem

$$-\nabla \cdot (\rho^\pm \nabla u^\pm) = f^\pm \quad \text{in } \Omega^\pm, \tag{5.1a}$$

$$u^\pm = 0 \quad \text{on } \partial\Omega^\pm \backslash \Gamma, \tag{5.1b}$$

$$[u] = \alpha \quad \text{on } \Gamma, \tag{5.1c}$$

$$[\rho \nabla u \cdot \boldsymbol{n}] = \beta \quad \text{on } \Gamma, \tag{5.1d}$$

where $u^\pm \equiv u|_{\Omega^\pm}$ and the jumps on Γ defined as before (4.2). We recall that the diffusion coefficients $\rho^+ \geq \rho^- > 0$ are constant. We will present a priori error analysis for the case $\alpha, \beta \equiv 0$. The method that we will present and analyze in this chapter for the case of homogeneous jump conditions is a variant (simplification without weighted averages) of the method introduced in [33]. This method includes a stabilization term, also known as *ghost penalty* stabilization term, with support on edges near the interface. See also [64] for the method without this stabilization term. The final goal of this chapter is to prove optimal error estimates independent of the constant of the discontinuous constant coefficients.

In this section we introduce a slightly simplified version of the unfitted Nitsche finite element method for high contrast interface problems by Burman and Zunino, Section 3.3 in [33]. The main idea behind this method differs substantially from those that help us to design the finite element approximations in the previous chapters. Here, by means of extension lemmas (see Section 2.4), we will consider the continuous solution of problem (5.1) as a pair of functions (u^-, u^+) with support slightly bigger than Ω^- and Ω^+, respectively.

5.1.2 Notation

We begin introducing the discrete sub-domains $\Omega_h^\pm$ containing the sub-domains $\Omega^\pm$

$$\Omega_h^\pm := \operatorname{int}\Big(\bigcup_{T\in\mathcal{T}_h^\pm} \overline{T}\Big). \tag{5.2}$$

In addition, we consider the edges subset of $\mathcal{E}_h^\Gamma$, Definition (2.2.8), restricted to the interior of $\Omega_h^\pm$

$$\mathcal{E}_h^{\Gamma,\pm} := \{e = \operatorname{int}(\partial T_1 \cap \partial T_2) : T_1, T_2 \in \mathcal{T}_h^\pm,\ \text{and } T_1 \cap \Gamma \neq \emptyset \text{ or } T_2 \cap \Gamma \neq \emptyset\}.$$

Let us define the broken Sobolev spaces (note that they differ from the ones defined in the previous chapter)

$$H_h^2(\Omega_h^\pm) := \{v \in H^1(\Omega_h^\pm) : v|_{T^\pm} \in H^2(T^\pm),\ \text{for all } T \in \mathcal{T}_h^\pm\}.$$

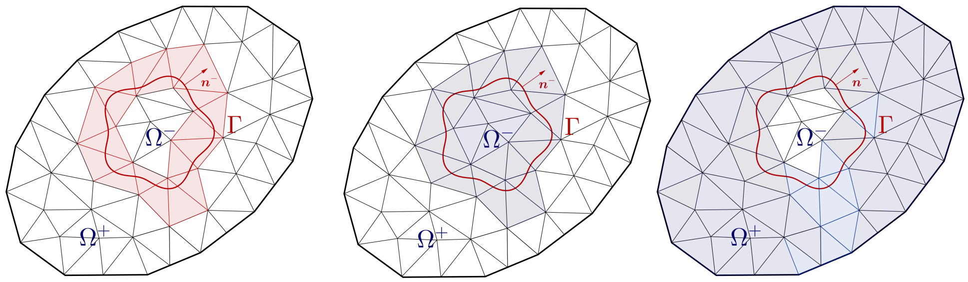

Figure 5.1: Illustration of definition of set $\mathcal{T}_h^\Gamma$ and discrete sub-domains $\Omega_h^\pm$. Left figure: elements in $\mathcal{T}_h^\Gamma$ (red transparent). Center figure: sub-domain Ω_h^- (blue transparent). Right figure: sub-domain Ω_h^+ (blue transparent).

Then, define the space of functions $V := H_h^2(\Omega_h^-) \times H_h^2(\Omega_h^+)$, and denote an element $v \in V$ by $v = (v^+, v^-)$. We will construct a finite element space conforming with V.

We fist define a standard finite element space of continuous piecewise linear polynomials with support in $\Omega_h^\pm$ by:

$$V_h^\pm := \{v \in \mathcal{C}(\overline{\Omega_h^\pm}) \cap H_0^1(\Omega) : v|_T \in \mathbb{P}^1(T), \forall T \in \mathcal{T}_h^\pm\}.$$

Then, the finite element subspace is defined by pairs of piecewise linear functions of V_h^- and V_h^+, i.e.

$$V_h := V_h^- \times V_h^+. \tag{5.3}$$

Abusing of notation, we will define for a function $v = (v^+, v^-) \in V_h$ the jumps across the interface as the jumps of the components

$$[v] = v^+ - v^- \quad \text{and} \quad [\rho \nabla v \cdot \boldsymbol{n}] = \rho^- \nabla v^- \cdot \boldsymbol{n}^- + \rho^+ \nabla v^+ \cdot \boldsymbol{n}^+. \tag{5.4}$$

5.1.3 The finite element method

We now consider a finite element method based on: the weak formulation of problem (5.1), penalty terms of the jump across the interface, and stabilization terms on edges in $\mathcal{E}_h^{\Gamma,\pm}$. Find $u_h = (u_h^-, u_h^+) \in V_h$, such that:

$$a_h(u_h, v) = \int_{\Omega^+} f^+ v^+ + \int_{\Omega^-} f^- v^-, \qquad \text{for all } v = (v^+, v^-) \in V_h, \tag{5.5}$$

where the bilinear form $a_h(\cdot,\cdot) : V \times V \to \mathbb{R}$ is defined by

$$\begin{aligned} a_h(w, v) = & \int_{\Omega^+} \rho^+ \nabla w^+ \cdot \nabla v^+ + \int_{\Omega^-} \rho^- \nabla w^- \cdot \nabla v^- \\ & + \int_\Gamma \left(\rho^- \nabla v^- \cdot \boldsymbol{n}^- [w] + \rho^- \nabla w^- \cdot \boldsymbol{n}^- [v]\right) + \sum_{T \in \mathcal{T}_h^\Gamma} \frac{\gamma}{h_T} \rho^- \int_{T_\Gamma} [w][v] \\ & + \gamma_g^- \sum_{e \in \mathcal{E}_h^{\Gamma,-}} |e| \int_e \rho^- [\![\nabla v^-]\!][\![\nabla w^-]\!] + \gamma_g^+ \sum_{e \in \mathcal{E}_h^{\Gamma,+}} |e| \int_e \rho^+ [\![\nabla v^+]\!][\![\nabla w^+]\!], \end{aligned} \tag{5.6}$$

for $v, w \in V$ and γ, γ_g^-, and γ_g^+ are positive parameters to be chosen. Note that the jumps $[\![\cdot]\!]$ in the flux stabilization terms (two last terms) are defined by (2.6).

The energy norm $\|\cdot\|_V$, induced by the bilinear form a_h, is defined for $v = (v^-, v^+) \in V$ by

$$\begin{aligned} \|v\|_V^2 = & \|\sqrt{\rho}\nabla v\|_{L^2(\Omega)}^2 + \sum_{T \in \mathcal{T}_h^\Gamma} \frac{1}{h_T} \|\sqrt{\rho^-}[v]\|_{L^2(T_\Gamma)}^2 \\ & + \sum_{e \in \mathcal{E}_h^{\Gamma,-}} |e| \, \|\sqrt{\rho^-}[\![\nabla v^-]\!]\|_{L^2(e)}^2 + \sum_{e \in \mathcal{E}_h^{\Gamma,+}} |e| \, \|\sqrt{\rho^+}[\![\nabla v^+]\!]\|_{L^2(e)}^2. \end{aligned}$$

Note that in this definition we make the abuse of notation of writing,

$$\|\sqrt{\rho}\nabla v\|_{L^2(\Omega)}^2 = \|\sqrt{\rho^-}\nabla v^-\|_{L^2(\Omega^-)}^2 + \|\sqrt{\rho^+}\nabla v^+\|_{L^2(\Omega^+)}^2,$$

for $v = (v^-, v^+) \in V$.

Remark 5.1. We point out that the terms in (5.6) involving integration on Γ can be generalized to

$$\int_\Gamma \left(\{\rho\nabla v\}_w \,[u_h] + \{\rho\nabla u_h\}_w \,[v]\right) ds + \sum_{T\in\mathcal{T}_h^\Gamma} \frac{\gamma}{h_T}\tilde{\rho} \int_{T_\Gamma} [u_h][v] ds.$$

The weighted average

$$\{\rho\nabla v \cdot \boldsymbol{n}^-\}_w := (w_-\, \rho^-\nabla v_- + w_+\, \rho^+\nabla v_+) \cdot \boldsymbol{n}^-$$

where the weights $w_-(x) \in [0,1]$ and $w_+(x) = 1 - w_-(x)$ and $\tilde{\rho}$ are chosen properly, see [34]. The case $w_-(x) = 1$ and $\tilde{\rho}(x) = \rho^-(x)$ reduces to the one in (5.6). Another choice considered in the literature (see [46, 32, 50]) is the harmonic average given by $w_- = \frac{\rho^+}{\rho^+ + \rho^-}$ and $\tilde{\rho} = \frac{2\rho^+\rho^-}{\rho^+ + \rho^-}$. In this case we obtain

$$\{\rho\nabla v \cdot \boldsymbol{n}^-\}_w = \frac{\tilde{\rho}}{2}\,(\nabla v_- + \nabla v_+) \cdot \boldsymbol{n}^-.$$

In this chapter we concentrate in the analysis of the choice (5.6), however, since $\rho^- \le \tilde{\rho} \le 2\rho^-$, the analysis for the harmonic average case follows straightforwardly.

5.2 Standard a priori error analysis

5.2.1 Stability and best approximation results

We will need the following technical proposition for the proof of coercivity; proof can be found in Appendix A.1.3.

Lemma 5.2.1. *Consider a node z of the triangulation $\mathcal{T}_h$ such that $z \in \overline{\Omega}^-$. Let ω_z be the patch of elements associated to z, i.e. $\omega_z = \operatorname{int}\left(\cup\{\overline{T} : T \in \mathcal{T}_h \text{ and } z \in \partial T\}\right)$. Then, for h small enough, there exists an element $T_z \in \omega_z$ such that:*

$$|T_z \cap \Omega^-| \geq C h_{T_z}^2, \tag{5.7}$$

where $C > 0$ is a constant independent of h_{T_z}.

Coercivity of the bilinear form a_h is proved below.

Lemma 5.2.2. *There exists a constant $c > 0$ such that*

$$c\|v\|_V^2 \leq a_h(v, v), \qquad \textit{for all } v \in V_h. \tag{5.8}$$

Proof. Let $v \in V_h$. Observe that the bilinear form a_h is symmetric, then it follows

$$\begin{aligned} a_h(v,v) =& \|\sqrt{\rho}\nabla v\|_{L^2(\Omega)}^2 + 2\int_\Gamma \rho^- \nabla v^- \cdot \boldsymbol{n}^-[v] ds + \sum_{T \in \mathcal{T}_h^\Gamma} \frac{\gamma}{h_T} \|\sqrt{\rho^-}[v]\|_{L^2(T_\Gamma)}^2 \\ &+ \gamma_g^- \sum_{e \in \mathcal{E}_h^{\Gamma,-}} |e|\rho^- \|[\![\nabla v^-]\!]\|_{L^2(e^-)}^2 + \gamma_g^+ \sum_{e \in \mathcal{E}_h^{\Gamma,+}} |e|\rho^+ \|[\![\nabla v^+]\!]\|_{L^2(e)}^2). \end{aligned}$$

In order to prove (5.8) it is enough to bound the non positive term (second term). Let $T \in \mathcal{T}_h^\Gamma$, the applying Cauchy-Schwarz inequality we obtain

$$\left|\int_{T_\Gamma} \rho^- \nabla v^- \cdot \boldsymbol{n}^-[v]\, ds\right| \leq \left(\sqrt{\rho^- h_T} \|\nabla v^- \cdot \boldsymbol{n}^-\|_{L^2(T_\Gamma)}\right)\left(\sqrt{\frac{\rho^-}{h_T}} \|[v]\|_{L^2(T_\Gamma)}\right).$$

Summing over $T \in \mathcal{T}_h^\Gamma$ and applying arithmetic-geometric inequality give

$$\left|\int_\Gamma \rho^- \nabla v^- \cdot \boldsymbol{n}^-[v] ds\right| \leq \sum_{T \in \mathcal{T}_h^\Gamma} \left(\varepsilon \rho^- h_T \|\nabla v^- \cdot \boldsymbol{n}^-\|_{L^2(T_\Gamma)}^2 + \frac{\rho^-}{\varepsilon h_T} \|[v]\|_{L^2(T_\Gamma)}^2\right).$$

Let $T \in \mathcal{T}_h^\Gamma$ and let $z \in \overline{\Omega}^-$ be a node of T. By Proposition 5.2.1, there exists a triangle T_z satisfying (5.7). Now, consider the shortest sequence of edges $E(T) = \{e_1, e_2, ..., e_N\}$ such that

$$\begin{cases} z \in \overline{e_j}, & j = 1, ..., N, \\ e_1 \subset \partial T \text{ and } e_N \subset \partial T_z, & \\ e_j, e_{j+1} \subset \partial T_j,\ T_j \in \mathcal{T}_h, & j = 1, ..., N-1. \end{cases}$$

Note that by its definition $E(T) \subset \mathcal{E}_h^{\Gamma,-}$. Then, observing that the tangential jump of ∇v^- is zero along edges, we have

$$\begin{aligned} h_T \rho^- \|\nabla v^- \cdot \boldsymbol{n}^-\|^2_{L^2(T_\Gamma)} &\leq h_T \rho^- \frac{|T_\Gamma|}{|e_1|} \|\nabla v^-\|^2_{L^2(e_1)} \leq \frac{1}{\gamma_0^2} \rho^- |e_1| \, \|\nabla v^-\|^2_{L^2(e_1)} \\ &\leq \frac{1}{\gamma_0^2} \rho^- |e_1| \left(\|[\![\nabla v^-]\!]\|^2_{L^2(e_1)} + \|\nabla v^-|_{T_1}\|^2_{L^2(e_1)} \right) \\ &\leq \frac{1}{\gamma_0^2} \rho^- |e_1| \, \|[\![\nabla v^-]\!]\|^2_{L^2(e_1)} + \frac{1}{\gamma_0^4} \rho^- |e_2| \, \|\nabla v^-|_{T_1}\|_{L^2(e_2)} \\ &\vdots \\ &\leq c(\gamma_0) \rho^- \sum_{e \in E(T)} |e| \, \|[\![\nabla v^-]\!]\|^2_{L^2(e)} + C(\gamma_0) \rho^- |e_N| \, \|\nabla v^-|_{T_z}\|_{L^2(e_N)} \\ &\leq c(\gamma_0) \rho^- \sum_{e \in E(T)} |e| \, \|[\![\nabla v^-]\!]\|^2_{L^2(e)} + \tilde{C}(\gamma_0) \|\sqrt{\rho^-} \nabla_k v^-\|^2_{L^2(T_z)}, \end{aligned}$$

where γ_0 is the shape regularity constant defined in (2.2).

Hence, considering that each nodal patch contains finite number of elements implies that, after summing over $T \in \mathcal{T}_h^\Gamma$, the terms above are repeated at most finitely many times. Then, it follows

$$\sum_{T \in \mathcal{T}_h^\Gamma} \rho^- h_T \|\nabla v^- \cdot \boldsymbol{n}^-\|^2_{L^2(T_\Gamma)} \leq \tilde{C}(\gamma_0) \left(\|\sqrt{\rho^-} \nabla v\|^2_{L^2(\Omega^-)} + \sum_{e \in \mathcal{E}_h^{\Gamma,-}} |e| \rho^- \|[\![\nabla v^-]\!]\|^2_{L^2(e)} \right).$$

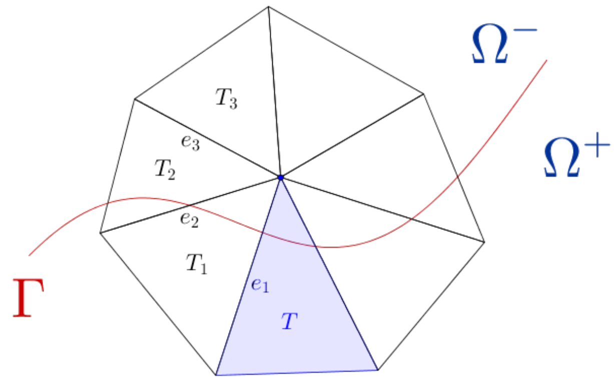

Figure 5.2: Proof of Lemma 5.8. Illustration of set $E(T) \subset \mathcal{E}_h^{\Gamma,-}$.

Therefore, coercivity follows by choosing γ large enough in terms of $C(\gamma_0)$ and ε. $\square$

With the aim of proving continuity of the bilinear form a_h, we define the following augmented norm:

$$\|v\|_{V_A}^2 = \|v\|_V^2 + \sum_{T\in\mathcal{T}_h^\Gamma} h_T \|\sqrt{\rho^-}\nabla v^- \cdot \boldsymbol{n}^-\|_{L^2(T_\Gamma)}^2. \tag{5.9}$$

Continuity of the bilinear form follows from its definition and Cauchy-Schwarz inequality. The result is stated as follows:

Lemma 5.2.3. *(Continuity) Suppose that $v^\pm, w^\pm \in H_h^2(\Omega^\pm)$. Then, there exists a constant $C > 0$, independent of v and w, such that*

$$a_h(w, v) \leq C\,\|w\|_{V_A}\,\|v\|_{V_A}.$$

Additionally, if $w^\pm \in H_h^2(\Omega^\pm)$ and $v \in V_h$ we have

$$a_h(w, v) \leq C\|w\|_{V_A}\,\|v\|_V. \tag{5.10}$$

In order to discuss the Galerkin orthogonality of method (5.5)-(5.6) we consider the extension operators introduced in Section 2.4.2 Proposition 2.4.4. A particular case is proved in Appendix A.5 by means of an even extension. From now on we simply denote $u^{\pm}_E$ by $u^{\pm}$.

Lemma 5.2.4. *(Galerkin orthogonality) Suppose that* u *solves the* (5.1) *and suppose that* $u|_{\Omega^{\pm}} \in H^2(\Omega^{\pm})$. *Then, we have that*

$$a_h(u, v) = (f, v), \quad \forall v \in V_h,$$

where we use the notation $u = (u^+, u^-)$. *Hence, Galerkin orthogonality holds:*

$$a_h(u - u_h, v) = 0, \quad \forall v \in V_h.$$

The main result of this section, the best approximation result, is stated below. It follows easily from coercivity, continuity, Galerkin orthogonality and from a generalization of Cea's Lemma. See for example Chapter III [26]. We give some details for completeness.

Theorem 5.2.1. *(Best approximation) Let* $\Omega \subseteq \mathbb{R}^2$ *be an open polygonal domain. Let* u *be a solution of problem* (5.1) *and assume that* $u|_{\Omega^{\pm}} \in H^2(\Omega^{\pm})$. *Let* u_h *be solution of the discrete problem* (5.5). *Then, there exists a constant* $C > 0$ *independent of* h, *such that*

$$\|u - u_h\|_V \leq C \inf_{v \in V_h} \|u - v\|_{V_A}.$$

Proof. Let $v \in V_h$, then we have by coercivity, Galerkin orthogonality and continuity that

$$\|u_h - v\|_V^2 \leq c\, a_h(u_h - v, u_h - v) = c\, a_h(u - v, u_h - v) \leq c\, C\, \|u - v\|_{V_A} \|u_h - v\|_V.$$

Now, triangle inequality implies that for any $v \in V_h$

$$\|u - u_h\|_V \leq \|u_h - v\|_V + \|u - v\|_V.$$

Therefore, the result is complete after combining the last two inequalities and taking the infimum over $v \in V_h$. □

5.2.2 Energy error estimates

In order to prove an error estimate in terms of the V-norm we introduce the following interpolation operator: Define $I_h : V \to V_h$ such that

$$(I_h u)^{\pm} = J_{\text{sz}} u^{\pm}, \quad \text{for } u = (u^+, u^-) \in V,$$

where J_{sz} is the Scott-Zhang interpolant (see Definition 2.2.12) onto the standard continuous piecewise linear polynomials. Consequently, the following estimate for the interpolation error follows from the properties of the Scott-Zhang interpolation operator and the extension result: Lemma 2.4.4.

Lemma 5.2.5. *Consider the definition of the interpolation operator I_h given above. Then, there exists a constant $C > 0$, independent of h, such that:*

$$\|u - I_h u\|_{V_A} \leq Ch(\sqrt{\rho^+}\|D^2 u\|_{L^2(\Omega^+)} + \sqrt{\rho^-}\|D^2 u\|_{L^2(\Omega^-)}).$$

In addition we state a standard regularity estimate introduced in Section 2.4.1 Proposition 2.4.3.

An energy error estimate follows from Theorem 5.2.1, Lemma 5.2.5 and Proposition 2.4.3. We state it in Corollary below.

Corollary 5.2.1. *(Standard energy error estimate) Let u be a solution of problem* (5.1)*, and let u_h be the solution of the discrete problem* (5.5)*. Suppose that Ω is convex. Then, there exists $C > 0$ independent of $\rho^{\pm}$, such that*

$$\|u - u_h\|_V \leq \frac{C\,h}{\sqrt{\rho^-}} \|f\|_{L^2(\Omega)}.$$

Remark 5.2. Constant C dependents in the extension constant C_E (2.27) and the regularity constant C_{reg} (2.23).

5.3 Error estimate for the flux

In order to prove the main result of this paper, the error estimate for the flux, we need a discrete extension result.

Lemma 5.3.1. *(Discrete extension) Assume that the triangulation $\mathcal{T}_h$ is quasi-uniform. Let $v_h \in V_h^+$. Then, there exists a function $Ev_h \in V_h^c = \{v \in C_0(\Omega) : v|_T \in \mathbb{P}^1(T), \forall T \in \mathcal{T}_h\}$, such that $Ev_h = v_h$ in Ω_h^+ and*

$$\|Ev_h\|_{H^1(\Omega)} \leq C\|v_h\|_{H^1(\Omega_h^+)},$$

with $C > 0$ independent of h.

Proof. See Appendix A.6. □

Considering the discrete extension lemma, we state a bound for the H^1-norm in Ω_h^+. The proof follows easily using a Proposition 5.2.1 (with roles of Ω^+ and Ω^-

reversed).

Lemma 5.3.2. *Let $v \in V_h^+$. Then, we have*

$$\|v\|^2_{H^1(\Omega_h^+)} \leq C \left(\|v\|^2_{H^1(\Omega^+)} + \sum_{e \in \mathcal{E}_h^{\Gamma,+}} |e| \, \|[\![\nabla v]\!]^2_{L^2(e)} \right).$$

Now we are in position to state and prove the main result of this paper.

Theorem 5.3.1. *Let u be a solution of problem* (5.1) *and let u_h be solution of the discrete problem* (5.5)*. Assume that Ω is convex and the triangulation is quasi-uniform. Then, there exists a constant $C > 0$, independent of h and $\rho^{\pm}$, such that*

$$\|\rho \nabla(u - u_h)\|_{L^2(\Omega)} \leq Ch\|f\|_{L^2(\Omega)}.$$

We remind the reader that

$$\|\rho \nabla(u - u_h)\|^2_{L^2(\Omega)} = \|\rho^- \nabla(u - u_h)^-\|^2_{L^2(\Omega^-)} + \|\rho^+ \nabla(u - u_h)^+\|^2_{L^2(\Omega^+)}.$$

Proof. Observe that the bound in Ω^- is given by Corollary 5.2.1

$$\|\rho^- \nabla(u - u_h)^-\|_{L^2(\Omega^-)} \leq Ch\|f\|_{L^2(\Omega)}.$$

Thus, it remains to prove

$$\|\rho^+ \nabla(u - u_h)^+\|_{L^2(\Omega^+)} \leq C\, h\|f\|_{L^2(\Omega)}. \tag{5.11}$$

Consider the function $v_h = (I_h u - u_h)^+ \in V_h^+$. If Ω^+ is the inclusion, i.e., $\partial\Omega^+ \cap \partial\Omega = \emptyset$, we redefine v_h so that it has average zero on Ω^+, i.e., $v_h = v_h - \frac{1}{|\Omega^+|}\int_{\Omega^+} v_h$.

Either case Poincare's inequality holds:

$$\|v_h\|_{H^1(\Omega^+)} \leq C\|\nabla v_h\|_{L^2(\Omega^+)} = C\|\nabla(I_h u - u_h)^+\|_{L^2(\Omega^+)},$$

for a constant $C > 0$. Applying Lemma 5.3.1 it follows that there exists an extension $Ev_h \in V_h^c$ such that $Ev_h = v_h$ in Ω_h^+, and $\|Ev_h\|_{H^1(\Omega)} \leq C\|v_h\|_{H^1(\Omega_h^+)}$. Combining this estimate with Lemma 5.3.2, we have

$$\|Ev_h\|_{H^1(\Omega)} \leq C\Big(\|\nabla(I_h u - u_h)^+\|_{L^2(\Omega^+)} + \Big(\sum_{e\in\mathcal{E}_h^{\Gamma,+}} |e|\,\|[\![\nabla(I_h u - u_h)^+]\!]^2_{L^2(e)}\Big)^{1/2}\Big). \tag{5.12}$$

Consequently, using $((Ev_h)^-, (Ev_h)^+) \in V_h$ as test function (where $(Ev_h)^\pm := Ev_h|_{\Omega_h^\pm}$), and the consistency of the method (5.5)-(5.6), we obtain

$$\begin{aligned}
0 &= a_h(u - u_h, Ev_h)\\
&= \int_{\Omega^+} \rho^+\nabla(u-u_h)^+ \cdot \nabla(Ev_h)^+ + \int_{\Omega^-} \rho^-\nabla(u-u_h)^- \cdot \nabla(Ev_h)^-\\
&+ \int_\Gamma \rho^-\nabla Ev_h^- \cdot \boldsymbol{n}^-[u-u_h]ds\\
&+ \sum_{e\in\mathcal{E}_h^{\Gamma,-}} |e| \int_e \rho^-[\![\nabla(Ev_h)^-]\!][\![\nabla(u-u_h)^-]\!]\, ds\\
&+ \sum_{e\in\mathcal{E}_h^{\Gamma,+}} |e| \int_e \rho^+[\![\nabla(Ev_h)^+]\!][\![\nabla(u-u_h)^+]\!]\, ds.
\end{aligned}$$

Here we used that Ev_h is continuous across the interface Γ. Multiplying by ρ^+ and adding and subtracting $I_h u^+$ in the first and last term give

$$
\begin{aligned}
&\|\rho^+\nabla(I_h u - u_h)^+\|^2_{L^2(\Omega^+)} + \sum_{e\in\mathcal{E}_h^{\Gamma,+}} |e|\, \|\rho^+[\![\nabla(I_h u - u_h)^+]\!]\|^2_{L^2(e)} = \\
&-\rho^+\int_{\Omega^+}\rho^+\nabla(u - I_h u)^+\cdot\nabla(Ev_h)^+ - \rho^+\sum_{e\in\mathcal{E}_h^{\Gamma,+}}|e|\int_e \rho^+[\![\nabla(Ev_h)^+]\!][\![\nabla(u - I_h u)^+]\!]\,ds \\
&-\rho^+\int_{\Omega^-}\rho^-\nabla(u - u_h)^-\cdot\nabla(Ev_h)^- - \rho^+\int_\Gamma \rho^-\nabla(Ev_h)^-\cdot\boldsymbol{n}^-[u - u_h]ds \\
&-\rho^+\sum_{e\in\mathcal{E}_h^{\Gamma,-}}|e|\int_e \rho^-[\![\nabla(Ev_h)^-]\!][\![\nabla(u - u_h)^-]\!]\,ds =: I_1 + I_2,
\end{aligned}
$$

where I_1 denotes the first two terms and I_2 the last three terms. First we bound I_1. Applying Cauchy-Schwarz and arithmetic geometric inequalities, and using that $\nabla(Ev_h)^+ = \nabla(I_h u - u_h)^+$ in Ω_h^+ yield

$$
\begin{aligned}
2|I_1| \le &\|\rho^+\nabla(I_h u - u)^+\|^2_{L^2(\Omega^+)} + \sum_{e\in\mathcal{E}_h^{\Gamma,+}}|e|\,\|\rho^+[\![\nabla(I_h u - u)^+]\!]\|^2_{L^2(e)} \\
&+ \|\rho^+\nabla(I_h u - u_h)^+\|^2_{L^2(\Omega^+)} + \sum_{e\in\mathcal{E}_h^{\Gamma,+}}|e|\,\|\rho^+[\![\nabla(I_h u - u_h)^+]\!]\|^2_{L^2(e)}.
\end{aligned}
$$

Similarly, we apply Cauchy-Schwarz inequality for the three terms in I_2 after taking as common factor $\rho^+\sqrt{\rho^-}$, i.e.

$$\left|\sqrt{\rho^-}\int_{\Omega^-}\nabla(u-u_h)^-\cdot\nabla(Ev_h)^-dx\right|$$
$$\leq \|\sqrt{\rho^-}\nabla(u-u_h)^-\|_{L^2(\Omega^-)}\|\nabla(Ev_h)^-\|_{L^2(\Omega^-)},$$
$$\left|\sqrt{\rho^-}\int_{\Gamma}\nabla(Ev_h)^-\cdot\boldsymbol{n}^-[u-u_h]ds\right|$$
$$\leq \sum_{T\in\mathcal{T}_h^\Gamma}\frac{1}{\sqrt{h_T}}\|\sqrt{\rho^-}\,[u-u_h]\,\|_{L^2(T_\Gamma)}\sqrt{h_T}\|\nabla(Ev_h)^-\cdot\boldsymbol{n}^-\|_{L^2(T_\Gamma)},$$
$$\left|\sqrt{\rho^-}\sum_{e\in\mathcal{E}_h^{\Gamma,-}}|e|\int_e[\![\nabla(Ev_h)^-]\!][\![\nabla(u-u_h)^-]\!]ds\right|$$
$$\leq \sum_{e\in\mathcal{E}_h^{\Gamma,-}}|e|\|\sqrt{\rho^-}[\![\nabla(u-u_h)^-]\!]\|_{L^2(e)}\|[\![\nabla(Ev_h)^-]\!]\|_{L^2(e)}.$$

Observe that terms involving $u-u_h$ are all bounded by $\|u-u_h\|_V$. Hence,

$$|I_2|\leq C\,\rho^+\sqrt{\rho^-}\|u-u_h\|_V\Big(\|\nabla(Ev_h)^+\|_{L^2(\Omega^+)}$$
$$+\big(\sum_{T\in\mathcal{T}_h^\Gamma}h_T\|\nabla(Ev_h)^-\cdot\boldsymbol{n}^-\|^2_{L^2(T_\Gamma)}\big)^{1/2}+\big(\sum_{e\in\mathcal{E}_h^{\Gamma,-}}|e|\,\|[\![\nabla(Ev_h)^-]\!]\|^2_{L^2(e)}\big)^{1/2}\Big).$$

For the terms involving Ev_h we use inverse inequalities, obtaining

$$\Big(\sum_{T\in\mathcal{T}_h^\Gamma}h_T\|\nabla(Ev_h)^-\cdot\boldsymbol{n}^-\|^2_{L^2(T_\Gamma)}\Big)^{1/2}+\Big(\sum_{e\in\mathcal{E}_h^{\Gamma,-}}|e|\,\|[\![\nabla(Ev_h)^-]\!]\|^2_{L^2(e)}\Big)^{1/2}$$
$$\leq C\|\nabla Ev_h\|_{L^2(\Omega)}.$$

Thus, by the estimates above for I_1 and I_2 it follows that

$$I_1+I_2\leq\frac{1}{2}(\|\rho^+\nabla(I_hu-u)^+\|^2_{L^2(\Omega^+)}+\sum_{e\in\mathcal{E}_h^{\Gamma,+}}|e|\,\|\rho^+[\![\nabla(I_hu-u)^+]\!]\|^2_{L^2(e)})$$
$$+C\,\sqrt{\rho^-}\|u-u_h\|_V\|\rho^+\nabla Ev_h\|_{L^2(\Omega)}.$$

By approximation properties of the Scott-Zhang interpolant and Proposition 2.4.3, we have

$$\|\rho^+\nabla(I_hu-u)^+\|^2_{L^2(\Omega^+)} + \sum_{e\in\mathcal{E}_h^{\Gamma,+}} |e|\|\rho^+[\![\nabla(I_hu-u)^+]\!]\|^2_{L^2(e)} \tag{5.13}$$
$$\leq Ch^2(\rho^+)^2\|D^2u^+\|^2_{L^2(\Omega^+)} \leq Ch^2\|f\|^2_{L^2(\Omega)}.$$

Using the error estimate Corollary 5.2.1 and definitions of I_1 and I_2 we conclude

$$\|\rho^+\nabla(I_hu-u_h)^+\|^2_{L^2(\Omega^+)} + \sum_{e\in\mathcal{E}_h^{\Gamma,+}} |e|\,\|\rho^+[\![\nabla(I_hu-u_h)^+]\!]\|^2_{L^2(e)}$$
$$\leq C(h\|f\|_{L^2(\Omega)}\|\rho^+\nabla Ev_h\|_{L^2(\Omega)} + h^2\|f\|^2_{L^2(\Omega)}).$$

Therefore, applying (5.12) we have

$$\|\rho^+\nabla(I_hu-u_h)\|^2_{L^2(\Omega^+)} + \sum_{e\in\mathcal{E}_h^{\Gamma,+}} |e|\,\|\rho^+[\![\nabla(I_hu-u_h)^+]\!]\|^2_{L^2(e)} \leq Ch^2\|f\|^2_{L^2(\Omega)}.$$

Finally, applying triangle inequality, the estimate for the interpolation error (5.13), and last inequality we obtain the desired bound (5.11). □

We conclude this section by stating an L^2-error estimate. The proof follows easily from a duality argument (see [63]). We omit the details.

Lemma 5.3.3. *(L^2 error estimate) Assuming the hypothesis of Theorem 5.3.1 we have*

$$\|(u-u_h)^-\|_{L^2(\Omega^-)} + \|(u-u_h)^+\|_{L^2(\Omega^+)} \leq \frac{C}{\rho^-}h^2\|f\|_{L^2(\Omega)}.$$

Unfortunately, the result has a factor $\frac{1}{\rho^-}$ on the right hand side. At the present moment we do not see how to remove it.

5.4 Final discussion

In this section we discuss and state some straightforward extensions of method (5.5)-(5.6).

5.4.1 Non homogeneous jump conditions

We consider problem (5.1) with a non homogeneous jump conditions in equations (5.1c) and (5.1d), i.e.

$$-\nabla \cdot (\rho^{\pm} \nabla u^{\pm}) = f^{\pm} \qquad \text{in } \Omega^{\pm}, \tag{5.14a}$$

$$u^{\pm} = 0 \qquad \text{on } \partial\Omega^{\pm} \backslash \Gamma, \tag{5.14b}$$

$$[u] = \alpha \qquad \text{on } \Gamma, \tag{5.14c}$$

$$[\rho \nabla u \cdot \boldsymbol{n}] = \beta \qquad \text{on } \Gamma, \tag{5.14d}$$

where α, β are a smooth functions given on the interface. The method in this case follows from a standard derivation of the variational formulation:

$$\begin{aligned} a_h(u_h, v) = (f^+, v^+)_{\Omega^+} + (f^-, v^-)_{\Omega^-} + \int_\Gamma \big(\beta v^+ + \rho^- \nabla v^- \cdot \boldsymbol{n}^- \alpha\big) ds \\ + \sum_{T \in \mathcal{T}_h^\Gamma} \frac{\gamma}{h_T} \rho^- \int_{T_\Gamma} [v] \alpha ds, \end{aligned} \tag{5.15}$$

for all $v \in V_h$.

All the proofs would generalize easily. The only requirement is that a regularity result as in [38] holds for this slightly more complicated problem.

5.4.2 Three dimensional problem

To extend the method in three dimension is straightforward. In order to prove the same result one needs the regularity results from [38] to hold in three dimensions which we have not found in the literature. Moreover, we need to be able to prove the geometric result and extension results in three dimensions: Proposition 5.2.1 and Lemma 5.3.1. We believe that these results should hold.

5.4.3 Concluding remarks

In this chapter we proved error estimates for the stabilized unfitted Nitsche methods (5.5)-(5.6) for problem (5.1) independent of the contrast of the coefficients ρ^- and ρ^+. We also proved a nonstandard error estimate for the flux variable totally independent of the coefficients. The key ingredient in the proof of this estimate was a discrete extension from Ω^+ and Ω. This estimate is sharper than the energy estimate since it is independent of the discontinuous coefficients ρ^- and ρ^+.

As in the previous chapter, it would be interesting to investigate problems with interfaces of arbitrary curvature (observe that the analysis is restricted by the Assumption 2). In this direction, perhaps a combination of the method presented here and the multicale method by Chu et al. in [38] could be a possible approach.

5.5 Numerical examples

This section illustrates numerically the a priori error estimates proved in Section 5.2 and Section 5.3. We consider a two dimensional example with a non trivial immersed and closed interface. In particular, the example supports the optimal order of convergence for the error of the flux $\rho\nabla(u-u_h)$. We summarize our experimental results in tables, displaying the following errors and experimental orders of convergence (eoc):

$$e_h^0 := \|u-u_h\|_{L^2(\Omega)}, \qquad e_h^\infty := \|u-u_h\|_{L^\infty(\Omega)},$$
$$e_{h,\rho}^1 := \|\rho\nabla(u-u_h)\|_{L^2(\Omega)}, \qquad e_{h,\rho}^{1,\infty} := \|\rho\nabla(u-u_h)\|_{L^\infty(\Omega)},$$

$$\mathrm{eoc}(e) := \frac{\log(e_{h_{l+1}}/e_{h_l})}{\log(h_{l+1}/h_l)}.$$

Our theoretical results predict optimal convergence of: error e_h^0 (second order), and error e_h^1 (first order). We also test the convergence of the errors e_h^∞ and $e_h^{1,\infty}$.

The finite element approximation by scheme (5.5)-(5.6) is computed with a sequence of uniform triangulations that are non-fitted with the interface. The parameter of the triangulation is given by $h = 2^{-(l+3/2)}$, for $l = 1, ..., 7$. Computations were performed in MATLAB including the solution of the linear system by means of command "\".

Example 5.1. Consider problem (5.1) in a square domain $\Omega = (-1,1)^2$ and an immersed interface $\Gamma = \{(x,y) \in \Omega : x^2+y^2 = (1/3)^2\}$. We will test both cases: Ω^- as inclusion, and Ω^+ as inclusion. Consider the following exact solution:

$$u(x,y) = \begin{cases} \frac{r^\alpha}{\rho^-} & , \text{ if } (x,y) \in \Omega^-, \\ \frac{r^\alpha}{\rho^+} + \left(\frac{1}{3}\right)^\alpha \left(\frac{1}{\rho^-} - \frac{1}{\rho^+}\right) & , \text{ if } (x,y) \in \Omega^+, \end{cases} \tag{5.16}$$

where $r = \sqrt{x^2 + y^2}$ and $\alpha = 2$. We test with values of the diffusion coefficients $\rho^+ = 10^4$ and $\rho^- = 1$. Tables 5.1 and 5.2 summarize the results obtained by method (5.5)-(5.6) with stabilization parameters $\gamma = 10$ and $\gamma_g^\pm = 10$, with Ω^- and Ω^+ as inclusion, respectively.

l	e_h^0	eoc	e_h^∞	eoc	$e_{h,\rho}^1$	eoc	$e_{h,\rho}^{1,\infty}$	eoc
1	1.9e-2	–	5.5e-2	–	3.7e-1	–	5.9e-1	–
2	6.2e-3	1.64	1.5e-2	1.86	1.4e-1	1.38	2.7e-1	1.11
3	1.1e-3	2.46	2.8e-3	2.45	5.6e-2	1.31	1.2e-1	1.17
4	1.7e-4	2.69	5.0e-4	2.48	2.6e-2	1.11	5.4e-2	1.17
5	2.8e-5	2.66	9.8e-5	2.34	1.3e-2	1.03	2.4e-2	1.14
6	4.6e-6	2.59	1.9e-5	2.39	6.4e-3	1.01	1.2e-2	1.03
7	8.4e-7	2.45	4.2e-6	2.16	3.2e-3	1.00	6.0e-3	1.01

Table 5.1: Example 5.1: errors and experimental orders of convergence (eoc) with $\Omega^- = \{(x, y) \in \Omega : x^2 + y^2 < (1/3)^2\}$ and $\Omega^+ = \Omega\backslash(\Omega^- \cup \Gamma)$, using method (5.5)-(5.6).

l	e_h^0	eoc	e_h^∞	eoc	$e_{h,\rho}^1$	eoc	$e_{h,\rho}^{1,\infty}$	eoc
1	3.7e-2	–	5.9e-2	–	3.6e-1	–	6.0e-1	–
2	8.3e-3	2.15	1.3e-2	2.23	1.4e-1	1.41	2.7e-1	1.15
3	1.5e-3	2.45	2.9e-3	2.09	5.6e-2	1.29	1.2e-1	1.17
4	2.7e-4	2.50	5.8e-4	2.35	2.6e-2	1.09	5.3e-2	1.18
5	5.2e-5	2.35	9.8e-5	2.56	1.3e-2	1.02	2.4e-2	1.14
6	1.2e-5	2.16	2.1e-5	2.25	6.4e-3	1.01	1.2e-2	1.01
7	2.8e-6	2.06	4.2e-6	2.29	3.2e-3	1.00	5.8e-3	1.05

Table 5.2: Example 5.1: errors and experimental orders of convergence (eoc) with $\Omega^+ = \{(x, y) \in \Omega : x^2 + y^2 < (1/3)^2\}$ and $\Omega^- = \Omega\backslash(\Omega^+ \cup \Gamma)$, using method (5.5)-(5.6).

Optimal convergence of the errors, second order for e_h^0 and e_h^∞ and first order for $e_{h,\rho}^1$ and $e_{h,\rho}^\infty$, for Example 5.1 is observed in Tables 5.1 and 5.2 for both cases Ω^- and Ω^+ as inclusion.

In addition, in order to test the independence of the coefficient $\rho^\pm$ of our estimate in Theorem 5.3.1, we consider the exact solution (5.16) with a fix mesh corresponding to $h = 2^{-(5+3/2)}$. We compute errors e_h^0, $e_{h,\rho}^1$ and $e_{h,\sqrt{\rho}}^1 = \|\sqrt{\rho}(u - u_h)\|_{L^2(\Omega)}$ for decreasing values of ρ^- and increasing values of ρ^+. We summarize the results in Tables 5.3 and 5.4, corresponding to Ω^- as inclusion and Ω^+ as inclusion, respectively.

ρ^-	ρ^+	e_h^0	$e_{h,\rho}^1$	$e_{h,\sqrt{\rho}}^1$
1e+0	1e+1	3.0e-5	1.3e-2	5.5e-3
1e-1	1e+2	2.8e-4	1.3e-2	1.3e-2
1e-2	1e+3	2.8e-3	1.3e-2	4.0e-2
1e-3	1e+4	2.8e-2	1.3e-2	1.3e-1
1e-4	1e+5	2.8e-1	1.3e-2	4.0e-1

Table 5.3: Example 5.1: errors for mesh parameter $h = 2^{-(5+3/2)}$. $\Omega^- = \{(x,y) \in \Omega : x^2 + y^2 < (1/3)^2\}$ and $\Omega^+ = \Omega \backslash (\Omega^- \cup \Gamma)$, using method (5.5)-(5.6).

ρ^-	ρ^+	e_h^0	$e_{h,\rho}^1$	$e_{h,\sqrt{\rho}}^1$
1e+0	1e+1	5.4e-5	1.3e-2	1.2e-2
1e-1	1e+2	5.2e-4	1.3e-2	3.9e-2
1e-2	1e+3	5.2e-3	1.3e-2	1.2e-1
1e-3	1e+4	5.3e-2	1.3e-2	3.9e-1
1e-4	1e+5	3.9e-1	1.3e-2	1.2e+0

Table 5.4: Example 5.1: errors for mesh parameter $h = 2^{-(5+3/2)}$. $\Omega^+ = \{(x,y) \in \Omega : x^2 + y^2 < (1/3)^2\}$ and $\Omega^- = \Omega \backslash (\Omega^+ \cup \Gamma)$, using method (5.5)-(5.6).

Tables 5.3 and 5.4 show that error $e_{h,\rho}^1$ is practically invariant, corroborating that in the main result of our paper Theorem 5.3.1, the estimate is totally independent of the diffusion coefficients $\rho^\pm$. Errors e_h^0 and $e_{h,\sqrt{\rho}}^1$ seems to be dependent of the coefficients as our estimates in Section 5.2 show.

Example 5.2. Consider problem (5.1) in a square domain $\Omega = (-1,1)^2$ and an immersed interface $\Gamma = \{(x,y) \in \Omega : x^2 + y^2 = (1/3)^2\}$. We consider Ω^- as the inclusion. Consider the following exact solution:

$$u(x,y) = \begin{cases} 2y^2 - 2x^2 + 2 & , \text{ if } (x,y) \in \Omega^-, \\ \sin(3x)^2 & , \text{ if } (x,y) \in \Omega^+, \end{cases}$$

Note that in the this case the jump of the solution and the jump of the flux are nonzero. We test with stabilization parameters $\gamma = 10$ and $\gamma_g^{\pm} = 10$. Figure 5.3 plots the errors obtained by method (5.15)-(5.6) and displays the approximate solution.

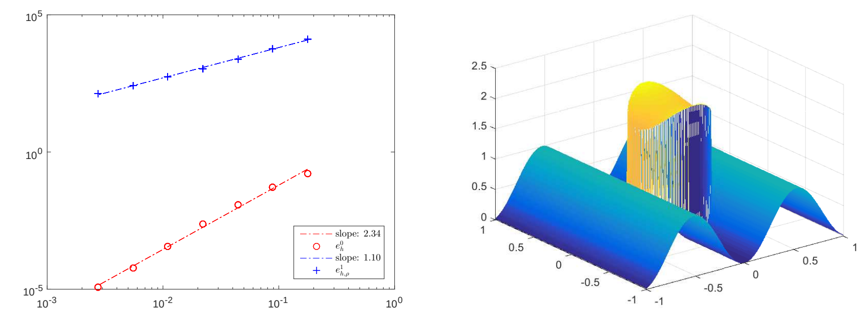

Figure 5.3: Example 5.2: Left figure: Plot on *Log* scale of errors e_h^0 and $e_{h,\rho}^1$ vs. h. Right figure: approximate solution by method (5.15)-(5.6) of problem (5.1).

We observe in Figure 5.3 that the errors e_h^0 and $e_{h,\rho}^1$ converge optimally, with an average ratio of convergence of 2.34 and 1.10, respectively.

Example 5.3. Consider the two dimensional domain $\Omega = (-1,1)^2$ with the immersed interface Γ defined by $\Gamma = \{(x,y) \in \Omega : \|(x,y)\|_2 = r = 1/18 + 0.2\sin(5s),\ s \in [0, 2\pi)\}$. We define Ω^- as the interior domain, i.e. $\partial\Omega^- = \Gamma$. We further consider the following exact solution

$$u(x,y) = \begin{cases} \frac{1}{\rho^-}(x^2+y^2)^2 & , \text{ if } (x,y) \in \Omega^-, \\ \frac{1}{\rho^+} y\sqrt{x^2+y^2} & , \text{ if } (x,y) \in \Omega^+, \end{cases}$$

We set the stabilization parameters to be: $\gamma = 10$, $\gamma_g^+ = 10$ and $\gamma_g^- = 10$.

l	e_h^0	eoc	e_h^∞	eoc	$e_{h,\rho}^1$	eoc	$e_{h,\rho}^{1,\infty}$	eoc
1	2.4e-2	–	7.1e-2	–	5.1e-1	–	1.0e+0	–
2	1.0e-2	1.23	2.6e-2	1.46	2.2e-1	1.18	7.8e-1	0.39
3	3.2e-3	1.68	1.4e-2	0.91	9.8e-2	1.19	5.1e-1	0.62
4	8.6e-4	1.91	4.4e-3	1.63	3.7e-2	1.41	2.9e-1	0.84
5	1.7e-4	2.35	1.0e-3	2.13	1.4e-2	1.43	1.4e-1	1.07
6	2.8e-5	2.60	1.9e-4	2.42	5.9e-3	1.23	6.2e-2	1.14

Table 5.5: Example 5.3: errors and experimental orders of convergence (eoc) with $\rho^- = 1$, $\rho^+ = 10^5$, using method (5.15)-(5.6).

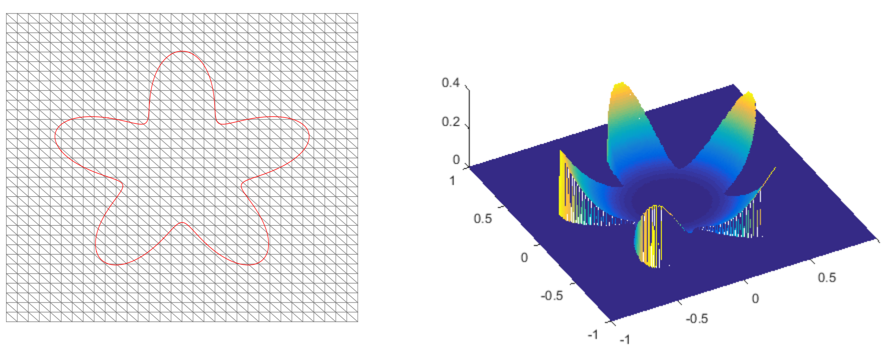

Figure 5.4: Example 5.3: Left figure: a non-fitted triangulation of the interface. Right figure: approximate solution by method (5.15)-(5.6) of problem (5.3).

Appendix A

Technical results and notes on implementation

A.1 Technical geometric lemmas

In this section we prove two technical lemmas involving geometrical estimates on elements intersected by the interface Γ. We remind the reader that we assume that Γ is a simple C^2 curve with an arc-length parameterization $\boldsymbol{X} : [0, |\Gamma|) \to \Gamma$, and Assumptions 1, 2 and 3 in Section 2.3.3.

Lemma A.1.1. *We assume that r is the radius of our tubular neighborhood of a curve Γ given in Proposition 2.3.1. We further assume that Γ is closed. The, for any $0 < \tau \leq r$, we can represent the tubular neighborhood as*

$$Tub(\tau) = \{x : \mathit{dist}(x, \Gamma) \leq \tau\}.$$

Proof. If $x_0 \in Tub(\tau)$ immediately implies that $\text{dist}(x_0, \Gamma) \leq \tau$.

Conversely, let x_0 such that $\text{dist}(x_0, \Gamma) \leq \tau$, for $0 < \tau < r$. By definition,

$$\text{dist}(x_0, \Gamma) = \min_{x \in \Gamma} \|x_0 - x\|_2 = \min_{s \in [0, |\Gamma|)} \|x_0 - \boldsymbol{X}(s)\|_2 =: \min_{s \in [0, |\Gamma|)} d_{x_0}(s).$$

Since the curve is closed, the minimum occurs for s_0 such that $d'_{x_0}(s_0) = 0$, which implies that

$$(\boldsymbol{X}(s_0) - x_0) \cdot \boldsymbol{t}(s_0) = 0,$$

for $s \in [0, |\Gamma|)$. Hence, x_0 belongs to a line segment centered and normal to the curve and since we are assuming that $\text{dist}(x_0, \Gamma) \leq \tau$ we have that $x_0 \in N_{\boldsymbol{X}(s_0)}(\tau)$, and then $x_0 \in Tub(\tau)$. $\square$

Remark A.1. Moreover, for any $x \in Tub(r)$ there exists a unique $x_\Gamma \in \Gamma$ such that $\text{dist}(x, x_\Gamma) = \text{dist}(x, \Gamma)$ and $x - x_\Gamma$ is perpendicular to Γ at x_Γ.

Lemma A.1.2. *For an element $T \in \mathcal{T}_h^\Gamma$, consider the segment L_T connecting the intersections of Γ with two different edges of T. Define*

$$d := \max_{x \in T_\Gamma} \operatorname{dist}(x, L_T).$$

Then, $d \leq |L_T|/2$.

Proof. Since the extreme points of L_T intersect Γ, we observe that any point on the segment L_T is at most at a distance $|L_T|/2$ from Γ. Observe that the maximum distance is reached when the normal to the curve points in the same direction than the normal to the segment L_T, i.e.

$$d = \operatorname{dist}(x_\Gamma, L_T) = \|x_\Gamma - x_{L_T}\|_2 = \operatorname{dist}(x_{L_T}, T_\Gamma) = \min_{x \in T_\Gamma} \|x_{L_T} - x\|_2 < |L_T|/2,$$

for $x_\Gamma \in \Gamma$ and $x_{L_T} \in L_T$. $\square$

Lemma A.1.3. *For every $x \in \Gamma$ consider the line segments $N_x(r)$ of length $2r$ with r the radius of the tubular neighborhood of Γ Proposition 2.3.1, centered at x and perpendicular to Γ at x. Let $x_1, x_2 \in \Gamma$ with $x_1 = \boldsymbol{X}(s_1)$ and $x_2 = \boldsymbol{X}(s_2)$ for $0 \leq s_1 \leq s_2 \leq |\Gamma|$. Consider the tubular section*

$$tub(r; x1, x2) = \bigcup \{N_x(r) : x = \boldsymbol{X}(s), s \in (s_1, s_2)\}.$$

Then, the area of the tubular section is given by

$$|tub(r; x1, x2)| = 2r|\ell|,$$

where ℓ is the curve segment in Γ between s_1 and s_2. For $\boldsymbol{X}$ are-length parameterization $|\ell| = s_2 - s_1$.

Proof. Define the curve on $Tub(r)$

$$\boldsymbol{X}^{\pm}(s) = \boldsymbol{X}(s) \pm \varepsilon \boldsymbol{n}(s), \quad \varepsilon(0, r).$$

We compute the arc-length of curves $\boldsymbol{X}^{\pm}$ for $s \in (s_1, s_2)$. Note that, using arc-length parameterization and Frenet formulas (see [44])

$$\frac{d\boldsymbol{X}^{\pm}(s)}{ds} = \boldsymbol{t}(s)(1 \mp \varepsilon\kappa(s)), \quad s \in (s_1, s_2),$$

where $\kappa(s)$ is the curvature of Γ. Then the arc-length are given by

$$\ell^{\pm}(\varepsilon) := \int_{s_1}^{s_2} \|\frac{d\boldsymbol{X}^{\pm}(s)}{ds}\|_2 ds = (s_2 - s_1) \mp \varepsilon \int_{s_1}^{s_2} \kappa(s) ds,$$

for $\varepsilon(0, r)$. Now we compute the are of the tubular section,

$$|tub(r; s_1, s_2)| = \int_0^r \ell^+(\varepsilon) d\varepsilon + \int_0^r \ell^-(\varepsilon) d\varepsilon = 2r(s_2 - s1),$$

which proves the result. □

Lemma A.1.4. *Consider the Γ_s a segment of the curve Γ and L_T the straight segment connecting the two end points of Γ_s. Assume that $|L_T| \leq r$, where r is the radius of r is the radius of the r-tubular neighborhood. Then, it holds*

$$|\Gamma_s| \leq 2|L_T|.$$

Proof. Let x_1, x_2 be the endpoints of the line segment L_T. For $i = 1, 2$, let N_i be the line that is normal to Γ at x_i. Let $\tilde{S}$ be the infinite region enclosed by N_1 and N_2, then let $S = Tub(r/2) \cap \tilde{S}$ be the tubular section of Γ_s. We see that the area of S is given by $|S| = r|\Gamma_s|$. Let M_1 and M_2 be two lines that are parallel to L_T and distance r from L_T. Consider the trapezoid, R, enclosed by N_i, M_i, $i = 1, 2$. We note that the area of R is given by $|R| = 2r|L_T|$. The result will follow if we show that $S \subset R$ since this will imply that $r|\Gamma_s| \leq 2r|L_T|$.

To this end, we first note that the line segment $L_T \subset Tub(r/2)$ since the distance of any point in L_T to Γ is less than $|L_T|/2$ which we are assuming is less than $r/4$ (Assumption $2h < r/2$). Let $x \in S$, then we know there exists a unique point $x_\Gamma \in \Gamma_s$ where the distance from x to x_Γ is less than $r/2$ and the line, which we denote by L_x, that passes through x and x_Γ is perpendicular to Γ at x_Γ. We know that L_x intersects L_T and we call this point y. We also know that distance distance between y and x_Γ is less than $r/4$ since $y \in L_T \subset Tub(r/4)$. Hence, we have shown that $\text{dist}(y, x) \leq 3r/4$. This, of course implies that the distance of x to the infinite line L_T^{ext} (which is the line that contains the line segment L_T) is at most r. In other words, x is in between the two lines M_1 and M_2. Since x was in the tubular section S it was in between the two lines N_1 and N_2 and hence x belongs to the trapezoid R. $\square$

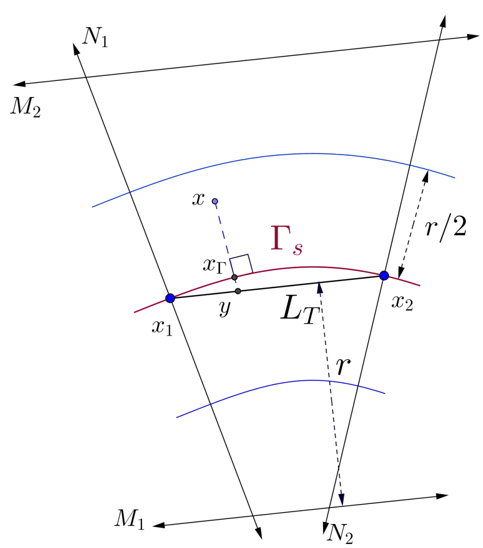

Figure A.1: Proof of Lemma A.1.4. Illustration of a curve segment Γ_s, straight line segment L_T connecting the end points of Γ_s, the tubular section of radius S, and the trapezoid R.

A.1.1 Proof of Lemma 4.3.1.

Let $e = \mathrm{int}\,(\partial T_1 \cap \partial T_2) \in \mathcal{E}_h^\Gamma$, with $T_1, T_2 \in \mathcal{T}_h$, and the previous definitions of $e^\pm = e \cap \Omega^\pm$. We analyze the case in Ω^-. The same analysis is valid in Ω^+. We proceed analyzing two cases depending on the intersection of the edge e with Γ:

(i) If $e \cap \Gamma = \emptyset$, $(e = e^-)$. If either T_1 or T_2 does not belong to $\mathcal{T}_h^\Gamma$ the results is trivial. Consider the case where T_1 and T_2 belong to $\mathcal{T}_h^\Gamma$, the interface sections $T_{1,\Gamma}$ and $T_{2,\Gamma}$ are nonempty. We consider the midpoint m_e the segment e and the ball $B_{|e|/2}(m_e)$ of radius $|e|/2$ and $|e|/2$ and centered at m_e. If the interface does not cross the ball $B_{|e|/2}(m_e)$ then we have

$$|T_1^-| \geq |B_{|e|/2}(m_e) \cap T_1|.$$

Denote by $\underline{\alpha}$ the minimum angle of the triangulation (given by shape regularity), and let $\tilde{\alpha} = \min\{\underline{\alpha}, \pi/4\}$. Now consider the isosceles triangle $\tilde{T}_1$ with base edge e and base angles $\tilde{\alpha}$. Then, clearly $\tilde{T}_1 \subset B_{|e|/2}(m_e) \cap T_1$ and $|\tilde{T}_1| = (|e^-|/2)^2 \tan\{\tilde{\alpha}\}$. Therefore, $|T_1^-| \geq (|e^-|/2)^2 \tan\{\tilde{\alpha}\}$. Assume then that the interface crosses the ball $B_{|e|/2}(m_e)$ in T_1. Observe that this implies that there exists a point in $T_{1,\Gamma}$ which normal passes through m_e with distance less than $|e|/2$. Now, if $T_{2,\Gamma}$ crosses the ball then we will have two points on Γ at a distance less than $|e|/2$ whose normal passes through m_e which contradicts the tubular neighborhood assumption. Therefore

$$\max_{i=\{1,2\}} |T_i^-| \geq \left(\frac{|e|}{2}\right)^2 \tan\{\tilde{\alpha}\}.$$

(ii) If $e \cap \Gamma \neq \emptyset$. Similarly as in the previous case, consider m_e the midpoint of e^- and the ball of radius $|e^-|/2$ centered at m_e. We observe that this ball can not cross both $T_{1,\Gamma}$ and $T_{2,\Gamma}$. Therefore

$$\max_{i=\{1,2\}} |T_i^-| \geq \left(\frac{|e^-|}{2}\right)^2 \tan\{\tilde{\alpha}\}.$$

A.1.2 Proof of Lemma 4.3.6.

We analyze the case in Ω^-. We first observe that, by triangle inequality we have

$$|l_T| \ \leq \sum_{i=1}^{3} |e_i^-| \ \leq \ 3 \max_{i=\{1,2,3\}} |e^-|.$$

Therefore, using Lemma A.1.4

$$|T_\Gamma| \ \leq \ 6 \max_{i=1,2,3} |e_i^-|.$$

Same analysis is valid to prove the statement in Ω^+.

A.1.3 Proof of Proposition 5.2.1

Consider a node z of the triangulation $\mathcal{T}_h$ and the patch of elements Δ_z (defined in Proposition A.1.3) associated to z. Since we are assuming that h is small enough and the interface is smooth we have that: the interface intersects each edge of triangulation at most once, or the interface coincides with an edge. with an edge. Therefore, if $z \in \overline{\Omega^-}$, there exists at least one node $z' \in \overline{\Delta}_z$ with $z' \in \overline{\Omega^-}$, and the edge $\overline{e}$ connecting z and z' is completely contained in $\overline{\Omega}^-$. If there exists more than one node satisfying this property then it would follow that an element of the patch of z is fully contained in Ω^-. We then prove the remaining case. See Figure A.2 for an illustration of these definitions.

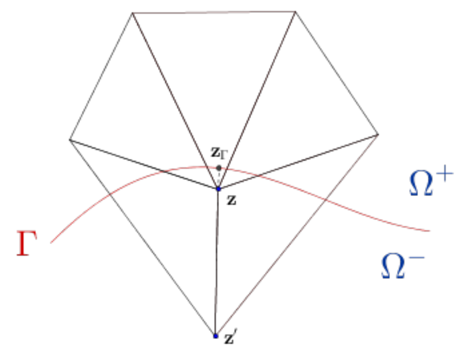

Figure A.2: Appendix A.1.3, proof of Proposition 5.2.1. Illustration of definitions.

Let z_Γ the point on Γ resulting of extending the segment e connecting z and z'. Denote by A_1 and A_2 the regions separated by the segment $e_\Gamma = \operatorname{int}(\overline{z' z_\Gamma})$, such that $A_1 \cup A_2 \cup e_\Gamma = \Delta_z \cap \Omega^-$. Then, by Lemma 4 in [63], we have

$$|e_\Gamma|^2 \leq C \max\{|A_1|, |A_2|\}.$$

Thus, the result follows from $|e| \leq |e^\Gamma|$ and shape regularity.

A.2 Proof of estimate (3.26)

We first use a dyadic decomposition of Ω. $\Omega = \Omega^* \cup \bigcup_{j=1}^J \Omega_j$ where $\Omega_j := \{x \in \Omega : d_{j+1} \leq |x - z| \leq d_j\}$, and $d_j = 2^{-j}$. Here, $J = \log_2(1/h)$ and $\Omega^* = \Omega \cap B_h$ where B_h is the ball of radius h centered z.

Let us use the notation $D_j = \Omega_j \cap \partial R_h \backslash \partial\Omega$ and $D^* = \Omega^* \cap \partial R_h \backslash \partial\Omega$ then we have

$$\|D_{\boldsymbol{n}} g\|_{L^1(\partial R_h \backslash \partial\Omega)} = \|D_{\boldsymbol{n}} g\|_{L^1(D^*)} + \sum_{j=1}^{J} \|D_{\boldsymbol{n}} g\|_{L^1(D_j)}$$

First we bound the first term. Using Cauchy-Schwarz inequality and the fact the one dimensional measure of D^* is h we have

$$\|D_{\boldsymbol{n}} g\|_{L^1(D^*)} \leq C h^{1/2} \|\nabla g\|_{L^2(D^*)}.$$

If we use a trace inequality then we have

$$\begin{aligned} h^{1/2}\|\nabla g\|_{L^2(D^*)} &\leq C(\|\nabla g\|_{L^2(\Omega^* \cap B_h)} + h\|D^2 g\|_{L^2(\Omega^* \cap B_h)}) \\ &\leq C(\|\nabla g\|_{L^2(\Omega)} + h\|D^2 g\|_{L^2(\Omega)}). \end{aligned}$$

Elliptic regularity will give

$$\|\nabla g\|_{L^2(\Omega)} + h\|D^2 g\|_{L^2(\Omega)} \leq C(\|\delta_h\|_{L^2(\Omega)} + h\|\delta_h\|_{H^1(\Omega)}) \leq \frac{C}{h},$$

which shows that

$$\|D_{\boldsymbol{n}} g\|_{L^1(D^*)} \leq \frac{C}{h}.$$

To take care of the sum we use Cauchy-Schwarz inequality again and get

$$\sum_{j=1}^{J} \|D_{\boldsymbol{n}} g\|_{L^1(D_j)} \leq \sum_{j=1}^{J} d_j \|\nabla g\|_{L^\infty(D_j)}$$

Using the Green's function representation of g and the fact that D_j is distance d_j away from z one can show (see [62])

$$\|\nabla g\|_{L^\infty(D_j)} \leq \frac{C}{d_j}.$$

Hence,

$$\sum_{j=1}^{J} \|D_{\boldsymbol{n}} g\|_{L^1(D_j)} \le C \sum_{j=1}^{J} \frac{1}{d_j} = C \sum_{j=1}^{J} \frac{1}{d_j} = C(2^{J+1} - 1) \le \frac{C}{h}.$$

A.3 Derivation of jumps (3.32) and (3.33)

We define for $\epsilon > 0$ the set $\Omega_\epsilon = \{x \in \Omega : \quad dist(x, \Gamma) < \epsilon\}$, where $dist$ is the standard distance function. We will also denote $\Gamma_\epsilon^\pm = \partial\Omega_\epsilon \cap \Omega^\pm$. From equation (3.31a), taking divergence, multiplying by an arbitrary $\phi \in C^2$ of compact support in Ω_ϵ and integrating we obtain

$$\begin{aligned} \int_{\Omega_\epsilon} \nabla \cdot \nabla p \, \phi dx &= \int_{\Omega_\epsilon} \nabla \cdot f \phi dx + \int_{\Omega_\epsilon} \nabla \cdot \boldsymbol{B} \phi dx \\ &= \int_{\Omega_\epsilon} \nabla \cdot f \phi dx - \int_{\Gamma} \boldsymbol{\beta} \cdot \nabla \phi ds. \end{aligned} \tag{A.1}$$

For the left-hand side of the equation above we integrate by parts twice obtaining

$$\begin{aligned} \int_{\Omega_\epsilon} \nabla \cdot \nabla p \, \phi dx = & \int_{\Gamma_\epsilon^+} Dp^+ \cdot \boldsymbol{n} \phi ds + \int_{\Gamma_\epsilon^-} Dp^- \cdot \boldsymbol{n} \phi ds \\ & - \int_{\Gamma_\epsilon^+} D\phi \cdot \boldsymbol{n} p^+ ds - \int_{\Gamma_\epsilon^-} D\phi \cdot \boldsymbol{n} p^- ds + \int_{\Omega_\epsilon} p \nabla \cdot \nabla \phi dx. \end{aligned}$$

By the definitions of $\Gamma_\epsilon^\pm$ we can fix its normal vectors by the normal vector to the interface Γ. Then, taking the limit as ϵ goes to zero we obtain

$$\lim_{\epsilon \to 0} \int_{\Omega_\epsilon} p \nabla \cdot \nabla \phi dx = 0 \tag{A.2}$$

$$\lim_{\epsilon \to 0} \int_{\Omega_\epsilon} \nabla \cdot \nabla p \phi dx \quad = \quad \int_{\Gamma} [Dp \cdot \boldsymbol{n}] \, \phi ds - \int_{\Gamma} D\phi \cdot \boldsymbol{n} \, [p] \, ds \tag{A.3}$$

We need to write the right-hand side in (A.1) in terms of the normal and tangential derivative. Let θ be the angle between the x direction (x-axis) and $\boldsymbol{n}$ direction and let $R(\theta)$ the rotation matrix defined by

$$R(\theta) = \begin{pmatrix} \cos(\theta) & -\sin(\theta) \\ \sin(\theta) & \cos(\theta) \end{pmatrix}$$

Then, $\nabla\phi = (D_{\boldsymbol{n}}\phi, D_{\boldsymbol{t}}\phi)R(\theta)^t$. Using this equivalency in (A.1) and integration by parts we obtain

$$\begin{aligned} \int_\Gamma \boldsymbol{\beta}\cdot\nabla\phi ds &= \int_\Gamma \boldsymbol{\beta}\cdot\left((D_{\boldsymbol{n}}\phi, D_{\boldsymbol{t}}\phi)R(\theta)^t\right) ds \\ &= \int_\Gamma (\boldsymbol{\beta}R(\theta))\cdot(D_{\boldsymbol{n}}\phi, D_{\boldsymbol{t}}\phi)ds \\ &= \int_\Gamma \hat{\boldsymbol{\beta}}\cdot(D_{\boldsymbol{n}}\phi, D_{\boldsymbol{t}}\phi)ds \\ &= \int_\Gamma \hat{\beta}_1 D_{\boldsymbol{n}}\phi ds - \int_\Gamma \frac{\partial}{\partial s}\hat{\beta}_2\phi ds \end{aligned}$$

Here we have defined $\hat{\boldsymbol{\beta}} = \boldsymbol{\beta}R(\theta)$. Matching this result with the limits in (A.2) we can conclude that

$$[p] = \hat{\beta}_1 \qquad [D_{\boldsymbol{n}}p] = \frac{\partial}{\partial s}\hat{\beta}_2. \tag{A.4}$$

Now, to get the normal jump of the gradient of the velocity we applied equation (3.31d), resulting

$$[D_{\boldsymbol{n}}\boldsymbol{u}] = \boldsymbol{\beta} + [p\boldsymbol{n}] = \boldsymbol{\beta} + \hat{\beta}_1\boldsymbol{n}. \tag{A.5}$$

A.4 Notes on implementation

A.4.1 Quadrature over curved elements.

The method defined in (5.5) requires the integration, over an element $T \in \mathcal{T}_h^\Gamma$, of $\nabla w_T^u \cdot \nabla v$. Now, since the correction function w_T^u is defined as piecewise polynomial of degree k on each piece of the restriction $T^\pm = T \cap \Omega^\pm$, we need some quadrature formulas on this region, say curved elements (polygons with one edge curved). To do so, we observe that L_T divides T in two regular polygons $\tilde{T}^\pm$, one is a triangle and the other a quadrilateral, see figure A.3. In order to make the presentation clearer, we will write the integral in terms of the coordinates system $(\tau,\, \eta)$ (associated to the vector $\boldsymbol{\tau}$ and $\boldsymbol{\eta}$, with $\boldsymbol{\eta}$ pointing outward T^-) such that the origin is the midpoint of L_T, the point $\frac{y_T+z_T}{2}$. Let $f \in C^{n+1}(T)$, then we write

$$\int_{T^\pm} f(x,y)dxdy \;=\; \int_{\tilde{T}^\pm} f(x,y)dxdy \pm \int_{-r_T/2}^{r_T/2}\int_0^{\gamma(\tau)} f(\tau,\eta)d\eta d\tau \qquad \text{(A.6)}$$

where, $\gamma(\tau)$ is the equation for the curve Γ on T. The first integral in (A.6) is over a polygon (triangle or quadrilateral) and we can use quadrature rules over polygons to approximate it, whereas the second integral is related to the curve, and we will use some Gaussian quadratures. First step, we take n Gaussian points $\{\tau_i\}_{i=1}^n$ over the segment L_T, equivalently, the interval $[-r_T/2, r_T/2]$ in the $(\tau,\, \eta)$-axis, and for each point we compute its projection onto the curve Γ in the $\boldsymbol{\eta}-$direction, say $\gamma(\tau_i)$. Now we compute, the Gaussian points for the segment $[0, \gamma(\tau_i)]$, we denote them by

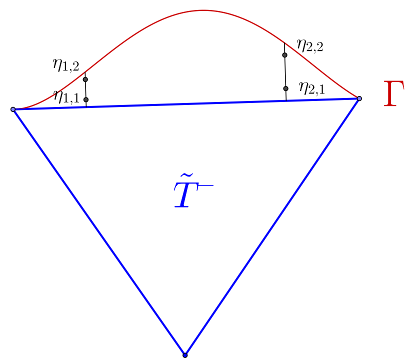

Figure A.3: Illustration of the Gaussian points over segments $Q_0^{1,T}, Q_1^{1,T}$ for quadrature purposes.

$\{\eta_{i,j}\}_{j=1}^n$. Therefore

$$\int_{-r_T/2}^{r_T/2}\int_0^{\gamma(\tau)} f(\tau,\eta)d\eta d\tau \;\approx\; \sum_{i=1}^n \frac{r_T}{2}\omega_i \sum_{j=1}^n \frac{|\gamma(\tau_i)|}{2}\omega_j f(\tau_i,\eta_{i,j})$$

where ω_i are the weights in the interval $[-1,1]$, and . See Figure A.3 for illustration of this notation. See also Figure 3.1. The error of the quadrature rule is of order $\mathcal{O}(r_T^{2n})$, and the constant is dependent on the derivatives $\|D^{(2n-k)}f\|_{L^\infty}\|\gamma^{(k)}\|_{L^\infty}$, $k=0,...,2n$. Observe that since the term involves the derivative of γ the quadrature rule is in general not exact.

A.4.2 Construction of basis functions of $S^1(T)$

In this section we define basis functions $\{w_1,w_2,w_3\}$ of the space $S^1(T)$, for $T\in\mathcal{T}_h^\Gamma$. Consider $\{x_1,x_2,x_3\}$ nodes of the element T. Let $\{\lambda_1,\lambda_2,\lambda_3\}$ be the barycentric coordinates of a point $x\in T$ with respect to $\{x_1,x_2,x_3\}$. Consider the following representation

$$w_i(x)=\begin{cases} w_i^-(x), & \text{if } x\in T^-;\\ w_i^+(x), & \text{if } x\in T^+.\end{cases}\quad w_i^\pm(x)=\sum_{j=1}^3 a_{i,j}^\pm\lambda_j(x).$$

We construct $\{w_1, w_2, w_3\}$, a set of basis functions of the space $S^1(T)$, by satisfying the following conditions: for $i = 1, 2, 3$

$$\begin{cases} w_i(x_j) = \delta_{i,j} & \text{for } j = 1,2,3; \\ [w_i(x_0)] = 0 & x_0 \in T_\Gamma; \\ [D_{\boldsymbol{t}_0} w_i] = 0 & \boldsymbol{t}_0 = \boldsymbol{t}(x_0); \\ [D_{\boldsymbol{n}_0} w_i = 0] & \boldsymbol{n}_0 = \boldsymbol{n}(x_0); \end{cases} \quad \text{where} \quad \delta_{i,j} = \begin{cases} 1, & \text{if } i = j \\ 0, & \text{if } i \neq j. \end{cases}$$

These conditions are written in a system of size 6×6 using the barycentric coordinates representation of $w_i^\pm$, i.e., we find the unknowns coefficients $\{a_{i,j}^\pm\}_{j=1}^3$ of w_i for $i = 1, 2, 3$, solutions of:

$$\begin{pmatrix} \tilde{\delta}_{1,+} & 0 & 0 & \tilde{\delta}_{1,-} & 0 & 0 \\ 0 & \tilde{\delta}_{2,+} & 0 & 0 & \tilde{\delta}_{2,-} & 0 \\ 0 & 0 & \tilde{\delta}_{3,+} & 0 & 0 & \tilde{\delta}_{3,-} \\ \lambda_1(x_0) & \lambda_2(x_0) & \lambda_3(x_0) & -\lambda_1(x_0) & -\lambda_2(x_0) & -\lambda_3(x_0) \\ -D_{\boldsymbol{t}_0}\lambda_1 & -D_{\boldsymbol{t}_0}\lambda_2 & -D_{\boldsymbol{t}_0}\lambda_3 & D_{\boldsymbol{t}_0}\lambda_1 & D_{\boldsymbol{t}_0}\lambda_2 & D_{\boldsymbol{t}_0}\lambda_3 \\ -\rho^+ D_{\boldsymbol{n}_0}\lambda_1 & -\rho^+ D_{\boldsymbol{n}_0}\lambda_2 & \rho^+ D_{\boldsymbol{n}_0}\lambda_3 & \rho^- D_{\boldsymbol{n}_0}\lambda_1 & \rho^- D_{\boldsymbol{n}_0}\lambda_2 & \rho^- D_{\boldsymbol{n}_0}\lambda_3 \end{pmatrix} \begin{pmatrix} a_{i,1}^+ \\ a_{i,2}^+ \\ a_{i,3}^+ \\ a_{i,1}^- \\ a_{i,2}^- \\ a_{i,3}^- \end{pmatrix} = \begin{pmatrix} \delta_{i,1} \\ \delta_{i,2} \\ \delta_{i,3} \\ 0 \\ 0 \\ 0 \end{pmatrix}$$

where

$$\tilde{\delta}_{j,\pm} = \begin{cases} 1, & \text{if } x_j \in T^\pm \\ 0, & \text{if } x_j \in T^\mp. \end{cases}$$

A.5 Proof of even extension

In this section we give an explicit construction of an even extension from Ω^+ to Ω. We apply this to continuous functions that are in $H^1(\Omega^+)$. The extension result (A.7) is a well-known result in partial differential equations. We sketch the proof with the aim to obtain the explicit construction of the extension, which will be used in the proof of Lemma 5.3.1.

For simplicity, assume that Ω^+ is the inclusion (i.e. $\partial\Omega^+ = \Gamma$). For $\epsilon > 0$ define the tubular neighborhood

$$R_\epsilon = \{x \in \Omega : d(x) := \text{dist}(x, \partial\Omega^+) \leq \epsilon\}.$$

Since Γ is smooth, and for ϵ small enough, for each $x \in R_\epsilon$ there exists a unique point $x_{\partial\Omega^+} \in \partial\Omega^+$ such that

$$|x - x_{\partial\Omega^+}| = \text{dist}(x, \partial\Omega^+).$$

Moreover, define the unit normal vector to $\partial\Omega^+$ pointing towards x as: $n(x) = (x - x_{\partial\Omega^+})/|x - x_{\partial\Omega^+}|$. Hence, for each $x \in R_\epsilon$ we define its "reflection" $\widetilde{x} = \widetilde{x}(x)$ by

$$\widetilde{x} = x_{\partial\Omega^+} - d(x)n(x).$$

Now, given $v \in C(\overline{\Omega^+})$ we define $\widetilde{G}v \in C(\Omega^+ \cup R_\epsilon)$ such that:

$$\widetilde{G}v(x) = \begin{cases} v(x), & \text{if } x \in \overline{\Omega^+} \\ v(\widetilde{x}), & \text{if } x \in R_\epsilon \backslash \Omega^+. \end{cases}$$

Our extension is complete by considering a cutoff function $\eta \in C_c(\Omega^+ \cup R_\epsilon)$, such that $\eta \equiv 1$ on $\Omega^+ \cup R_{\epsilon/2}$. Of course, we extend η to all of Ω by zero. Thus, the extension $Gv \in C_c(\Omega)$ is defined as follows

$$Gv = \eta\widetilde{G}v.$$

The estimate is a well-known result.

$$\|Gv\|_{H^1(\Omega)} \leq C\|v\|_{H^1(\Omega^+)}. \tag{A.7}$$

A.6 Proof of discrete extension Lemma 5.3.1

We first introduce notation. For each node x of the triangulation $\mathcal{T}_h$ we consider the patch associated to x, denoted by Δ_x. Moreover, we consider Δ_x^- as the restrictions to Ω^-, i.e.,

$$\Delta_x^- = \Delta_x \cap \Omega^-.$$

Considering definitions introduced in Appendix A.5, we define the reflection of Δ_x^-

$$\widetilde{\Delta}_x^- = \{\widetilde{y}(y) : y \in \Delta_x^-\} \subset \overline{\Omega^+}.$$

Let $v \in V_h^+$, then, by (A.7) there exists $Gv \in H_0^1(\Omega)$ such that $Gv = v$ in Ω^+, and

$$\|Gv\|_{H^1(\Omega)} \leq C\|v\|_{H^1(\Omega^+)}.$$

We proceed constructing a stable interpolation operator of the extended function Gv onto V_h^c, invariant on V_h^+. Define $P_1(Gv)$ for any node x of the triangulation $\mathcal{T}_h$ by

$$P_1(Gv)(x) = \begin{cases} v(x), & \text{if } x \in \overline{\Omega^+}, \\ \frac{1}{|\Delta_x^-|}\int_{\Delta_x^-} Gv(y)dy, & \text{if } x \in \Omega^-. \end{cases}$$

It is not difficult to show that

$$\|P_1(Gv)\|_{H^1(\Omega)} \leq C\|Gv\|_{H^1(\Omega)}. \tag{A.8}$$

Observe that this definition does not guarantee that $P_1(Gv)$ coincides with v for a node in $\Omega_h^+ \backslash \Omega^+$. Then we need to correct the definition of the interpolant on these nodes. The needed extension is defined as follows

$$Ev := P_2(Gv)(x) = \begin{cases} v(x), & \text{if } x \in \overline{\Omega}_h^+, \\ \frac{1}{|\Delta_x^-|}\int_{\Delta_x^-} Gv(y)dy, & \text{if } x \in \Omega\backslash\overline{\Omega}_h^+. \end{cases}$$

Notice that $P_2(Gv)$ and $P_1(Gv)$ agree at every node except the nodes x in the following set

$$S_h = \{x \in \Omega_h^+ \backslash \Omega^+ : x \text{ is a node of some triangle } T \in \mathcal{T}_h^\Gamma\}.$$

Define also the collection of triangles that have a node in S.

$$\mathcal{M}_h = \{T \in \mathcal{T}_h : \text{ at least one of three vertices of } T \text{ belongs to } S_h\}.$$

If we define $e_h = P_2(Gv) - P_1(Gv)$ we see that

$$\|\nabla e_h\|^2_{L^2(\Omega)} = \sum_{T\in\mathcal{M}_h} \|\nabla e_h\|^2_{L^2(T)}.$$

For each $T \in \mathcal{M}_h$, let $x_T \in S$ be such that $|e_h(x_T)| = \max_{y\in T}|e_h(y)|$. Then it is simple to show, using inverse estimates, that

$$\|\nabla e_h\|_{L^2(T)} \leq C\,|e_h(x_T)|.$$

By definition we have

$$|e_h(x_T)| = \left| v(x_T) - \frac{1}{|\Delta^-_{x_T}|}\int_{\Delta^-_{x_T}} Gv(y)dy \right| = \left| v(x_T) - \frac{1}{|\Delta^-_{x_T}|}\int_{\widetilde{\Delta}^-_{x_T}} Gv(\widetilde{y})J(\widetilde{y})d\widetilde{y} \right|,$$

where $J(\widetilde{y})$ is the Jacobian of the map $\widetilde{y}(y) \to y$. Applying the definition of Gv from the previous section, using that $v(\widetilde{x}_T) = v(x_T)$, and the fact that $\int_{\widetilde{\Delta}^-_{x_T}} J(\widetilde{y})d\widetilde{y} = |\Delta^-_{x_T}|$ we get

$$|e_h(x_T)| = \left| \frac{1}{|\Delta^-_{x_T}|}\int_{\widetilde{\Delta}^-_{x_T}} (v(\widetilde{x}_T) - v(\widetilde{y}))J(\widetilde{y})d\widetilde{y} \right| \leq C \,\text{diameter}\,(\widetilde{\Delta}^-_{x_T})\|\nabla v\|_{L^\infty(\widetilde{\Delta}^-_{x_T})}.$$

We see that $\widetilde{\Delta}^-_{x_T} \subset B_{\frac{d}{2}h}(T) = \{y \in \Omega^+_h : \text{dist}(y,T) < \frac{d}{2}h\}$ for a d large enough but independent of h and T.

Using an inverse estimate we have

$$\text{diameter}\,(\widetilde{\Delta}^-_{x_T})\|\nabla v\|_{L^\infty(\widetilde{\Delta}^-_{x_T})} \leq C\|\nabla v\|_{L^2(B_{d\,h}(T))}.$$

Hence, we get

$$\|\nabla e_h\|^2_{L^2(\Omega)} \leq C \sum_{T\in\mathcal{M}_h} \|\nabla v\|^2_{L^2(B_{d\,h}(T))} \leq C\,\|\nabla v\|^2_{L^2(\Omega^+_h)}.$$

Finally, using the triangle inequality we get

$$\|\nabla Ev\|_{L^2(\Omega)} \leq \|\nabla P_1(Gv)\|_{L^2(\Omega)} + C\|\nabla v\|_{L^2(\Omega^+_h)}.$$

The result now follows from using (A.8) and Poincare's inequality.

Bibliography

1. S. Adjerid, M. Ben-Romdhane, and T. Lin, *Higher degree immersed finite element methods for second-order elliptic interface problems*, Int. J. Numer. Anal. Model., 11 (2014), pp. 541–566.

2. D. N. Arnold, *An Interior Penalty Finite-Element Method with Discontinuous Elements*. Thesis (Ph.D.)–The University of Chicago.

3. ——, *An interior penalty finite element method with discontinuous elements*, SIAM J. Numer. Anal., 19 (1982), pp. 742–760.

4. D. N. Arnold, F. Brezzi, B. Cockburn, and L. D. Marini, *Unified analysis of discontinuous Galerkin methods for elliptic problems*, SIAM J. Numer. Anal., 39 (2001/02), pp. 1749–1779.

5. I. Babuška, *The finite element method with lagrangian multipliers*, Numerische Mathematik, 20, pp. 179–192.

6. ——, *The finite element method for elliptic equations with discontinuous coefficients*, Computing (Arch. Elektron. Rechnen), 5 (1970), pp. 207–213.

7. ——, *The finite element method with penalty*, Mathematics of computation, 27 (1973), pp. 221–228.

8. I. Babuška and U. Banerjee, *Stable generalized finite element method (SGFEM)*, Comput. Methods Appl. Mech. Engrg., 201/204 (2012), pp. 91–111.

9. I. Babuška, U. Banerjee, and J. E. Osborn, *Survey of meshless and generalized finite element methods: A unified approach*, Acta Numerica, 12 (2003), pp. 1–125.

10. I. Babuška, G. Caloz, and J. E. Osborn, *Special finite element methods for a class of second order elliptic problems with rough coefficients*, SIAM J. Numer. Anal., 31 (1994), pp. 945–981.

11. I. Babuška and J. Melenk, *The partition of unity method*, International Journal for Numerical Methods in Engineering, 40 (1997), pp. 727–758.

12. N. Barrau, R. Becker, E. Dubach, and R. Luce, *A robust variant of NXFEM for the interface problem*, C. R. Math. Acad. Sci. Paris, 350 (2012), pp. 789–792.

13. J. W. Barrett and C. M. Elliott, *Finite element approximation of the Dirichlet problem using the boundary penalty method*, Numerische Mathematik, 49 (1986), pp. 343–366.

14. J. T. Beale and A. T. Layton, *On the accuracy of finite difference methods for elliptic problems with interfaces*, Commun. Appl. Math. Comput. Sci., 1 (2006), pp. 91–119 (electronic).

15. R. Becker, E. Burman, and P. Hansbo, *A Nitsche extended finite element method for incompressible elasticity with discontinuous modulus of elasticity*, Comput. Methods Appl. Mech. Engrg., 198 (2009), pp. 3352–3360.

16. T. Belytschko and T. Black, *Elastic crack growth in finite elements with minimal remeshing*, International journal for numerical methods in engineering, 45 (1999), pp. 601–620.

17. M. Ben Romdhane, *Higher-Degree Immersed Finite Elements for Second-Order Elliptic Interface Problems*, PhD thesis, Virginia Polytechnic Institute and State University, 2011.

18. M. P. Bendsoe and O. Sigmund, *Topology optimization: theory, methods, and applications*, Springer Science & Business Media, 2013.

19. D. Boffi, *The immersed boundary method for fluid-structure interactions: mathematical formulation and numerical approximation*, Boll. Unione Mat. Ital. (9), 5 (2012), pp. 711–724.

20. D. Boffi, N. Cavallini, and L. Gastaldi, *Finite element approach to immersed boundary method with different fluid and solid densities*, Math. Models Methods Appl. Sci., 21 (2011), pp. 2523–2550.

21. ——, *The finite element immersed boundary method with distributed lagrange multiplier*, SIAM Journal on Numerical Analysis, 53 (2015), pp. 2584–2604.

22. D. Boffi and L. Gastaldi, *A finite element approach for the immersed boundary method*, Comput. & Structures, 81 (2003), pp. 491–501. In honour of Klaus-Jürgen Bathe.

23. D. Boffi, L. Gastaldi, and L. Heltai, *Numerical stability of the finite element immersed boundary method*, Mathematical Models and Methods in Applied Sciences, 17 (2007), pp. 1479–1505.

24. ——, *On the cfl condition for the finite element immersed boundary method*, Computers & structures, 85 (2007), pp. 775–783.

25. D. Boffi, L. Gastaldi, L. Heltai, and C. S. Peskin, *On the hyper-elastic formulation of the immersed boundary method*, Computer Methods in Applied Mechanics and Engineering, 197 (2008), pp. 2210–2231.

26. D. Braess, *Finite elements: Theory, fast solvers, and applications in solid mechanics*, Cambridge University Press, 2007.

27. S. C. Brenner and L. R. Scott, *The mathematical theory of finite element methods*, vol. 15 of Texts in Applied Mathematics, Springer-Verlag, New York, 1994.

28. F. Brezzi and R. S. Falk, *Stability of higher-order hood-taylor methods*, SIAM Journal on Numerical Analysis, 28 (1991), pp. 581–590.

29. E. Burman, *Ghost penalty*, C. R. Math. Acad. Sci. Paris, 348 (2010), pp. 1217–1220.

30. E. Burman and P. Hansbo, *Fictitious domain finite element methods using cut elements: I. A stabilized Lagrange multiplier method*, Comput. Methods Appl. Mech. Engrg., 199 (2010), pp. 2680–2686.

31. ——, *Fictitious domain methods using cut elements: III. A stabilized Nitsche method for Stokes' problem*, ESAIM Math. Model. Numer. Anal., 48 (2014), pp. 859–874.

32. E. Burman and P. Zunino, *A domain decomposition method based on weighted interior penalties for advection-diffusion-reaction problems*, SIAM J. Numer. Anal., 44 (2006), pp. 1612–1638 (electronic).

33. ——, *Numerical approximation of large contrast problems with the unfitted Nitsche method*, in Frontiers in numerical analysis—Durham 2010, vol. 85 of Lect. Notes Comput. Sci. Eng., Springer, Heidelberg, 2012, pp. 227–282.

34. Z. Cai, X. Ye, and S. Zhang, *Discontinuous Galerkin finite element methods for interface problems: a priori and a posteriori error estimations*, SIAM J. Numer. Anal., 49 (2011), pp. 1761–1787.

35. B. Camp, T. Lin, Y. Lin, and W. Sun, *Quadratic immersed finite element spaces and their approximation capabilities*, Advances in Computational Mathematics, 24 (2006), pp. 81–112.

36. Z. Chen and J. Zou, *Finite element methods and their convergence for elliptic and parabolic interface problems*, Numer. Math., 79 (1998), pp. 175–202.

37. A. J. Chorin, *A numerical method for solving incompressible viscous flow problems*, Journal of computational physics, 2 (1967), pp. 12–26.

38. C.-C. Chu, I. G. Graham, and T.-Y. Hou, *A new multiscale finite element method for high-contrast elliptic interface problems*, Math. Comp., 79 (2010), pp. 1915–1955.

39. P. G. Ciarlet, *The finite element method for elliptic problems*, North-Holland Publishing Co., Amsterdam-New York-Oxford, 1978. Studies in Mathematics and its Applications, Vol. 4.

40. K. Copps, *The design and the implementation of the generalized finite element method*. Thesis (Ph.D.)–Texas A&M University.

41. M. Crouzeix and P.-A. Raviart, *Conforming and nonconforming finite element methods for solving the stationary stokes equations i*, Revue française d'automatique, informatique, recherche opérationnelle. Mathématique, 7 (1973), pp. 33–75.

42. A. Dadone and B. Grossman, *An immersed body methodology for inviscid flows on cartesian grids*, AIAA paper, 1059 (2002), p. 2002.

43. A. Demlow, D. Leykekhman, A. H. Schatz, and L. B. Wahlbin, *Best approximation property in the W^1_∞ norm for finite element methods on graded meshes*, Math. Comp., 81 (2012), pp. 743–764.

44. M. P. do Carmo, *Differential geometry of curves and surfaces*, Prentice-Hall, Inc., Englewood Cliffs, N.J., 1976. Translated from the Portuguese.

45. J. Dolbow and T. Belytschko, *A finite element method for crack growth without remeshing*, Int. J. Numer. Meth. Eng, 46 (1999), pp. 131–150.

46. M. Dryja, *On discontinuous Galerkin methods for elliptic problems with discontinuous coefficients*, Comput. Methods Appl. Math., 3 (2003), pp. 76–85 (electronic). Dedicated to Raytcho Lazarov.

47. M. Dryja and O. B. Widlund, *Domain decomposition algorithms with small overlap*, SIAM J. Sci. Comput., 15 (1994), pp. 604–620. Iterative methods in numerical linear algebra (Copper Mountain Resort, CO, 1992).

48. G. Dziuk and C. M. Elliott, *Finite element methods for surface pdes*, Acta Numerica, 22 (2013), pp. 289–396.

49. Y. Efendiev and T. Y. Hou, *Multiscale finite element methods: theory and applications*, vol. 4, Springer Science & Business Media, 2009.

50. A. Ern, A. F. Stephansen, and P. Zunino, *A discontinuous Galerkin method with weighted averages for advection-diffusion equations with locally small and anisotropic diffusivity*, IMA J. Numer. Anal., 29 (2009), pp. 235–256.

51. L. C. Evans, *Partial differential equations*, vol. 19 of Graduate Studies in Mathematics, American Mathematical Society, Providence, RI, second ed., 2010.

52. L. J. Fauci and C. S. Peskin, *A computational model of aquatic animal locomotion*, J. Comput. Phys., 77 (1988), pp. 85–108.

53. A. L. Fogelson and C. S. Peskin, *A fast numerical method for solving the three-dimensional Stokes equations in the presence of suspended particles*, J. Comput. Phys., 79 (1988), pp. 50–69.

54. T.-P. Fries and T. Belytschko, *The extended/generalized finite element method: an overview of the method and its applications*, Internat. J. Numer. Methods Engrg., 84 (2010), pp. 253–304.

55. D. Gilbarg and N. S. Trudinger, *Elliptic partial differential equations of second order*, vol. 224 of Grundlehren der Mathematischen Wissenschaften [Fundamental Principles of Mathematical Sciences], Springer-Verlag, Berlin, second ed., 1983.

56. V. Girault, R. H. Nochetto, and R. Scott, *Stability of the finite element Stokes projection in $W^{1,\infty}$*, C. R. Math. Acad. Sci. Paris, 338 (2004), pp. 957–962.

57. E. Givelberg, *Modeling elastic shells immersed in fluid*, Communications on pure and applied mathematics, 57 (2004), pp. 283–309.

58. Y. Gong, B. Li, and Z. Li, *Immersed-interface finite-element methods for elliptic interface problems with nonhomogeneous jump conditions*, SIAM J. Numer. Anal., 46 (2007/08), pp. 472–495.

59. Y. Gong and Z. Li, *Immersed interface finite element methods for elasticity interface problems with non-homogeneous jump conditions*, Numer. Math. Theory Methods Appl., 3 (2010), pp. 23–39.

60. P. Grisvard, *Elliptic problems in nonsmooth domains*, vol. 24 of Monographs and Studies in Mathematics, Pitman (Advanced Publishing Program), Boston, MA, 1985.

61. J. Guzmán and D. Leykekhman, *Pointwise error estimates of finite element approximations to the Stokes problem on convex polyhedra*, Math. Comp., 81 (2012), pp. 1879–1902.

62. J. Guzmán, M. A. Sánchez, and M. Sarkis, *On the accuracy of finite element approximations to a class of interface problems*, Mathematics of Computations, accepted. Tech. report Scientific Computing Group, Brown University 2014-6., (2014).

63. ——, *A finite element method for high-contrast interface problems with error estimates independent of contrast*, Submitted. ArXiv preprint arXiv:1507.03873, (2015).

64. A. Hansbo and P. Hansbo, *An unfitted finite element method, based on Nitsche's method, for elliptic interface problems*, Comput. Methods Appl. Mech. Engrg., 191 (2002), pp. 5537–5552.

65. P. Hansbo, *Nitsche's method for interface problems in computational mechanics*, GAMM-Mitt., 28 (2005), pp. 183–206.

66. X. He, *Bilinear immersed finite elements for interface problems*, PhD thesis, Virginia Polytechnic Institute and State University, 2009.

67. X. He, T. Lin, and Y. Lin, *Immersed finite element methods for elliptic interface problems with non-homogeneous jump conditions*, Int. J. Numer. Anal. Model., 8 (2011), pp. 284–301.

68. ——, *The convergence of the bilinear and linear immersed finite element solutions to interface problems*, Numer. Methods Partial Differential Equations, 28 (2012), pp. 312–330.

69. T. Y. Hou and B. T. Wetton, *Second-order convergence of a projection scheme for the incompressible Navier-Stokes equations with boundaries*, SIAM Journal on Numerical Analysis, 30 (1993), pp. 609–629.

70. T. Y. Hou and X.-H. Wu, *A multiscale finite element method for elliptic problems in composite materials and porous media*, Journal of computational physics, 134 (1997), pp. 169–189.

71. J. Huang and J. Zou, *Some new a priori estimates for second-order elliptic and parabolic interface problems*, J. Differential Equations, 184 (2002), pp. 570–586.

72. R. Kafafy, T. Lin, Y. Lin, and J. Wang, *Three-dimensional immersed finite element methods for electric field simulation in composite materials*, International journal for numerical methods in engineering, 64 (2005), pp. 940–972.

73. R. B. Kellogg, *Singularities in interface problems*, in Numerical Solution of Partial Differential Equations, II (SYNSPADE 1970) (Proc. Sympos., Univ. of Maryland, College Park, Md., 1970), Academic Press, New York, 1971, pp. 351–400.

74. R. B. Kellogg, *On the Poisson equation with intersecting interfaces*, Applicable Anal., 4 (1974/75), pp. 101–129. Collection of articles dedicated to Nikolai Ivanovich Muskhelishvili.

75. L. Lee and R. J. Leveque, *An immersed interface method for incompressible Navier-Stokes equations*, SIAM J. Sci. Comput., 25 (2003), pp. 832–856.

76. R. J. LeVeque and Z. Li, *Immersed interface methods for Stokes flow with elastic boundaries or surface tension*, SIAM J. Sci. Comput., 18 (1997), pp. 709–735.

77. R. J. LeVeque and Z. L. Li, *The immersed interface method for elliptic equations with discontinuous coefficients and singular sources*, SIAM J. Numer. Anal., 31 (1994), pp. 1019–1044.

78. Z. Li, *The immersed interface method: A numerical approach for partial differential equations with interfaces*, 1994. Thesis (Ph.D.)–University of Washington.

79. ——, *The immersed interface method using a finite element formulation*, Appl. Numer. Math., 27 (1998), pp. 253–267.

80. Z. Li and K. Ito, *The immersed interface method: numerical solutions of PDEs involving interfaces and irregular domains*, vol. 33, Siam, 2006.

81. Z. Li and M.-C. Lai, *The immersed interface method for the Navier-Stokes equations with singular forces*, J. Comput. Phys., 171 (2001), pp. 822–842.

82. Z. Li, T. Lin, Y. Lin, and R. C. Rogers, *An immersed finite element space and its approximation capability*, Numer. Methods Partial Differential Equations, 20 (2004), pp. 338–367.

83. Z. Li, T. Lin, and X. Wu, *New Cartesian grid methods for interface problems using the finite element formulation*, Numer. Math., 96 (2003), pp. 61–98.

84. T. Lin, Y. Lin, and X. Zhang, *Partially penalized immersed finite element methods for elliptic interface problems*, SIAM J. Numer. Anal., 53 (2015), pp. 1121–1144.

85. T. Lin and J. Wang, *An immersed finite element electric field solver for ion optics modeling*, in Proceedings of AIAA Joint Propulsion Conference, Indianapolis, IN, 2002, pp. 2002–4263.

86. T. Lin, Q. Yang, and X. Zhang, *Partially penalized immersed finite element methods for parabolic interface problems*, Numer. Methods Partial Differential Equations, 31 (2015), pp. 1925–1947.

87. A. N. Marques, J.-C. Nave, and R. R. Rosales, *A correction function method for Poisson problems with interface jump conditions*, J. Comput. Phys., 230 (2011), pp. 7567–7597.

88. A. Massing, M. G. Larson, A. Logg, and M. E. Rognes, *A stabilized Nitsche fictitious domain method for the Stokes problem*, J. Sci. Comput., 61 (2014), pp. 604–628.

89. ——, *A stabilized Nitsche overlapping mesh method for the Stokes problem*, Numer. Math., 128 (2014), pp. 73–101.

90. D. M. McQueen and C. S. Peskin, *Heart simulation by an immersed boundary method with formal second-order accuracy and reduced numerical viscosity*, in Mechanics for a New Mellennium, Springer, 2001, pp. 429–444.

91. J. M. Melenk, *On generalized finite-element methods.* Thesis (Ph.D.)–University of Maryland, College Park.

92. J. M. Melenk and I. Babuška, *The partition of unity finite element method: basic theory and applications*, Comput. Methods Appl. Mech. Engrg., 139 (1996), pp. 289–314.

93. L. A. Miller and C. S. Peskin, *When vortices stick: an aerodynamic transition in tiny insect flight*, Journal of Experimental Biology, 207 (2004), pp. 3073–3088.

94. Y. Mori, *Convergence proof of the velocity field for a Stokes flow immersed boundary method*, Comm. Pure Appl. Math., 61 (2008), pp. 1213–1263.

95. J. Nitsche, *Über ein variationsprinzip zur lösung von dirichlet-problemen bei verwendung von teilräumen, die keinen randbedingungen unterworfen sind*, in Abhandlungen aus dem mathematischen Seminar der Universität Hamburg, vol. 36, Springer, 1971, pp. 9–15.

96. C. S. Peskin, *Numerical analysis of blood flow in the heart*, J. Computational Phys., 25 (1977), pp. 220–252.

97. ——, *The immersed boundary method*, Acta Numer., 11 (2002), pp. 479–517.

98. C. S. Peskin and D. M. McQueen, *Modeling prosthetic heart valves for numerical analysis of blood flow in the heart*, J. Comput. Phys., 37 (1980), pp. 113–132.

99. C. S. Peskin and B. F. Printz, *Improved volume conservation in the computation of flows with immersed elastic boundaries*, J. Comput. Phys., 105 (1993), pp. 33–46.

100. R. Rannacher and R. Scott, *Some optimal error estimates for piecewise linear finite element approximations*, Math. Comp., 38 (1982), pp. 437–445.

101. P.-A. Raviart and J. M. Thomas, *A mixed finite element method for 2nd order elliptic problems*, in Mathematical aspects of finite element methods (Proc. Conf., Consiglio Naz. delle Ricerche (C.N.R.), Rome, 1975), Springer, Berlin, 1977, pp. 292–315. Lecture Notes in Math., Vol. 606.

102. A. H. Schatz and L. B. Wahlbin, *Interior maximum norm estimates for finite element methods*, Math. Comp., 31 (1977), pp. 414–442.

103. ——, *Interior maximum-norm estimates for finite element methods. II*, Math. Comp., 64 (1995), pp. 907–928.

104. L. R. Scott and S. Zhang, *Finite element interpolation of nonsmooth functions satisfying boundary conditions*, Math. Comp., 54 (1990), pp. 483–493.

105. R. Scott, *Optimal L^∞ estimates for the finite element method on irregular meshes*, Math. Comp., 30 (1976), pp. 681–697.

106. R. Stenberg, *On some techniques for approximating boundary conditions in the finite element method*, J. Comput. Appl. Math., 63 (1995), pp. 139–148. International Symposium on Mathematical Modelling and Computational Methods Modelling 94 (Prague, 1994).

107. T. Strouboulis, I. Babuška, and K. Copps, *The design and analysis of the generalized finite element method*, Comput. Methods Appl. Mech. Engrg., 181 (2000), pp. 43–69.

108. T. Strouboulis, K. Copps, and I. Babuška, *The generalized finite element method: an example of its implementation and illustration of its performance*, Internat. J. Numer. Methods Engrg., 47 (2000), pp. 1401–1417.

109. ——, *The generalized finite element method*, Comput. Methods Appl. Mech. Engrg., 190 (2001), pp. 4081–4193.

110. J. Xu, *Estimate of the Convergence Rate of Finite Element Solutions to Elliptic Equations of Second Order with Discontinuous Coefficients*, ArXiv e-prints, (2013).

111. H. Yu, *Three-dimensional computational modeling and simulation of platelet aggregation on parallel computers.* Thesis (Ph.D.)–The University of Utah.

112. X. Zhang, *Nonconforming immersed finite element methods for interface problems*, PhD thesis, Virginia Polytechnic Institute and State University, 2013.

113. P. Zunino, *Analysis of backward Euler/extended finite element discretization of parabolic problems with moving interfaces*, Comput. Methods Appl. Mech. Engrg., 258 (2013), pp. 152–165.

114. P. Zunino, L. Cattaneo, and C. M. Colciago, *An unfitted interface penalty method for the numerical approximation of contrast problems*, Appl. Numer. Math., 61 (2011), pp. 1059–1076.